NOTICE

CERTAIN DATA CONTAINED IN THIS DOCUMENT MAY BE DIFFICULT TO READ IN MICROFICHE PRODUCTS.

SAND--90-0416

DE91 000483

Distribution
Category UC-705

FINITE ELEMENT ERROR ESTIMATION AND ADAPTIVITY BASED ON PROJECTED STRESSES

Joseph Jung
Applied Mechanics Division III
Sandia National Laboratories
Albuquerque, New Mexico 87185

Abstract

This report investigates the behavior of a family of finite element error estimators based on projected stresses, i.e., continuous stresses that are a least squared error fit to the conventional Gauss point stresses. An error estimate based on element force equilibrium appears to be quite effective. Examples of adaptive mesh refinement for a one-dimensional problem are presented. Plans for two-dimensional adaptivity are discussed.

MASTER

CONTENTS

1. Introduction 9

2. Projected Stress 11

2.1 Formulation 11

2.2 One-Dimensional Behavior of Projected Stresses 12

2.2.1 One-Dimensional Model Problem 12

2.2.2 One-Dimensional Projected Sterss Results 13

2.3 Loubignac Iterations to Improve Stresses 13

3. Possible Error Estimates Based on Projected Stresses 20

4. Numerical Results 23

4.1 One-Dimensional 23

4.2 Two-Dimensional 28

4.2.1 A Plate with a Hole 28

4.2.2 A Uniformly Loaded Simply Supported Beam 43

4.2.3 A Short Cantilever Beam 51

5. Discussion of Error Results 58

6. Adaptivity 59

6.1 Simple One-Dimensional H-Type Adaptivity 59

6.2 Plans for Two-Dimensional Adaptivity 59

6.3 Closure 59

7. References 73

FIGURES

1. One-Dimensional Model Problem 14
2. Stress Comparison for n = 0, Two Elements 15
3. Stress Comparison for n = 0, Three Elements 15
4. Stress Comparison for n = 0, Four Elements 16
5. Stress Comparison for n = 0, Five Elements 16
6. Stress Comparison for n = 1, Two Elements 17
7. Stress Comparison for n = 1, Three Elements 17
8. Stress Comparison for n = 1, Four Elements 18
9. Stress Comparison for n = 1, Five Elements 18
10. Stress Improvement Using 4 Loubignac Iterations, n = 0 19
11. Stress Improvement Using 4 Loubignac Iterations, n = 1 19
12. Plot of Various Stress Quantities 22
13. Element Force Error for n = 0 (uniform loading) 24
14. Element Equilibrium Error for n = 0 (uniform loading) 24
15. Stress Error Norm for n = 0 (uniform loading) 25
16. Del Sigma Norm for n = 0 (uniform loading) 25
17. Element Force Error for n = 1 (linearly varying loading) 26
18. Element Equilibrium Error for n = 1 (linearly varying loading) 26
19. Stress Error Norm for n = 1 (linearly varying loading) 27
20. Del Sigma Norm for n = 1 (linearly varying loading) 27
21. Mesh 1 for the Hole Problem 29
22. Mesh 2 for the Hole Problem 29
23. Mesh 3 for the Hole Problem 30
24. Mesh 4 for the Hole Problem 30
25. L_2 Norm of True Stress Error, Mesh 1 31
26. L_2 Norm of True Stress Error, Mesh 2 31
27. L_2 Norm of True Stress Error, Mesh 3 32
28. L_2 Norm of True Stress Error, Mesh 4 32
29. True Del Sigma Error Norm, Mesh 1 33
30. True Del Sigma Error Norm, Mesh 2 33
31. True Del Sigma Error Norm, Mesh 3 34
32. True Del Sigma Error Norm, Mesh 4 34
33. Individual Stress Errors Around the Hold Boundary of Mesh 4 35
34. L_2 Norm Stress Error Around the Hole Boundary of Mesh 4 35
35. Element Force Error, Mesh 1 37
36. Element Force Error, Mesh 2 37
37. Element Force Error, Mesh 3 38
38. Element Force Error, Mesh 4 38
39. Stress Error Norm, Mesh 1 39
40. Stress Error Norm, Mesh 2 39
41. Stress Error Norm, Mesh 3 40
42. Stress Error Norm, Mesh 4 40
43. Del Sigma Norm, Mesh 1 41
44. Del Sigma Norm, Mesh 2 41
45. Del Sigma Norm, Mesh 3 42
46. Del Sigma Norm, Mesh 4 42
47. A Simply Supported Uniformly Loaded Beam 43
48. Mesh 1 of the Beam 44
49. Mesh 2 of the Beam 44
50. Mesh 3 of the Beam 45
51. Comparison of Projected Bending Stresses and Beam Theory at the Midspan of the Beam 45

52. Element Force Residual Norm for Mesh 1 46
53. Element Force Residual Norm for Mesh 2 46
54. Element Force Residual Norm for Mesh 3 47
55. Element Force Residual Norm for Mesh 3 at the Midspan of the Beam .. 47
56. Stress Error Norm for Mesh 1 48
57. Stress Error Norm for Mesh 2 48
58. Stress Error Norm for Mesh 3 49
59. Del Sigma Norm for Mesh 1 49
60. Del Sigma Norm for Mesh 2 50
61. Del Sigma Norm for Mesh 3 50
62. A Short Cantilever Beam Problem 51
63. Mesh 1 for the Short Cantilever Problem 52
64. Mesh 2 for the Short Cantilever Problem 52
65. Mesh 3 for the Short Cantilever Problem 53
66. Element Force Error Norm for Mesh 1 53
67. Element Force Error Norm for Mesh 2 54
68. Element Force Error Norm for Mesh 3 54
69. Stress Error Norm for Mesh 1 55
70. Stress Error Norm for Mesh 2 55
71. Stress Error Norm for Mesh 3 56
72. Del Sigma Norm for Mesh 1 56
73. Del Sigma Norm for Mesh 2 57
74. Del Sigma Norm for Mesh 3 57
75. H-Type Mesh Refinement for n = 0, 5% Error Tolerance
Using an Element Force Residual Error Measure
a. Iteration 1 60
b. Iteration 2 60
c. Iteration 3 61
76. Element Force Residual Error for n=0, 5% Error Tolerance 62
77. H-Type Mesh Refinement for n = 0, 5% Error Tolerance
Using a Del Sigma Error Measure
a. Iteration 1 63
b. Iteration 2 63
c. Iteration 3 64
78. Del Sigma Error for n = 0, 5% Error Tolerance 65
79. H-Type Mesh Refinement for n = 0, 5% Error Tolerance
Using an Element Force Residual Error Measure
a. Iteration 1 66
b. Iteration 2 66
c. Iteration 3 67
d. Iteration 4 67
80. Element Force Residuals for n = 1, 5% Error Tolerance..... 68
81. H-Type Mesh Refinement for n = 1, 5% Error Tolerance Using
a Del Sigma Error Measure
a. Iteration 1 69
b. Iteration 2 69
c. Iteration 3 70
d. Iteration 4 70
e. Iteration 5 71
82. Del Sigma Error for n = 1, 5% Error Tolerance 72

FINITE ELEMENT ERROR ESTIMATION AND
ADAPTIVITY BASED ON PROJECTED STRESSES

1. INTRODUCTION

In recent years, considerable effort has been devoted to finite element error estimation and control [see A. Noor and I. Babuska (1987) for a summary]. If a reliable error estimate can be obtained, it follows that the error estimate could be used to adaptively change the mesh in order to reduce the error to an acceptable level. Obtaining the error estimate, though, can be a formidable task since, in general, the only information available to the analyst is the approximate solution itself.

Among the most popular approaches is that developed by Babuska, et al., which attempts to estimate the error in the strain energy of the solution, the so-called energy norm. This estimator has the form of

$$\varepsilon^2 = \sum_{i=1}^{m} \left(\frac{h_i^2}{24K} \int_{r_i} r^2 \, d\Omega + \frac{h_i}{24K} \int_{I_i} J^2 \, dI \right)$$

with I_i being the element interface, r is the residual of the governing differential equation, J is the inter-element traction jump, m is the number of elements, K is the bulk modulus, and h_i is the characteristic length of the element. Such estimators require explicit determination of the inter-element traction jumps and integration along the element interfaces. Furthermore, most of the error for this estimator is in the traction term.

Zienkiewicz and Zhu (1987), proposed a new approach based on a projected stress field (a continuous stress field that is a least squared error fit to the conventional finite element stresses). The appeal of using a projected stress field was obvious--there was now more information that could be used to form an error estimate. If the projected stresses were taken to be approximately equal to the exact solution, one could write

$$\underset{\sim}{e}_{\sigma} = \underset{\sim}{\sigma}_{ex} - \underset{\sim}{\sigma}_{fe}$$

$$\approx \hat{\underset{\sim}{\sigma}} - \underset{\sim}{\sigma}_{fe}$$

where

$\underset{\sim}{\sigma}_{ex}$ are the exact stresses

$\underset{\sim}{\sigma}_{fe}$ are the finite element stresses

and

$\hat{\underset{\sim}{\sigma}}$ are the projected stresses

We now have a very simple and easy to use error estimator. The method for obtaining projected stresses will be discussed in this report.

The work in this report explores some new approaches for using projected stresses that are different from that presented by Zienkiewicz. In particular, attention is paid to possible error measures based on the residual at the equilibrium equations or the force residuals of element equilibrium. Both of these error measures are applicable to nonlinear as well as linear problems since they involve residuals of basic equations that are not influenced by whether the problem is linear or not.

Although this report focuses primarily on error estimation, some thought is given to adaptivity. There are a number of approaches to adaptivity, which are commonly called r, h, and p methods. The r method involves moving the node point locations to minimize the error with a given number of nodes. This approach is almost never used since it leads to a very complex set of nonlinear equations. The h method involves element subdivision to control the solution error, and the p method refers to increasing the order of approximation within the elements. The h and p methods have often been combined to obtain optimum convergence rates.

In this report, we will use some simple h type refinements for one-dimensional problems and will discuss plans for future two-dimensional work.

2. PROJECTED STRESS

2.1 FORMULATION

The error estimation techniques used in this report are based on projected stress fields (continuous stress fields over the domain of the problem). This stress field can be developed from a number of different approaches. We could start from a weighted residual statement (Zienkiewicz, et al., 1985), a least squared error statement (Hinton and Campbell, 1974), or the concept of conjugate approximations (Oden and Brauchli, 1971). All three approaches produce equivalent results.

The simplest derivation is probably the weighted residual approach. Let us first begin by defining a continuous stress field, $\hat{\underset{\sim}{\sigma}}$, based on element shape functions, N (usually the same shape functions as those used for the displacement interpolation), and nodal stress values, $\hat{\underset{\sim}{\sigma}}^*$, such that,

$$\hat{\underset{\sim}{\sigma}} = N \, \hat{\underset{\sim}{\sigma}}^* \tag{1}$$

We can now write a weighted residual statement in which the residual is the difference between the conventionally computed finite element stresses, $\underset{\sim}{\sigma}_{fe}$, and the projected stresses, $\hat{\underset{\sim}{\sigma}}$,

$$\int_\Omega N^T \left(\underset{\sim}{\sigma}_{fe} - \hat{\underset{\sim}{\sigma}} \right) d\Omega = 0 \tag{2}$$

which upon substitution of Equation (1) into (2) yields

$$\int_\Omega N^T \left(\underset{\sim}{\sigma}_{fe} - N \, \hat{\underset{\sim}{\sigma}}^* \right) d\Omega = 0$$

or

$$M \, \hat{\underset{\sim}{\sigma}}^* = \int_\Omega N^T \, \sigma_{fe} \, d\Omega \tag{3}$$

in which

$$M = \int_\Omega N^T \, N \, d\Omega \; . \tag{4}$$

The nodal stresses are obtained by solving this linear set of equations, which is symbolically written as

$$\hat{\underset{\sim}{\sigma}}^* = M^{-1} \int_\Omega N^T \, \underset{\sim}{\sigma}_{fe} \, d\Omega \; . \tag{5}$$

This operation is repeated for each component of stress.

The equivalent least squared error formulation is derived from the functional

$$EM = \int_\Omega \left(\hat{\underset{\sim}{\sigma}} - \underset{\sim}{\sigma}_{fe} \right)^2 d\Omega = \int_\Omega \left(N \, \hat{\underset{\sim}{\sigma}}^* - \underset{\sim}{\sigma}_{fe} \right)^2 d\Omega$$

Minimizing this functional yields

$$\frac{\partial EM}{\partial \hat{\underset{\sim}{\sigma}}^*} = \int_\Omega N^T N \, d\Omega \, \hat{\underset{\sim}{\sigma}}^* - \int_\Omega N^T \underset{\sim}{\sigma}_{fe} \, d\Omega = 0 \tag{6}$$

which is identical to Equation (3).

An interesting point is that the projected stresses can be interpreted as a least squared error fit to the conventional finite element stresses, which are themselves a least squared error fit to the exact solution (Herrmann, 1972). Thus, one would intuitively expect that the projected stresses would provide a fairly good continuous approximation to the exact solution with the least accurate approximations occurring on the boundaries of the body where the computed finite element stresses are the poorest. Furthermore, nodal points on the boundary are not completely surrounded by elements so that the natural weighting of stresses that occurs in the interior of the mesh is not as great on the boundary.

It is also interesting to notice that the matrix, M, consists of the products of shape functions integrated over the volume of each element, which closely resembles a typical finite element "mass" matrix. As with mass matrices, a "consistent" form is obtained if the integrations are performed with an integration scheme that evaluates the integrals exactly, while a simple diagonal "lumped" form is obtained if the integrals are evaluated only at the nodes. Zienkiewicz, et al. (1985) points out that the consistent form, in general, gives better results. The lumped form, however, leads to a system of equations that is extremely easy to solve. This lumped form yields a simple volume weighted nodal average of stresses.

2.2 ONE-DIMENSIONAL BEHAVIOR OF PROJECTED STRESSES

To examine how the projected stresses behave, let us examine a series of simple one-dimensional elasticity problems. We will consider the problem shown in Figure 1, and compare the projected stresses, finite element stresses, and the exact stresses.

2.2.1 One-Dimensional Model Problem

As the one-dimensional model problem, consider a circular bar of cross-sectional area, A, fixed at one end, and loaded along its length by the function f(x), Figure 1. Assuming linear elasticity, the governing differential equation is

$$EA \frac{d^2u}{dx^2} + f(x) = 0$$

with the boundary conditions

$$u|_{x=0} = 0$$

$$\left.\frac{du}{dx}\right|_{x=L} = 0 \ .$$

Let us consider a particular form for f(x), i.e., let

$$f(x) = \sigma_o \, P \left(\frac{x}{L} \right)^n \quad ; \quad n = 0, 1, 2, \ldots$$

where P is the perimeter of the bar.

The solution to this differential equation (for a given n) is

$$u = \frac{\sigma_o P}{EA(n+1)} \left[Lx - \frac{x^{(n+2)}}{L^n (n+2)} \right] .$$

The stress is given by

$$\sigma = E \frac{du}{dx}$$

$$\sigma = \frac{\sigma_o P}{A(n+1)} \left[L - \frac{x^{(n+1)}}{L^n} \right] .$$

2.2.2 <u>One-Dimensional Projected Stress Results</u>

For the first example problem, we let a bar of unit length and unit area be loaded by a uniform stress along its perimeter, ($\sigma_o = 1.$), i.e.,

$$f(x) = P \qquad (n = 0) \ .$$

The exact stresses, projected stresses, and finite element stresses for two, three, four, and five elements are shown in Figures 2 through 5. In general, we see that the stress results at the interior nodes are quite good and the maximum errors occur at the boundaries where there is only limited finite element stress information.

In the second example problem, the forcing function was taken to be

$$f(x) = P(x/L) \qquad (n = 1) \ .$$

Convergence of the projected stresses toward the exact solution is observed as the number of elements is increased, Figures 6 through 9.

These examples were performed using a uniform mesh refinement.

2.3 LOUBIGNAC ITERATIONS TO IMPROVE STRESSES

Loubignac, et al. (1977) and Cantin (1978) showed that it is possible to further improve the projected stress solution with an iteration process. This process consists of repetitively solving the incremental problem

$$K \, \Delta \underset{\sim}{u}_i = \underset{\sim}{f} - \int B^T \, \hat{\underset{\sim}{\sigma}}_i \, d\Omega$$

with

$$\underset{\sim}{u}_{i+1} = \underset{\sim}{u}_i + \Delta \underset{\sim}{u}_i$$

until the right-hand side residual or $\Delta \underset{\sim}{u}_i$ is acceptably small. These iterations are called Loubignac or Loubignac-Cantin iterations. Zienkiewicz, et al. (1985) recognized that this process is equivalent to solving a mixed formulation to the problem in which both stresses and displacements are problem unknowns.

The effectiveness of this procedure is shown in Figures 10 and 11 in which the stresses, after four Loubignac iterations, are plotted for the one-dimensional model problem with n = 0 and 1, each using four element meshes. A marked improvement in the projected stress solution is observed. Because the error measures examined in this report are based on the projected stresses, it is important to recognize that these stresses can be improved through an iterative process. Moreover, for nonlinear problems it may be possible to include these iterations in the iteration procedure for the overall nonlinear response at little extra cost [Zienkiewicz, et al. (1985)].

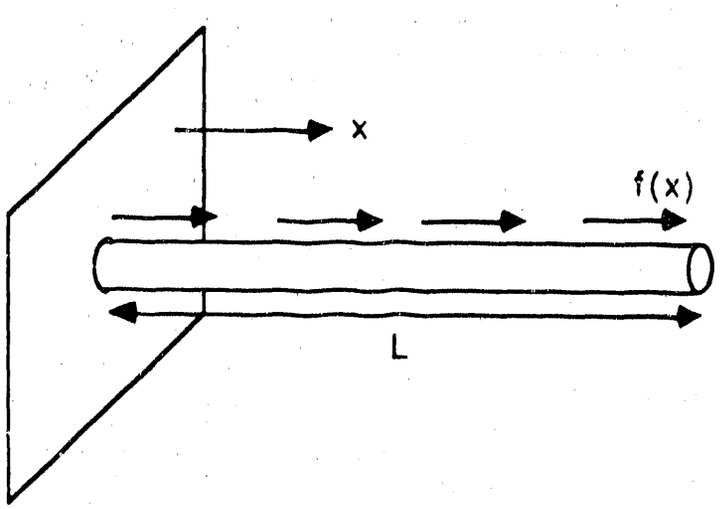

Figure 1. One-Dimensional Model Problem

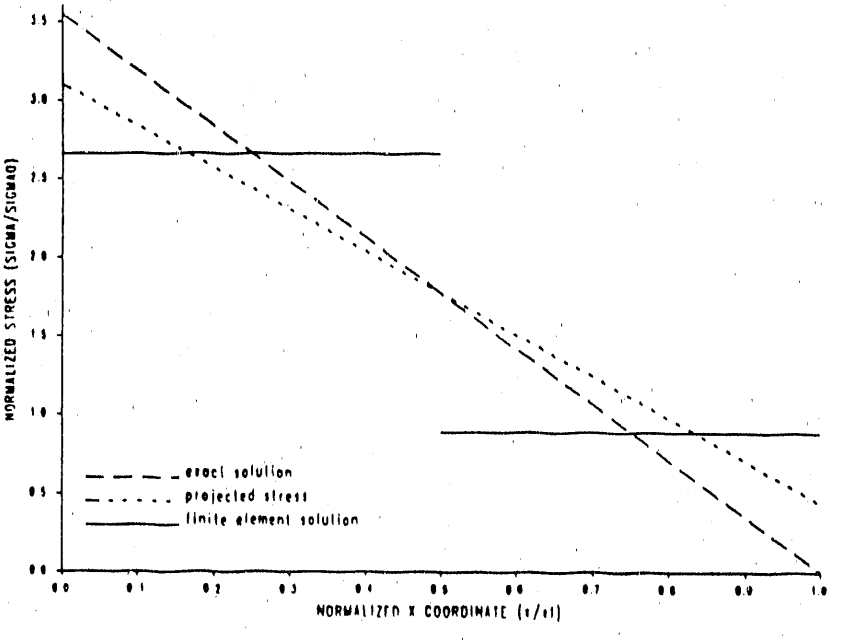

Figure 2. Stress Comparison for n = 0, Two Elements

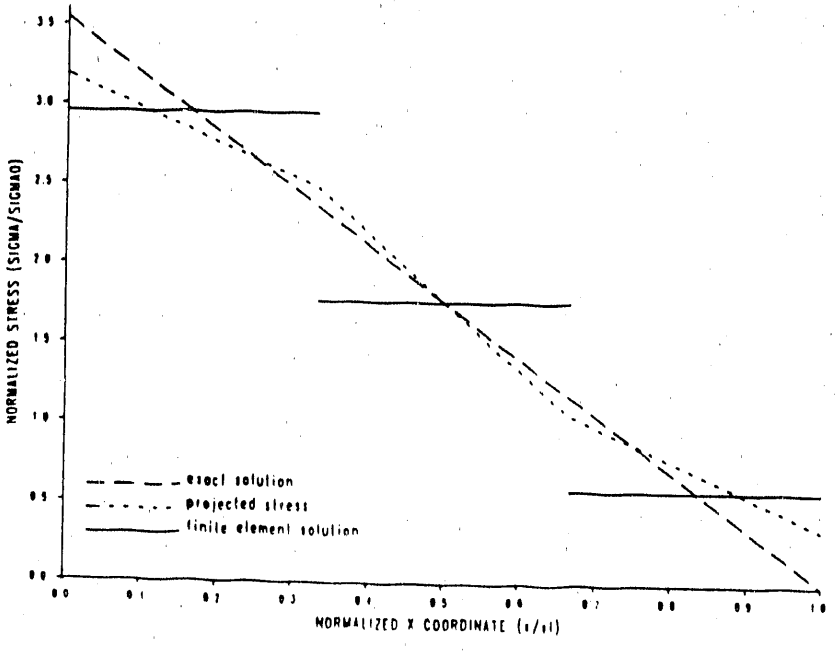

Figure 3. Stress Comparison for n = 0, Three Elements

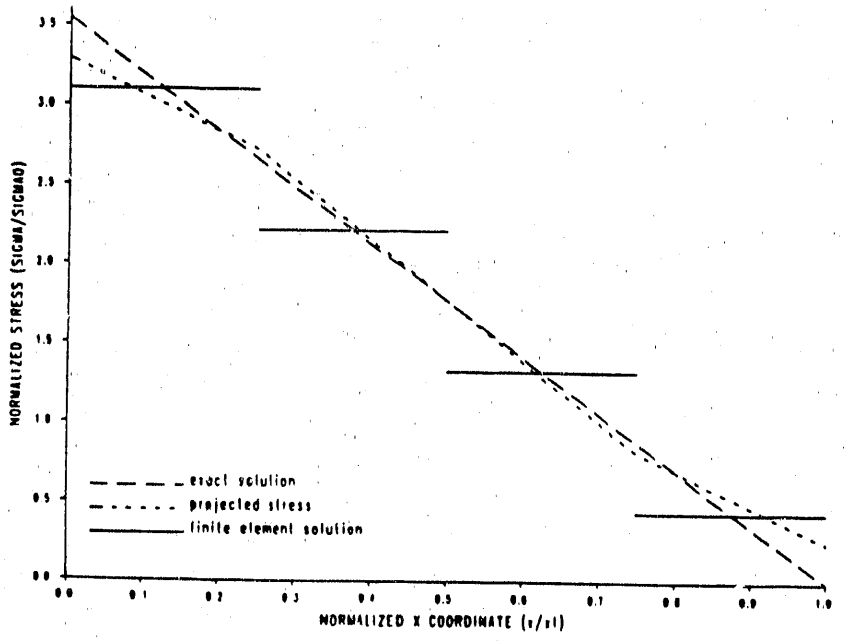

Figure 4. Stress Comparison for n = 0, Four Elements

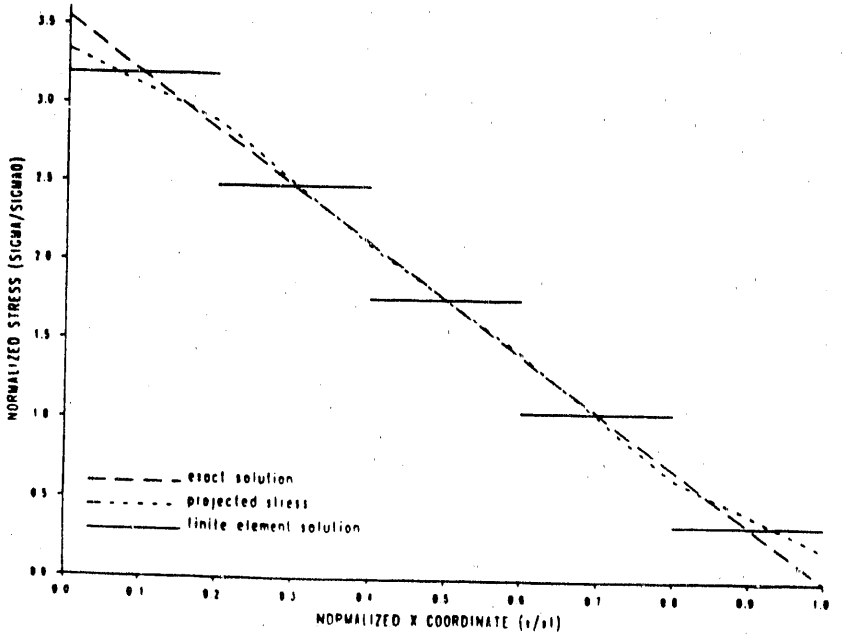

Figure 5. Stress Comparison for n = 0, Five Elements

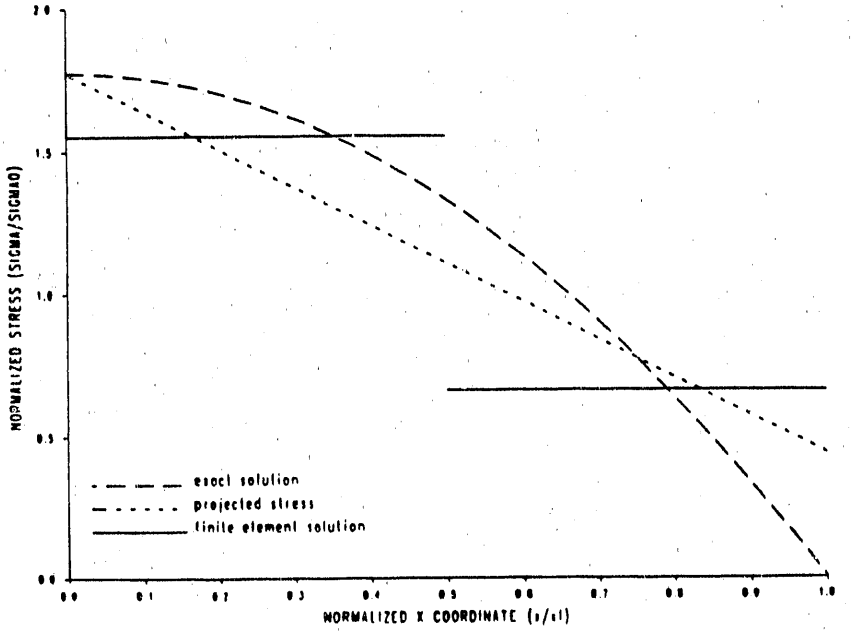

Figure 6. Stress Comparison for n = 1, Two Elements

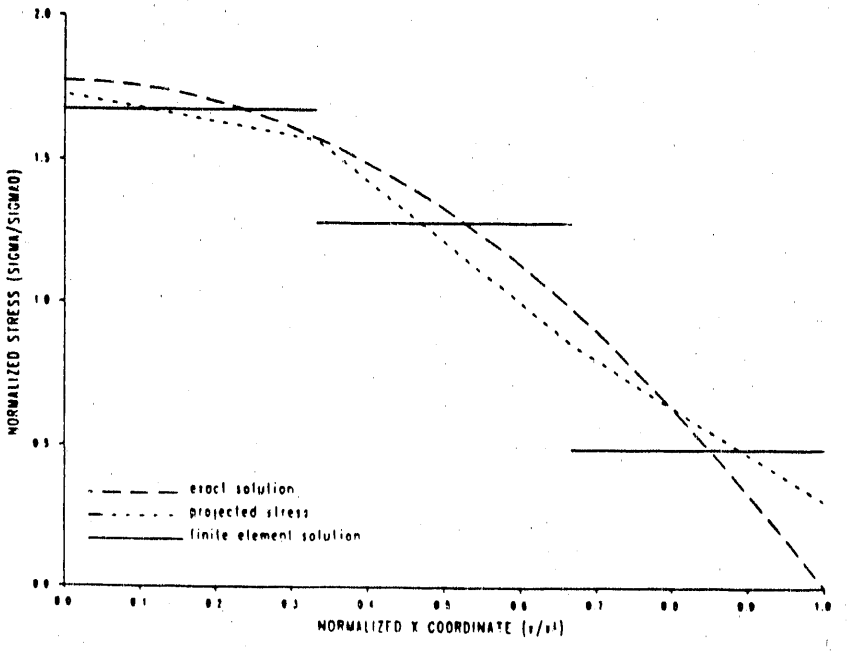

Figure 7. Stress Comparison for n = 1, Three Elements

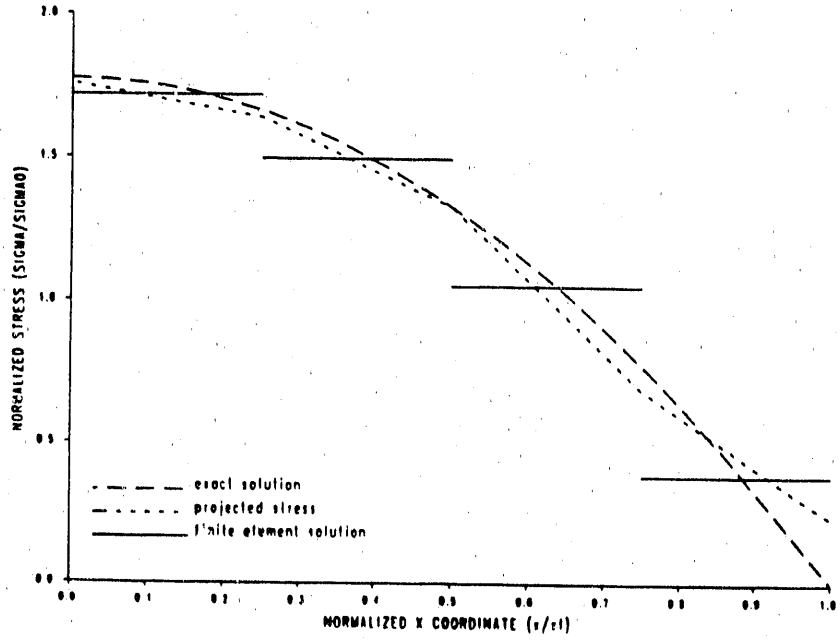

Figure 8. Stress Comparison for n = 1, Four Elements

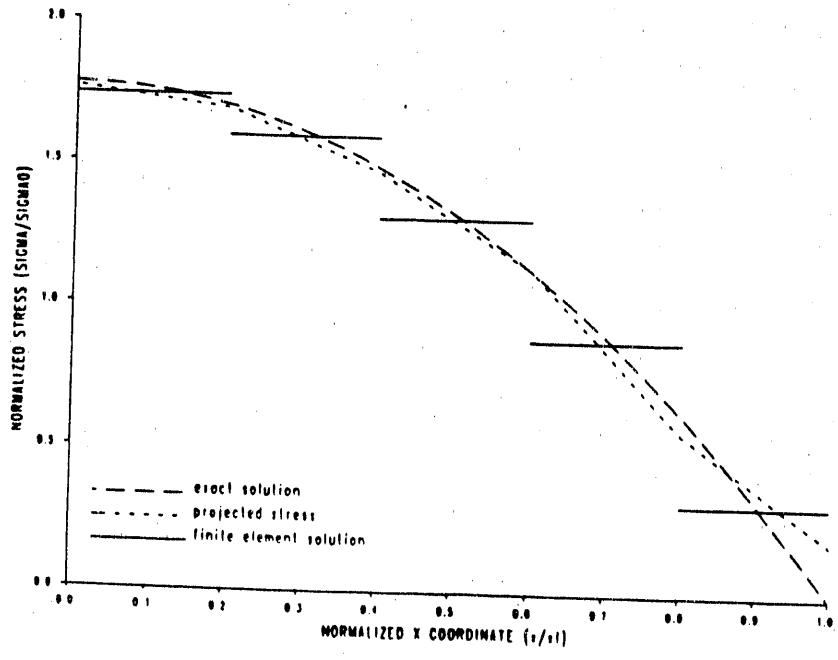

Figure 9. Stress Comparison for n = 1, Five Elements

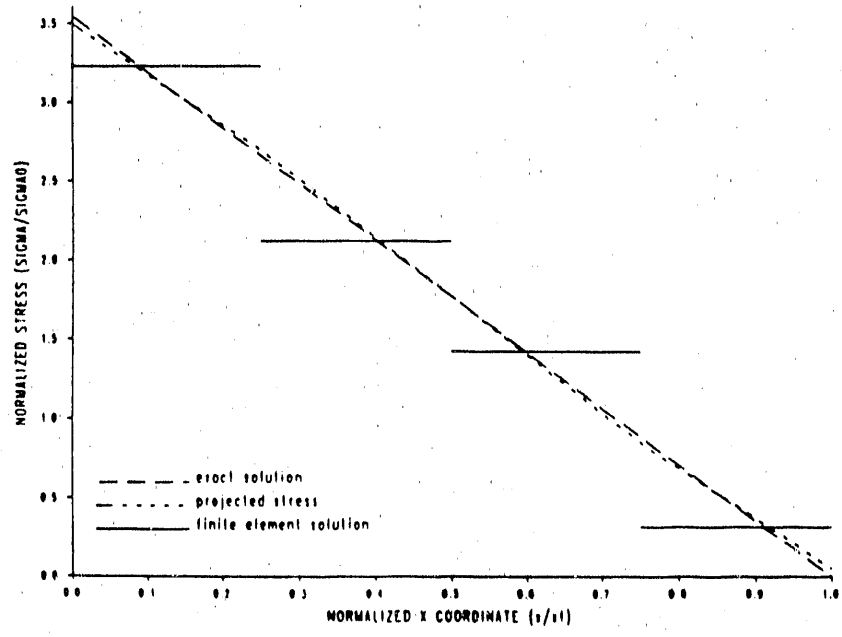

Figure 10. Stress Improvement Using 4 Loubignac Iterations, n = 0

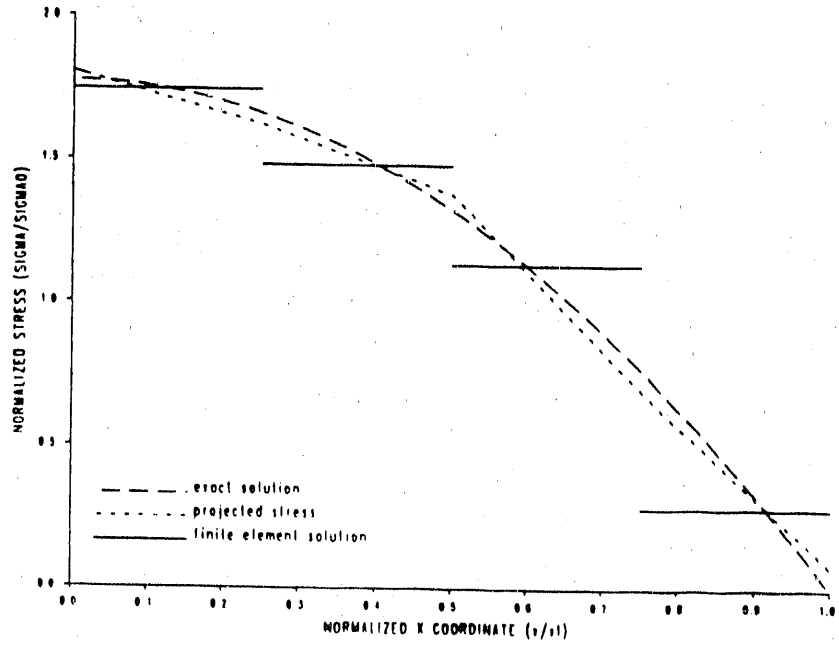

Figure 11. Stress Improvement Using 4 Loubignac Iterations, n = 1

3. POSSIBLE ERROR ESTIMATES BASED ON PROJECTED STRESSES

The current work focused on four possible error estimators based on the projected stresses. The simplest error estimator is probably the difference between the projected stress and the finite element stress, see Figure 12, as suggested by Zienkiewicz and Zhu (1987). In their work, the projected stress, $\hat{\underset{\sim}{\sigma}}$, was taken to be equal to the exact solution and, thus, the stress error can be written as

$$\underset{\sim}{e}^{\sigma} = \hat{\underset{\sim}{\sigma}} - \underset{\sim}{\sigma}_{fe} \tag{7}$$

where $\underset{\sim}{\sigma}_{fe}$ is the finite element stress.

Although elegantly simple, this definition of error may indicate an appreciable error even though the projected stress field approximates the exact solution well, Figure 12.

Zienkiewicz suggests that an integral form of the stress error estimator given in Equation (7) can be obtained by forming the so-called L_2 norm stress error for each element, i.e.,

$$|| \underset{\sim}{e}^{\sigma} ||_{L_2} = \left(\int_{\Omega} \underset{\sim}{e}^{\sigma T} \underset{\sim}{e}^{\sigma} \, d\Omega \right)^{1/2}$$

and then a new norm can be written as

$$\Delta\sigma = \left(\frac{|| \underset{\sim}{e}^{\sigma} ||^2_{L_2}}{\Omega} \right)^{1/2} . \tag{8}$$

This new norm defines the root mean square stress error in absolute terms.

However, this norm is not rotationally invariant, i.e., if we used the same mesh, but in a rotated coordinate system, we would not, in general, calculate the same value for the L_2 norm in both systems. A rotationally invariant version of the L_2 norm of a second order tensor, **A**, would be

$$|| \mathbf{A} ||_{L_2} = \left[\int_{\Omega} a_{ij} \, a_{ij} \, d\Omega \right]^{1/2} \tag{9}$$

Of course, this norm could also be written in a nonintegrated form as

$$| \mathbf{A} |_{L_2} = \left[a_{ij} \, a_{ij} \right]^{1/2} \tag{10}$$

Equation (10) is useful when we seek a discrete measure of Equation (7). We will use the norm

$$| e^{\sigma} |_{L_2} = \max_{x \varepsilon \Omega} \left[e^{\sigma}_{ij} \; e^{\sigma}_{ij} \right]^{1/2} \tag{11}$$

as the measure of discrete stress errors in each element.

In all of the calculations reported in this work, Equation (9) is used. In this spirit, the norm used in Equation (8) is

$$|| e_{\sigma} ||_{L_2} = \left[\int_{\Omega} e^{\sigma}_{ij} \; e^{\sigma}_{ij} \; d\Omega \right]^{1/2} \tag{12}$$

A third possible error measure could be based on evaluating the residual of the governing equilibrium equations. This can be accomplished by taking the appropriate derivatives of the projected stress fields and substituting these quantities into the equilibrium equations, e.g., in two dimensions,

$$\begin{aligned} \frac{\partial \sigma_x}{\partial x} + \frac{\partial \tau}{\partial y} &= 0 \\ \frac{\partial \tau}{\partial x} + \frac{\partial \sigma_y}{\partial y} &= 0 \; . \end{aligned} \tag{13}$$

In general, the equilibrium equations will not be satisfied and hence, there will be residuals that can be interpreted as an error measure. In terms of the element shape functions and nodal stress values, the equations for the residual would be (again in two dimensions)

$$\begin{aligned} \sum_{i=1}^{n} \frac{\partial N_i}{\partial x} \hat{\sigma}^{*}_{x_i} + \sum_{i=1}^{n} \frac{\partial N_i}{\partial y} \hat{\tau}^{*}_{i} &= R_x \\ \sum_{i=1}^{n} \frac{\partial N_i}{\partial x} \hat{\tau}^{*}_{i} + \sum_{i=1}^{n} \frac{\partial N_i}{\partial y} \hat{\sigma}^{*}_{y_i} &= R_y \; . \end{aligned} \tag{14}$$

The residuals are a direct result of having continuous stress fields and are intuitively appealing because in a standard displacement based finite element formulation, the equilibrium equations are only satisfied in the limit as the number of elements becomes very large.

A fourth error measure could be obtained by integrating the residuals in Equation (14) over the volume of the element to obtain element force residuals, i.e.,

$$\begin{aligned} \int_{\Omega} R_x \; d\Omega &= F_x \\ \int_{\Omega} R_y \; d\Omega &= F_y \end{aligned} \tag{15}$$

Alternatively, the divergence theorem could be applied to obtain a surface integral, if desired. These force residuals may be easier to work with than the residuals of Equation (14) because Equation (15) can be normalized by some characteristic force quantity in the problem while it may be difficult to find a characteristic stress derivative with which to normalize Equation (14).

An appropriate norm for Equation (15) is

$$|| F || = \left(F_x^2 + F_y^2 \right)^{1/2} . \tag{16}$$

For adaptive purposes, it is most useful to perform the indicated integrations over each element in order to obtain local error quantities. If a global estimate is desired, it is possible to sum these quantities as indicated in Zienkiewicz and Zhu (1987).

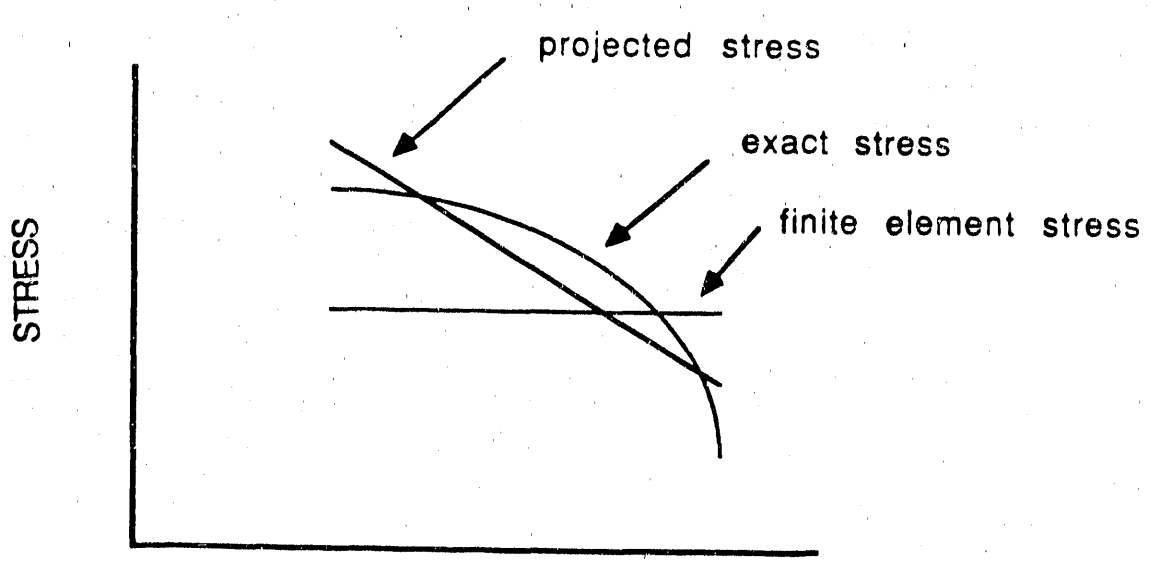

Figure 12. Plot of Various Stress Quantities

4. NUMERICAL RESULTS

In this section, we will examine the behavior of the proposed error estimators when applied to one-dimensional and two-dimensional elasticity problems. It is informative to see how these error estimators behave in the simpler one-dimensional setting before examining the two-dimensional problems.

4.1 ONE-DIMENSIONAL

In one dimension, we will again use the model problem presented in Section 2.2.1, Figure 1. The results for n = 0 and 1 (i.e., a uniform and linearly varying load distribution) with the mesh uniformly refined from 2 to 5 elements are presented Figures 13 through 20.

First, let us consider the case of n = 0, Figure 13 to 16. Figure 13 shows the element force residuals, Equation (15), normalized by the total reaction force. The curves show a fairly uniform decrease in the element force residuals as the number of elements is increased. The highest residuals exist at the ends of the rod. The results show that the force residuals in a given region may actually increase as the mesh is refined, if the starting mesh is very coarse.

Figure 14 shows the equilibrium residuals, Equation (14), evaluated at the center of each element. Essentially the same trends as the force residuals are obtained.

The element stress errors, Equation (11), are shown in Figure 15. Although a fairly uniform decrease in the element stress errors is noted as the number of elements is increased, there is a notable boundary insensitivity. The lowest errors are predicted to be at the boundaries, when in fact, the highest true errors occur there (see Figures 2 through 5).

The $\Delta\sigma$ norm, Equation (8), normalized by the maximum stress in the body is shown in Figure 16. This error estimate exhibits trends that are similar to the stress error norm.

Turning now to the problem with a linearly varying load (n = 1), Figures 17 to 20 show very similar convergence characteristics to those of n = 0 for all four error estimators. All of the error estimators detect that the finite element solution at the fixed boundary is relatively good; but again, the element stress error and $\Delta\sigma$ norms are insensitive to the error at the free end of the bar. The element force residuals and equilibrium residuals are sensitive to the free end error, however.

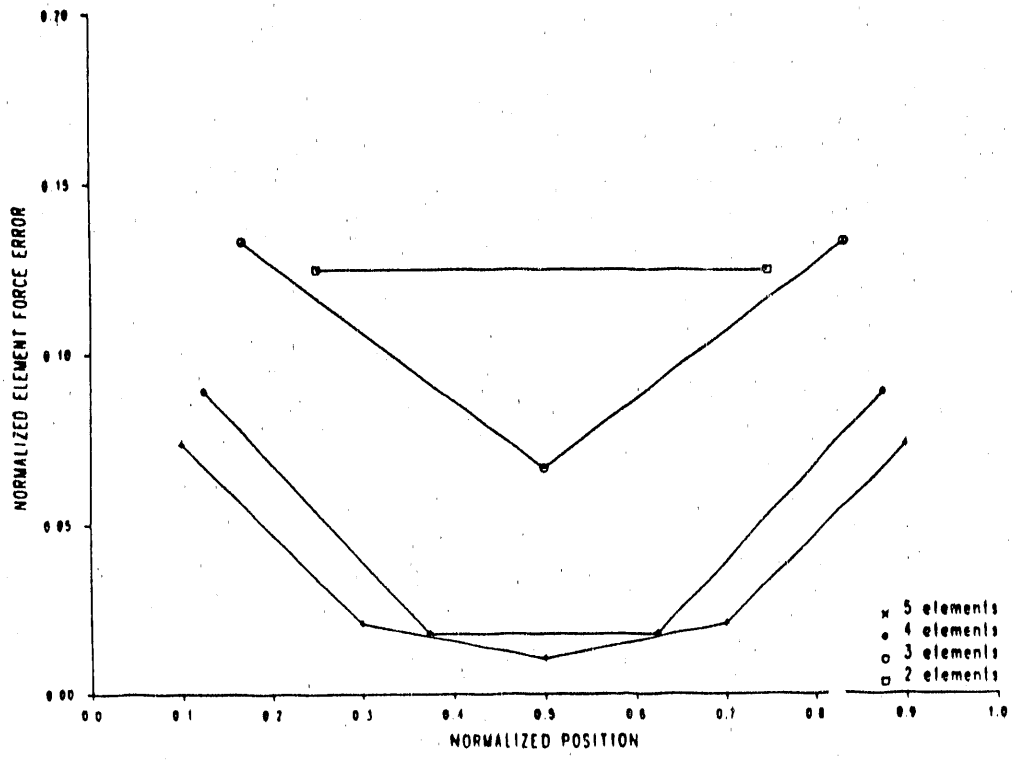

Figure 13. Element Force Error for n = 0 (uniform loading)

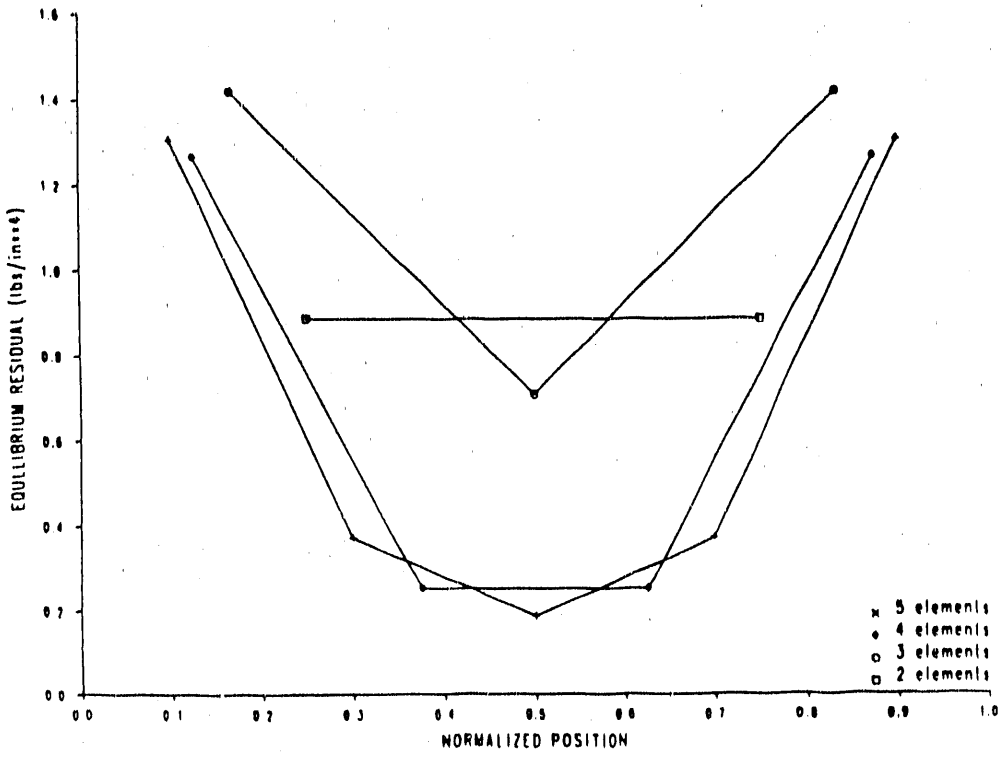

Figure 14. Element Equilibrium Error for n = 0 (uniform loading)

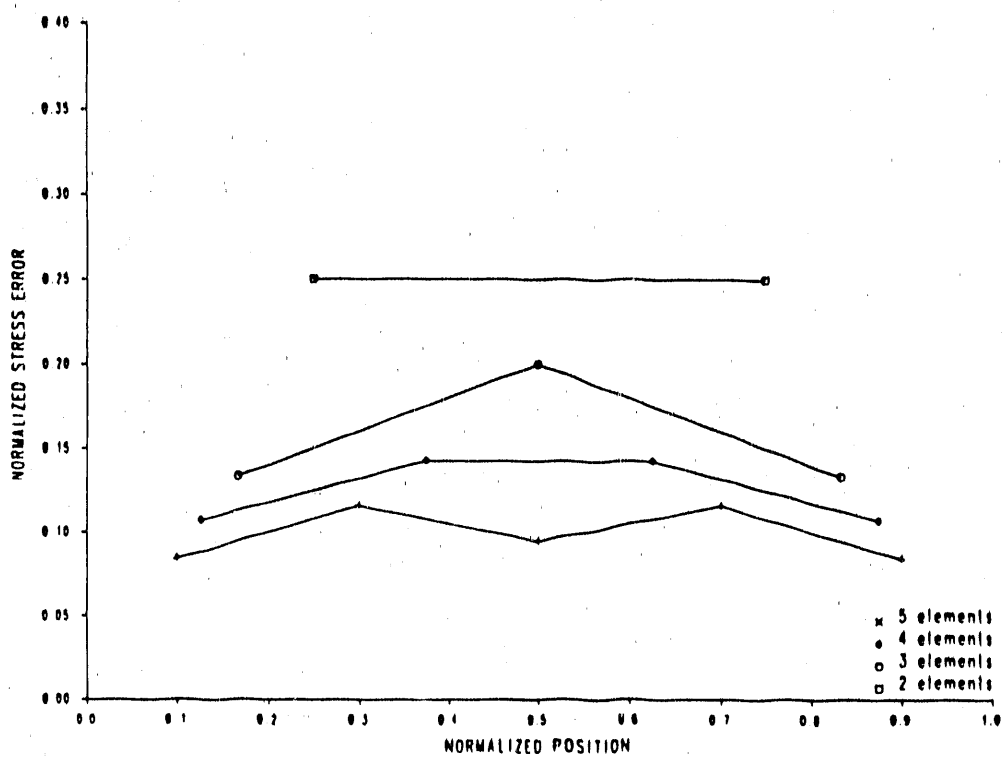

Figure 15. Stress Error Norm for n = 0 (uniform loading)

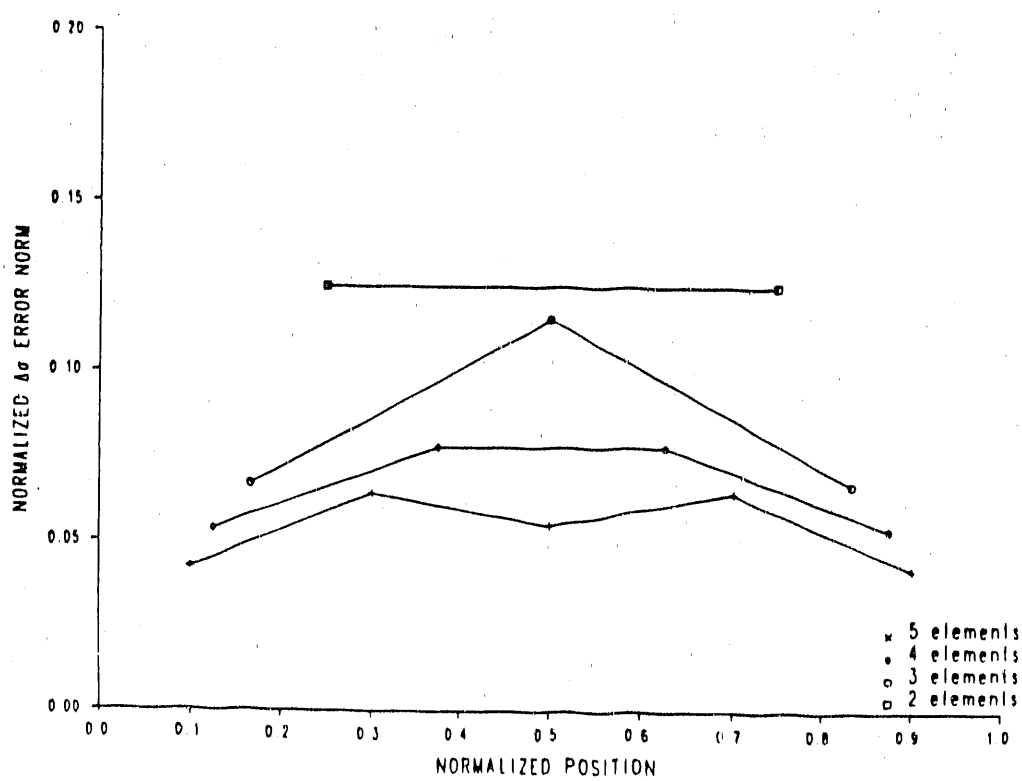

Figure 16. Del Sigma Norm for n = 0 (uniform loading)

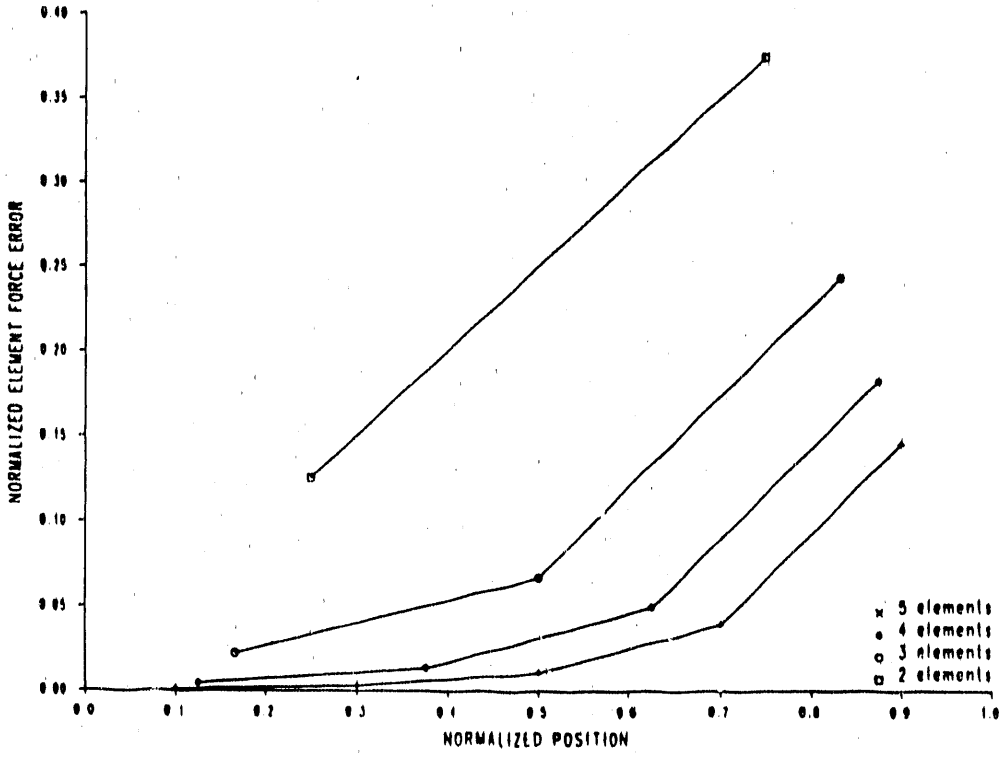

Figure 17. Element Force Error for n = 1 (linearly varying loading)

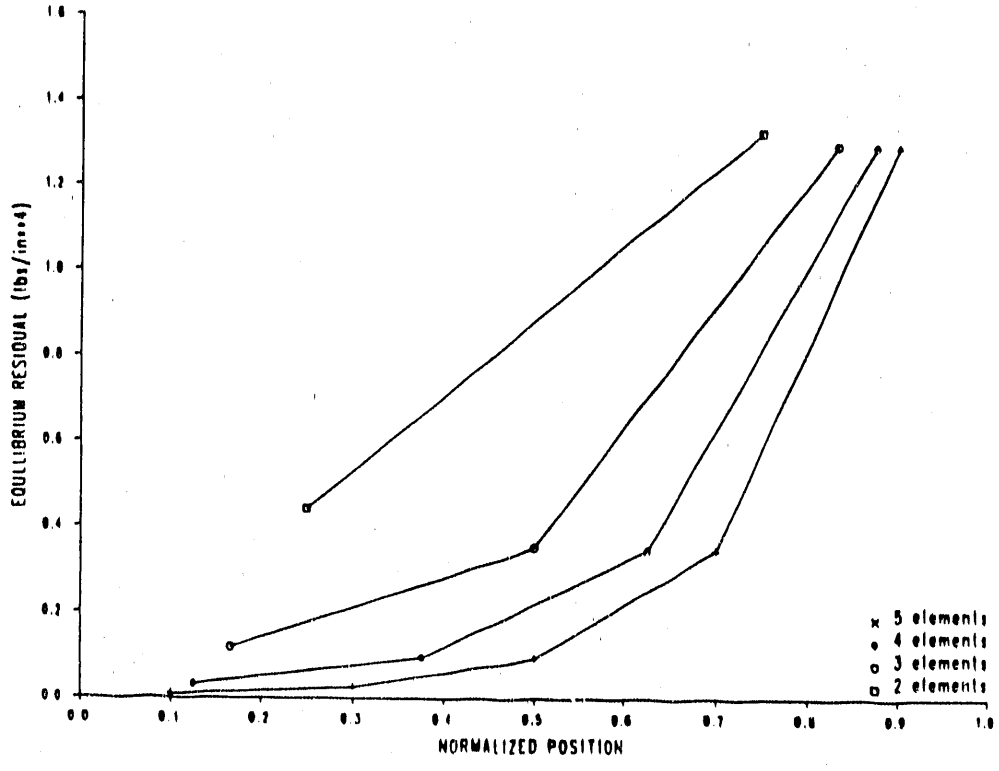

Figure 18. Element Equilibrium Error for n = 1 (linearly varying loading)

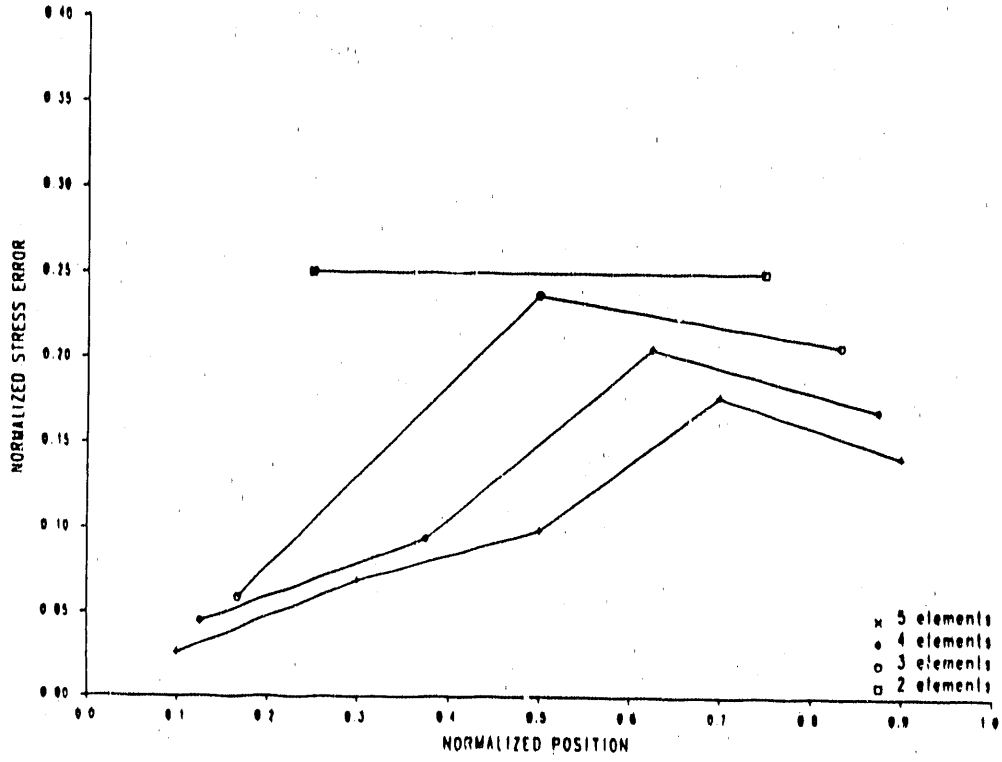

Figure 19. Stress Error Norm for n = 1 (linearly varying loading)

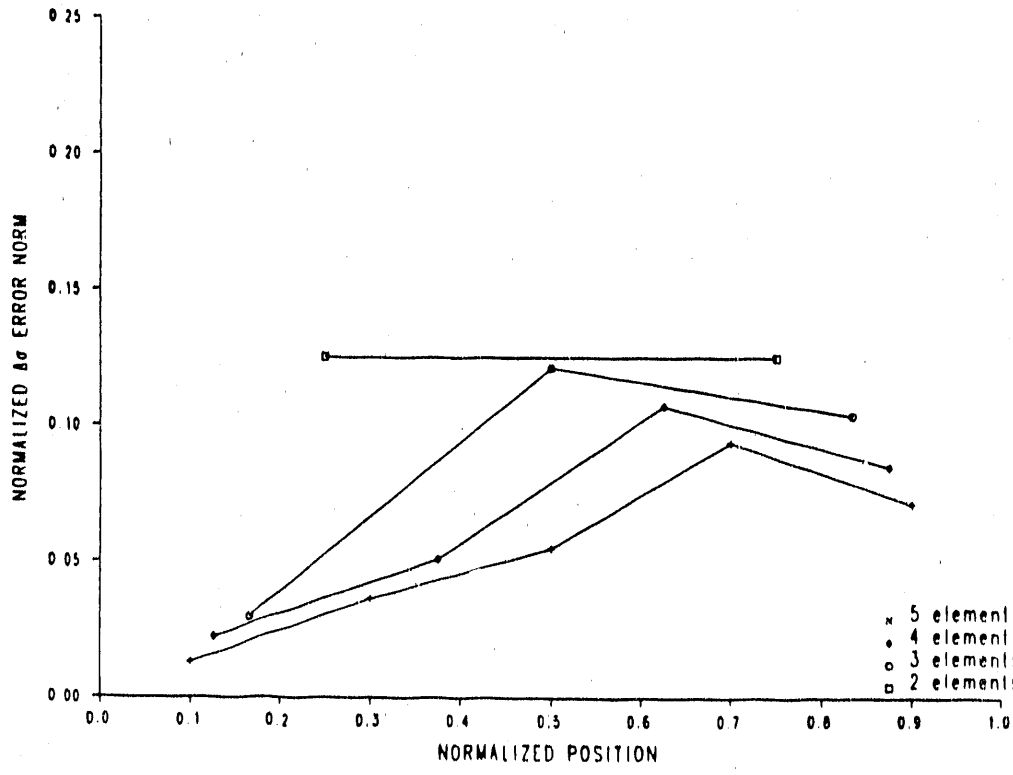

Figure 20. Del Sigma Norm for n = 1 (linearly varying loading)

4.2 TWO-DIMENSIONAL

A number of two-dimensional plane stress elasticity calculations were performed to examine the proposed error estimators. These problems consisted of a plate with a hole, a simply supported beam, and a short cantilever beam. As with the one-dimensional problems, a series of meshes for each problem was used to study behavior of the error estimators. The performance of only three of the four originally proposed error estimators will be presented. These included the stress error norm, the element force residual, and the $\Delta\sigma$ norm. The residual of the equilibrium equations yield such poor results for all cases that it was not included.

4.2.1 A Plate with a Hole

The problem of a uniformly loaded plate with a hole was analyzed using four different meshes having 90, 238, 478, and 798 degrees of freedom, Figures 21 through 24. The L_2 norm of the true errors in the projected stresses (based on the solution of a hole in an infinite plate) are shown in Figures 25 through 28. This error norm shows that the location of highest error varies with the mesh, but converges to a point on the hole boundary at about a 45 degree angle. There is a monotonic decrease of the maximum error in that norm as the mesh is refined. The true $\Delta\sigma$ error is shown in Figures 29 through 32. The location of the maximum error also moves as the mesh is refined, but settles down at approximately the same location as the L_2 norm of the stress errors. A monotonic decrease in the maximum value of this norm is also observed.

The reason the location of maximum error, as measured by these norms, is at the particular location indicated is because the shear stress error dominates the total error at approximately 45 degrees up the hole boundary. Figure 33 shows the individual stress error components around the hole boundary for Mesh 4. Figure 34 shows the associated L_2 norm of the stress error on the hole boundary.

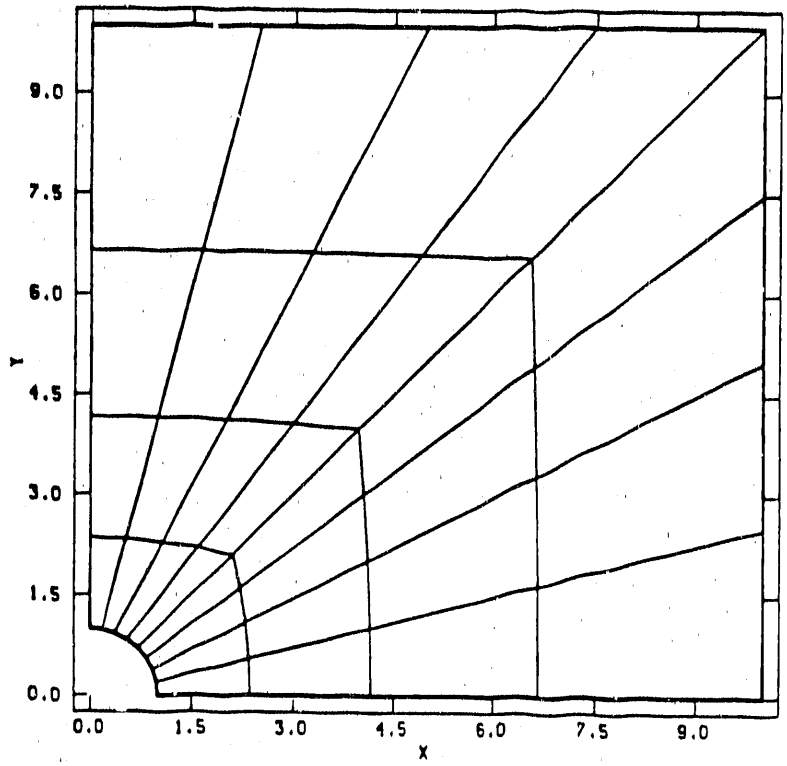

Figure 21. Mesh 1 for the Hole Problem

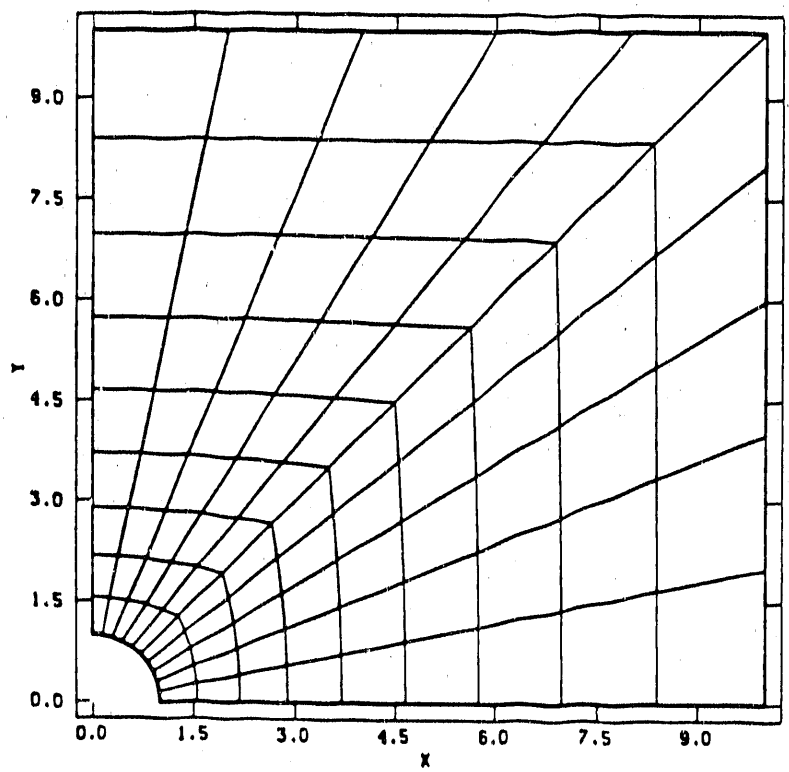

Figure 22. Mesh 2 for the Hole Problem

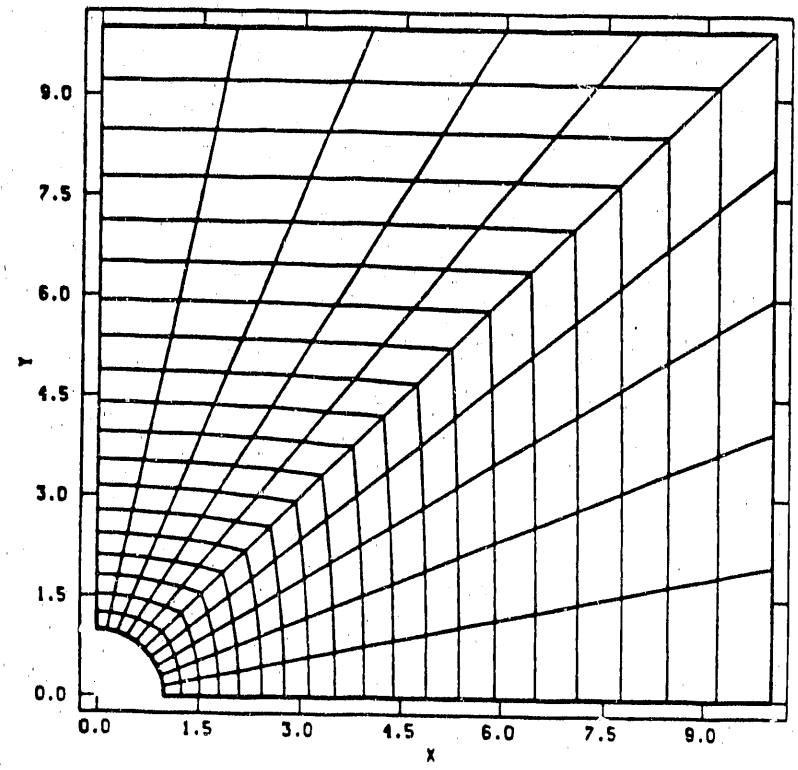

Figure 23. Mesh 3 for the Hole Problem

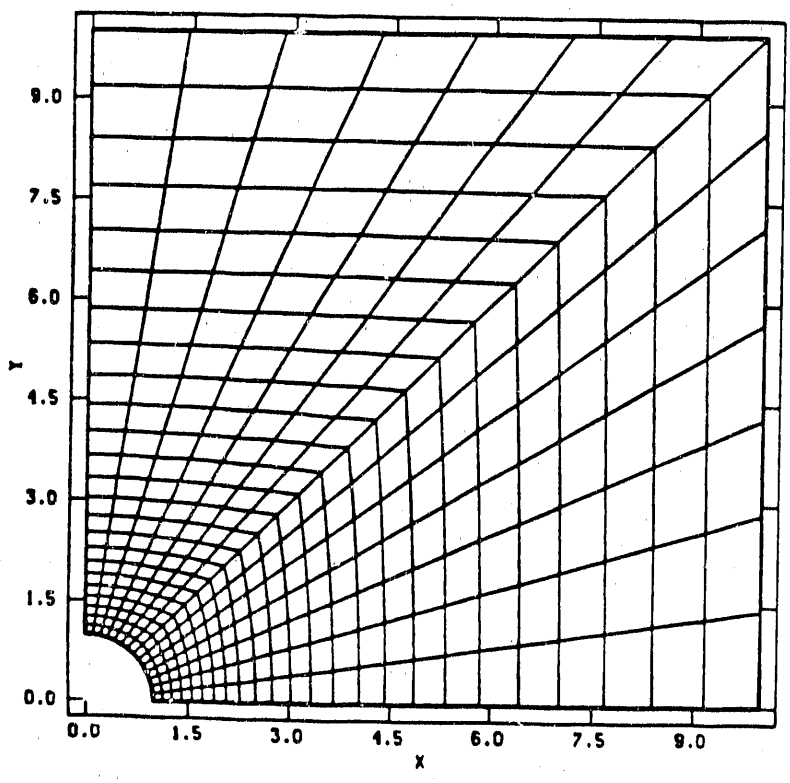

Figure 24. Mesh 4 for the Hole Problem

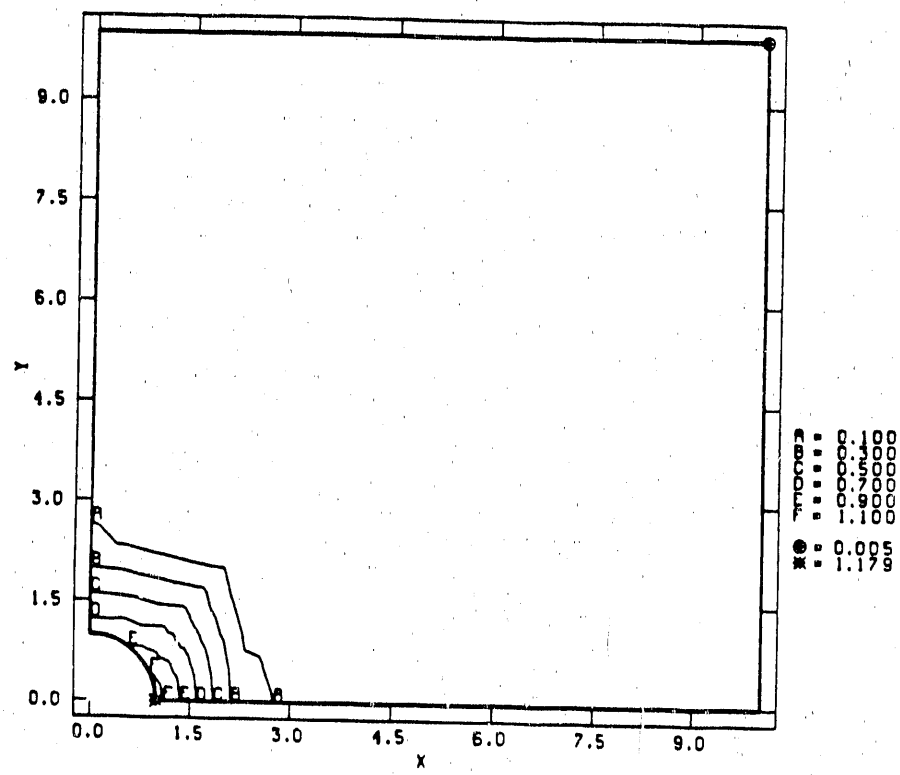

Figure 25. L_2 Norm of True Stress Error, Mesh 1

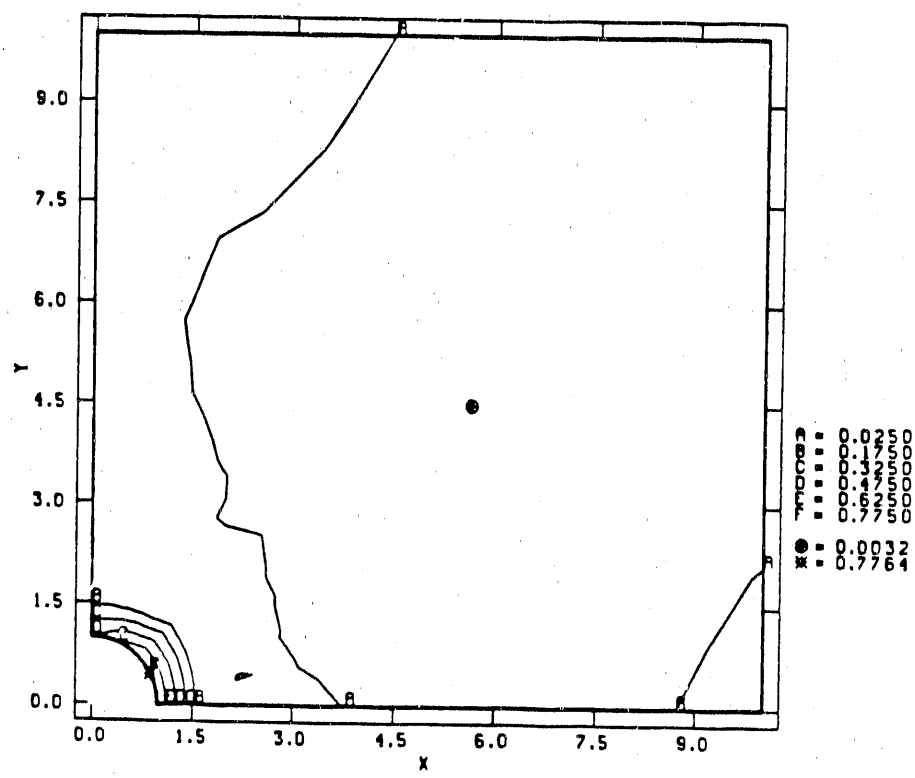

Figure 26. L_2 Norm of True Stress Error, Mesh 2

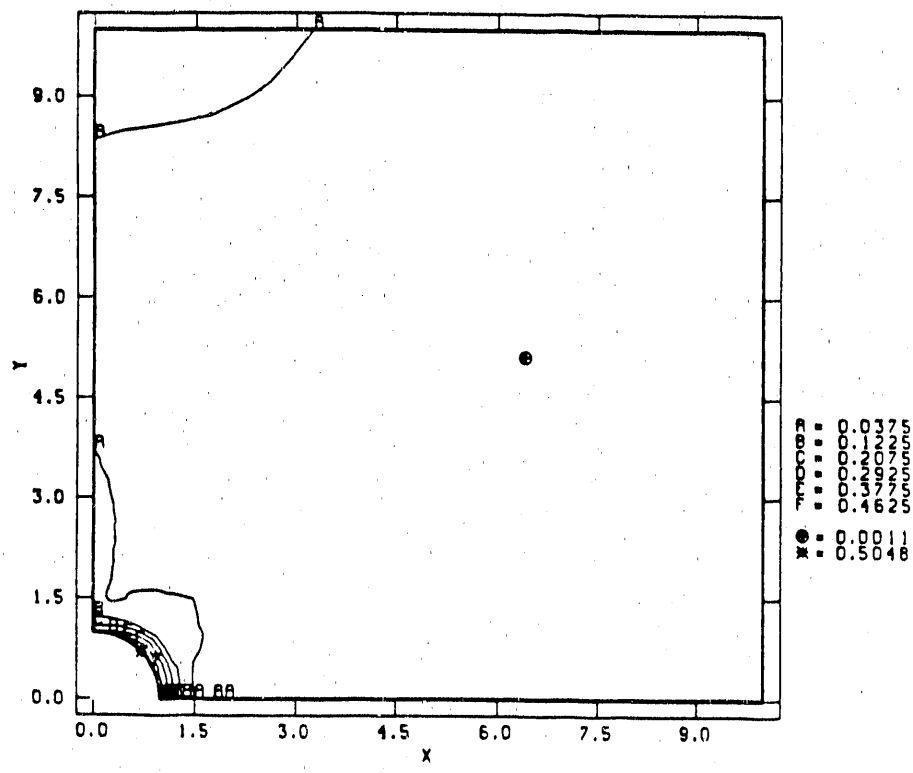

Figure 27. L_2 Norm of True Stress Error, Mesh 3

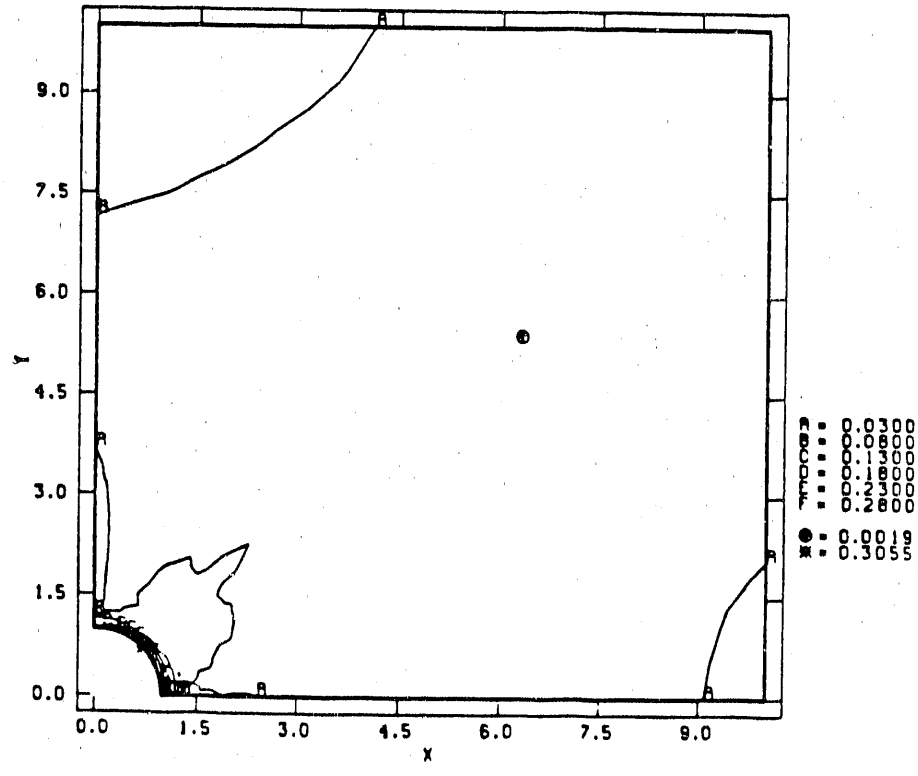

Figure 28. L_2 Norm of True Stress Error, Mesh 4

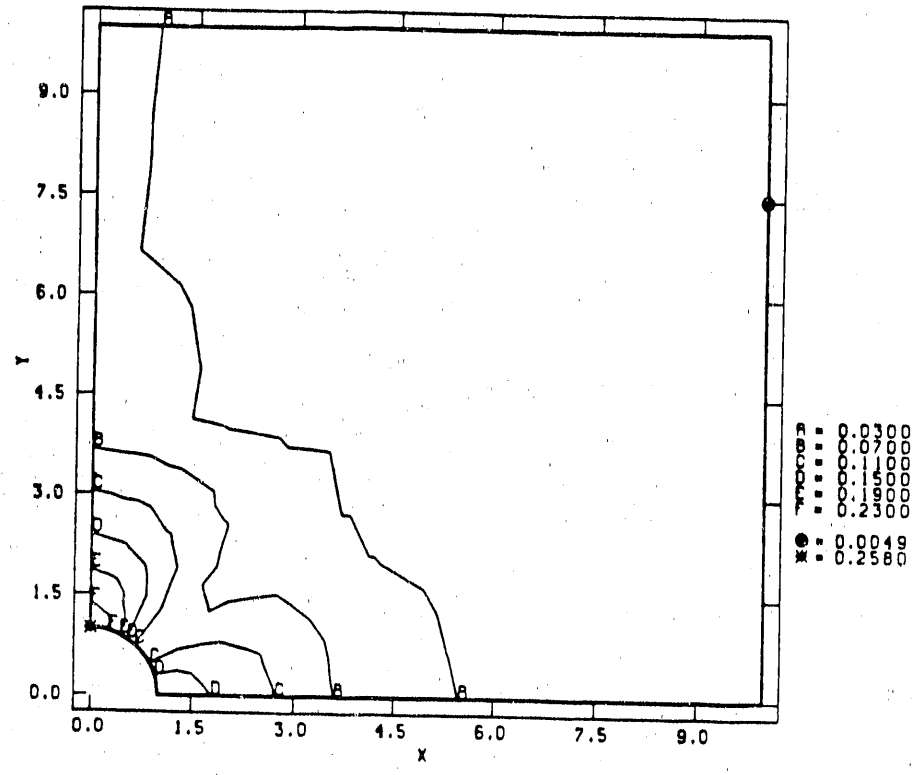

Figure 29. True Del Sigma Error Norm, Mesh 1

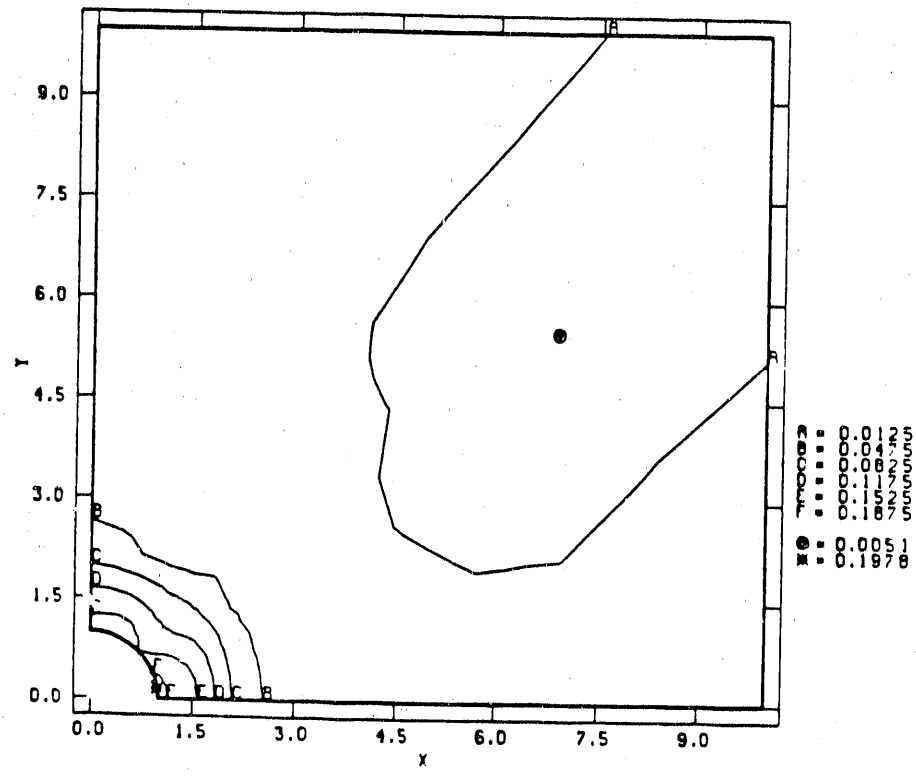

Figure 30. True Del Sigma Error Norm, Mesh 2

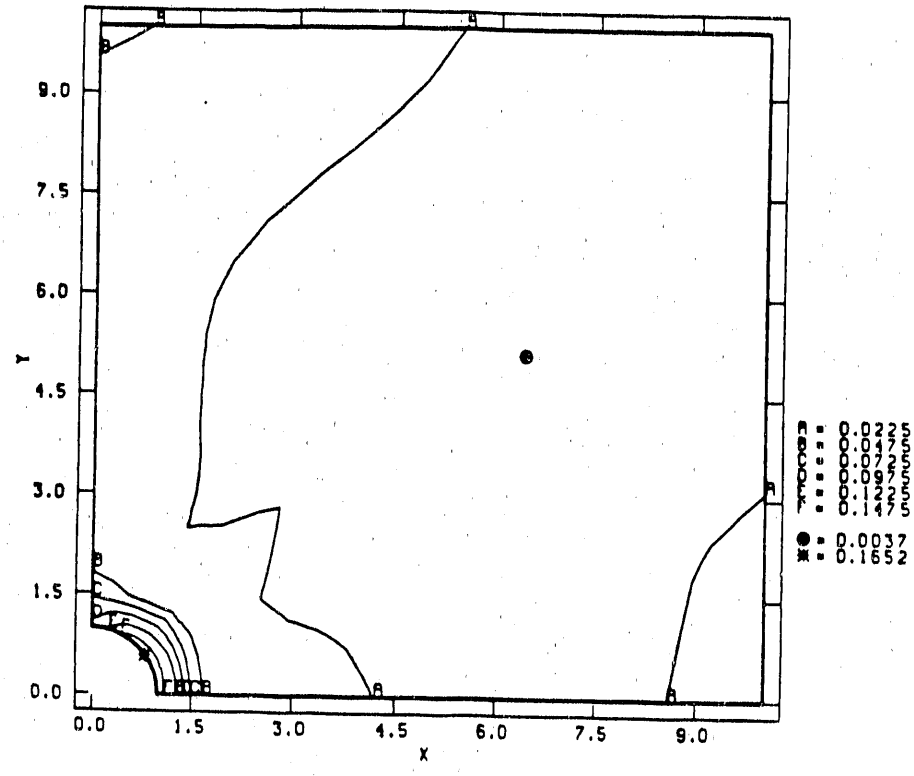

Figure 31. True Del Sigma Error Norm, Mesh 3

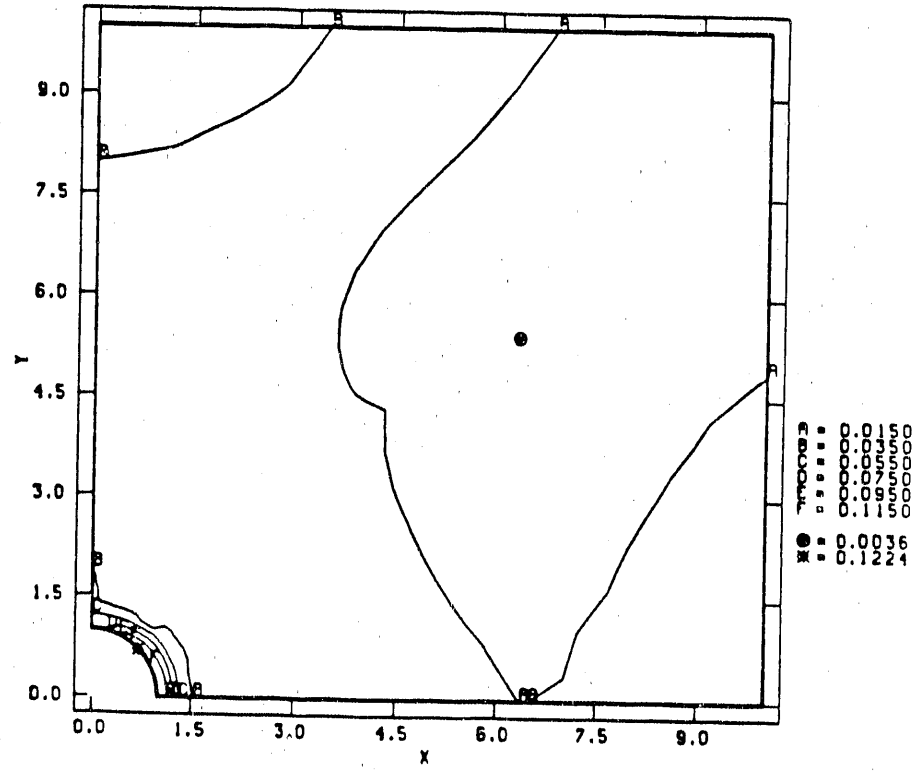

Figure 32. True Del Sigma Error Norm, Mesh 4

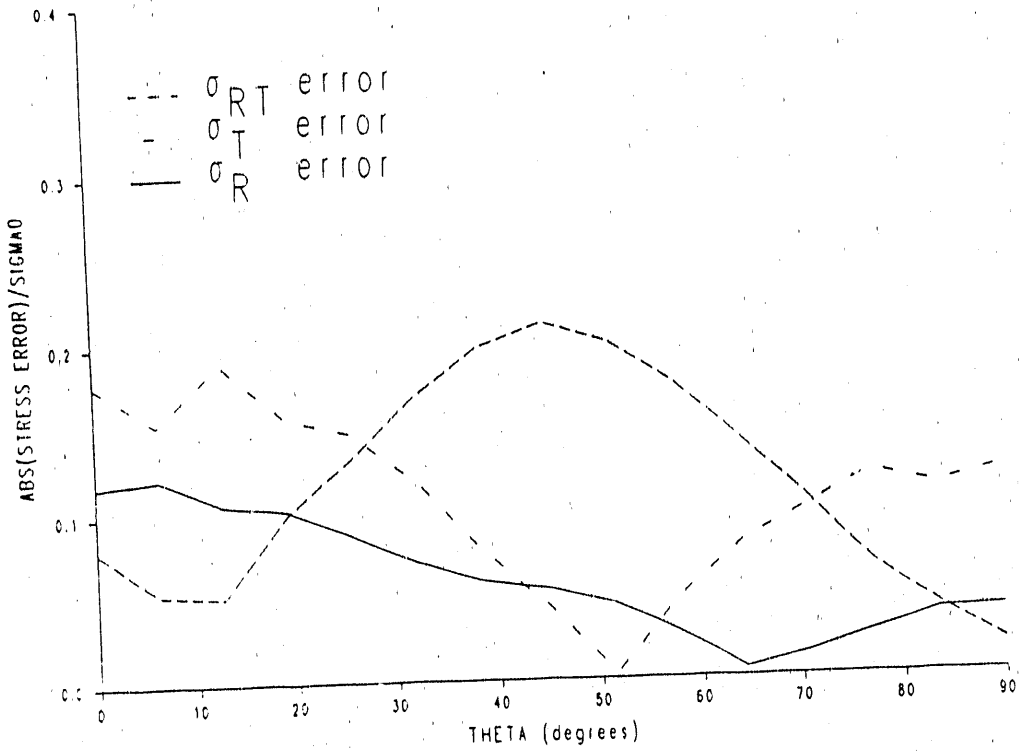

Figure 33. Individual Stress Errors Around the Hole Boundary of Mesh 4

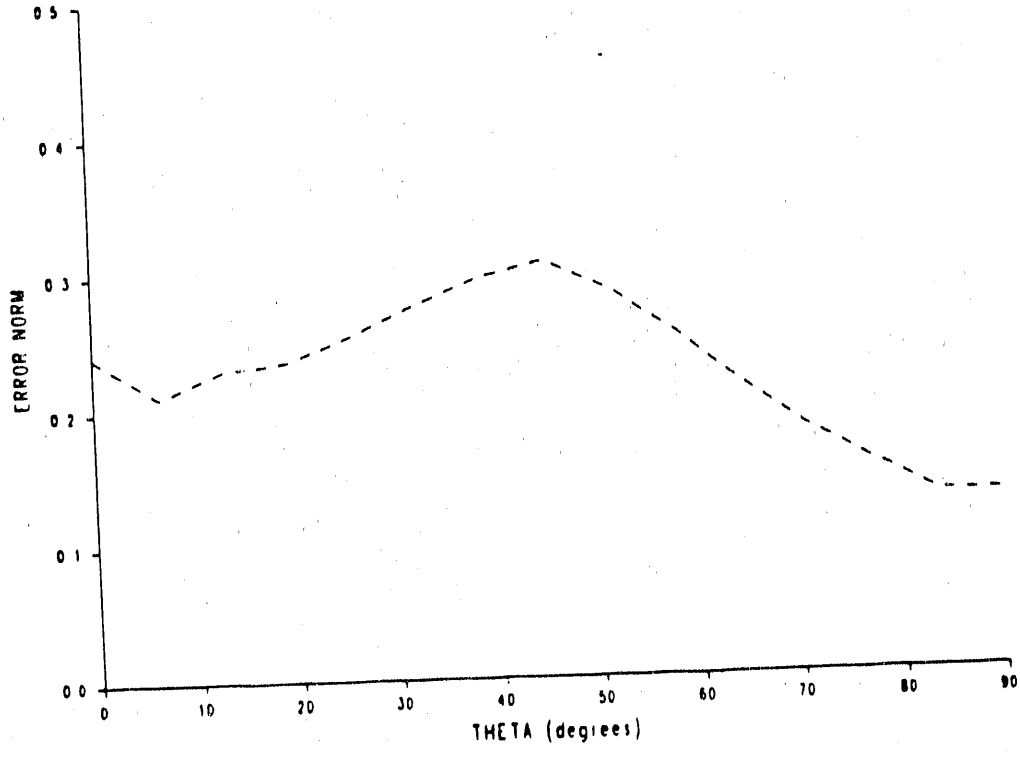

Figure 34. L_2 Norm Stress Error Around the Hole Boundary of Mesh 4

Now that we have considered the true errors, let us turn our attention to the element force equilibrium residual (normalized to the net reaction forces), Figures 35 through 38. This error measure behaves similarly to the L_2 norm of the exact stress errors and the exact $\Delta\sigma$ norms, Figures 25 to 31. The location of the maximum error is approximately the same as that for the exact error norms, and a monotonic decrease in the maximum values is observed.

The discrete version of the stress error norm, i.e., nonintegrated form of the L_2 norm of the maximum stress errors evaluated at the element nodes, is shown in Figures 39 through 42. The maximum error locations are not consistent with the exact error, Figures 25 to 28.

The $\Delta\sigma$ norm, Figures 43 to 46, also predicts maximum error locations that are inconsistent with the exact error norms.

Both the L_2 norm of the maximum stress errors and the $\Delta\sigma$ norm do not decrease monotonically as the mesh is refined. This is most likely due to the fact that these norms substitute the projected stresses for the exact stresses when calculating the error. The quality of the projected stresses is mesh dependent so the mesh must be "reasonably" fine for consistent estimates of the exact stresses to be obtained. Thus, these two norms would not be expected to decrease monotonically until the mesh has reached a certain degree of fineness.

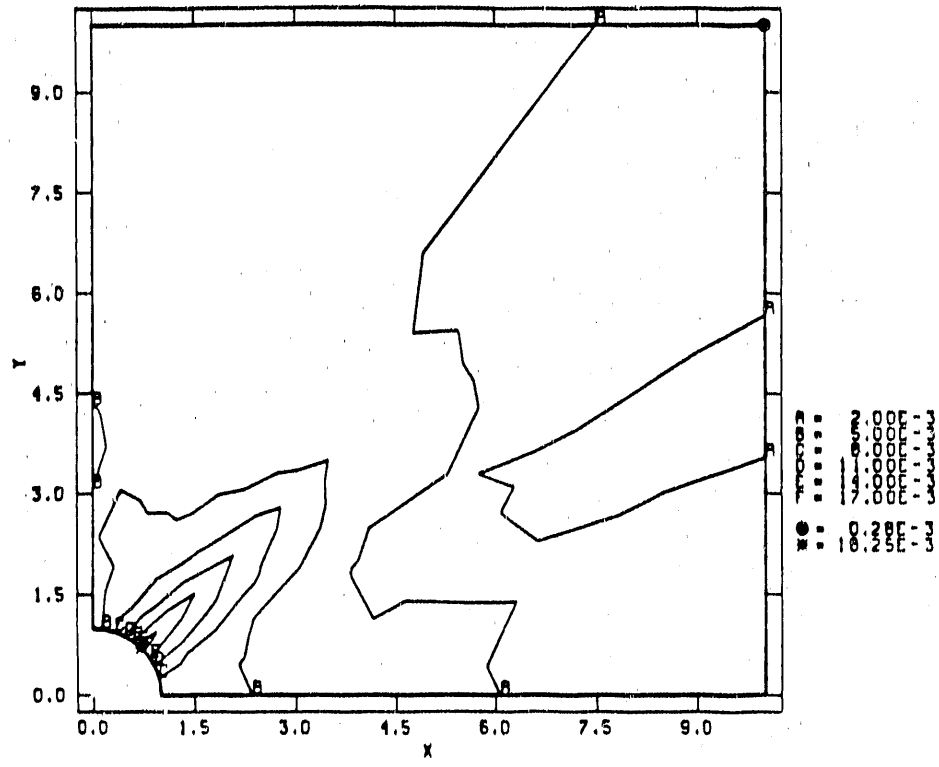

Figure 35. Element Force Error, Mesh 1

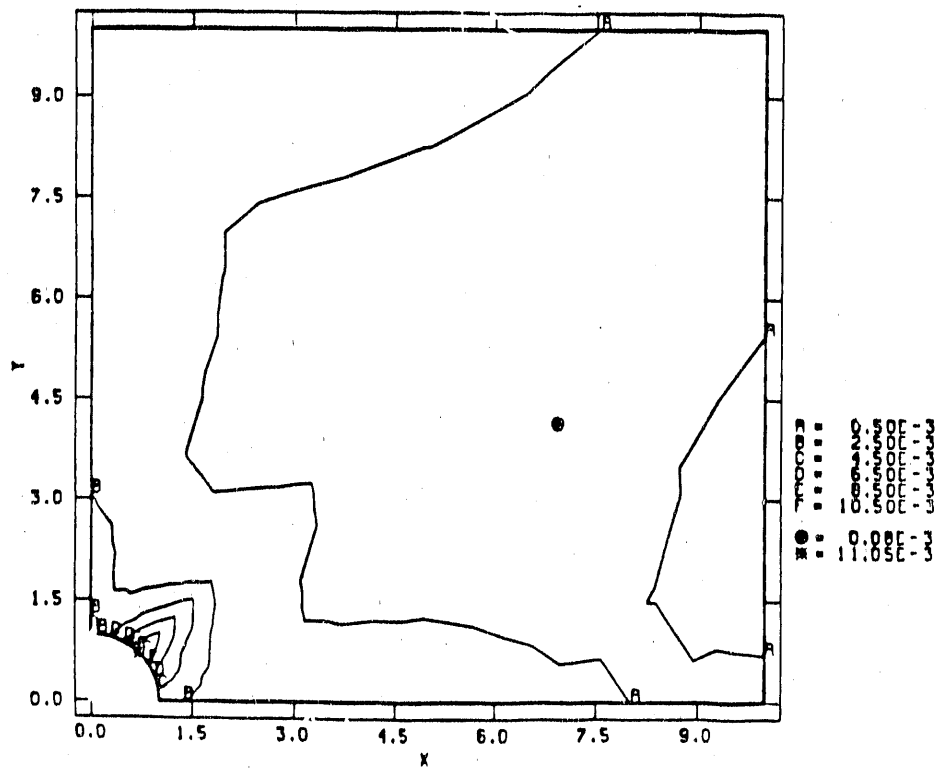

Figure 36. Element Force Error, Mesh 2

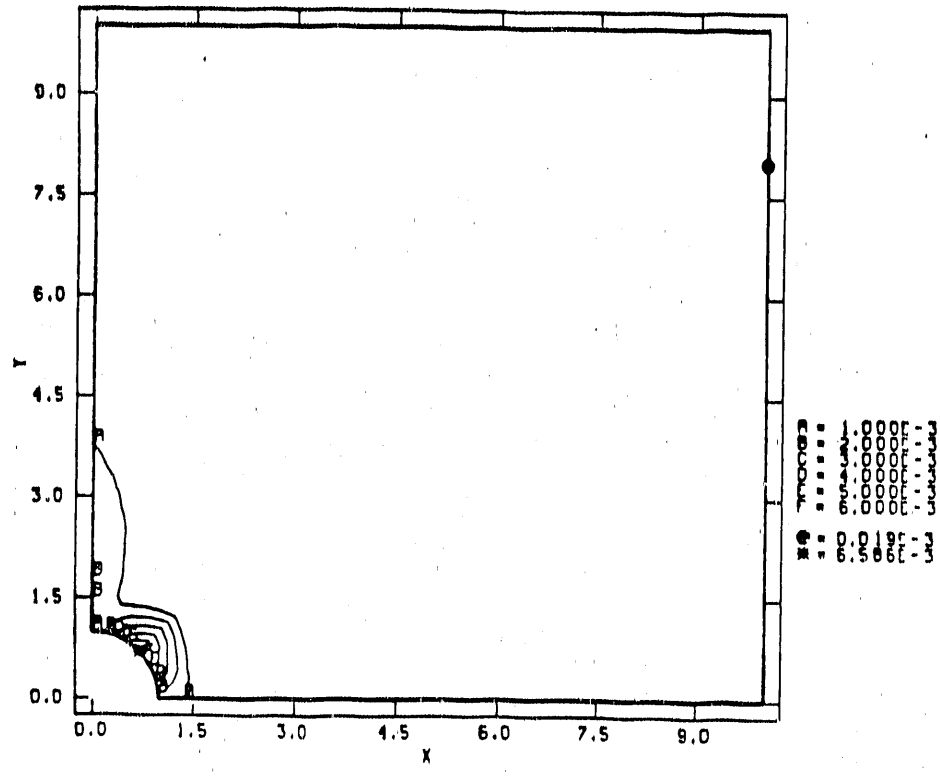

Figure 37. Element Force Error, Mesh 3

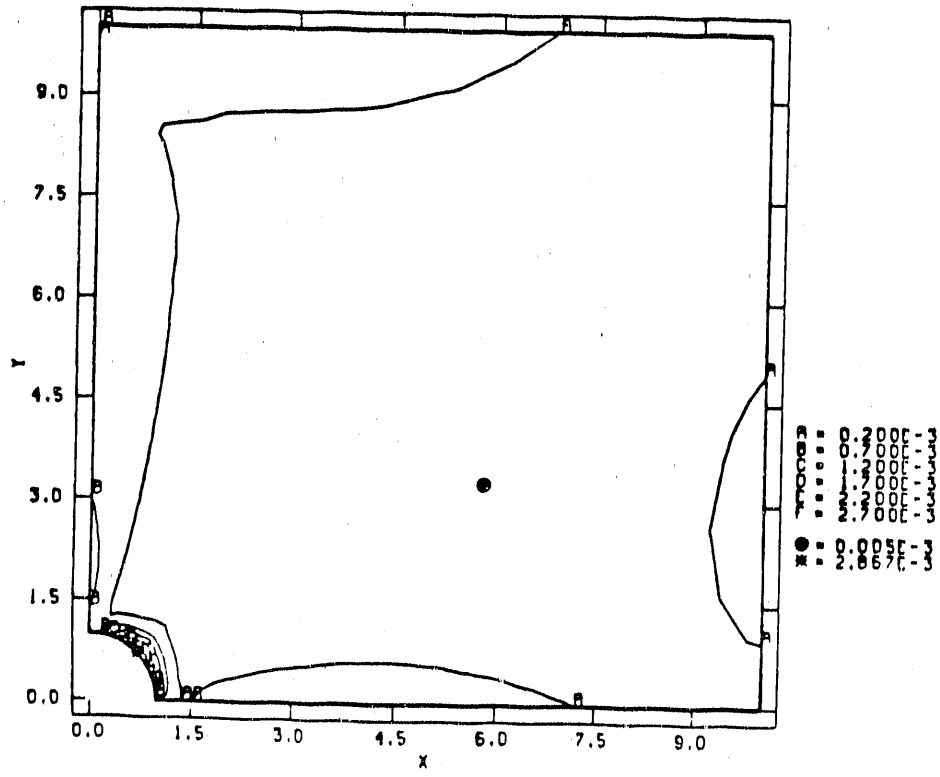

Figure 38. Element Force Error, Mesh 4

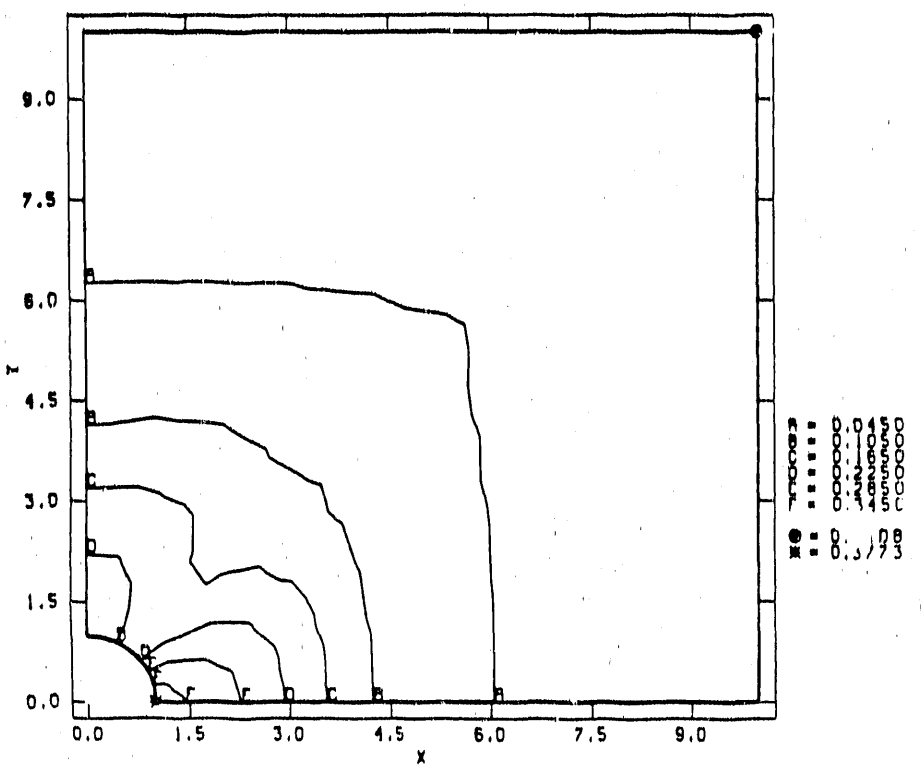

Figure 39. Stress Error Norm, Mesh 1

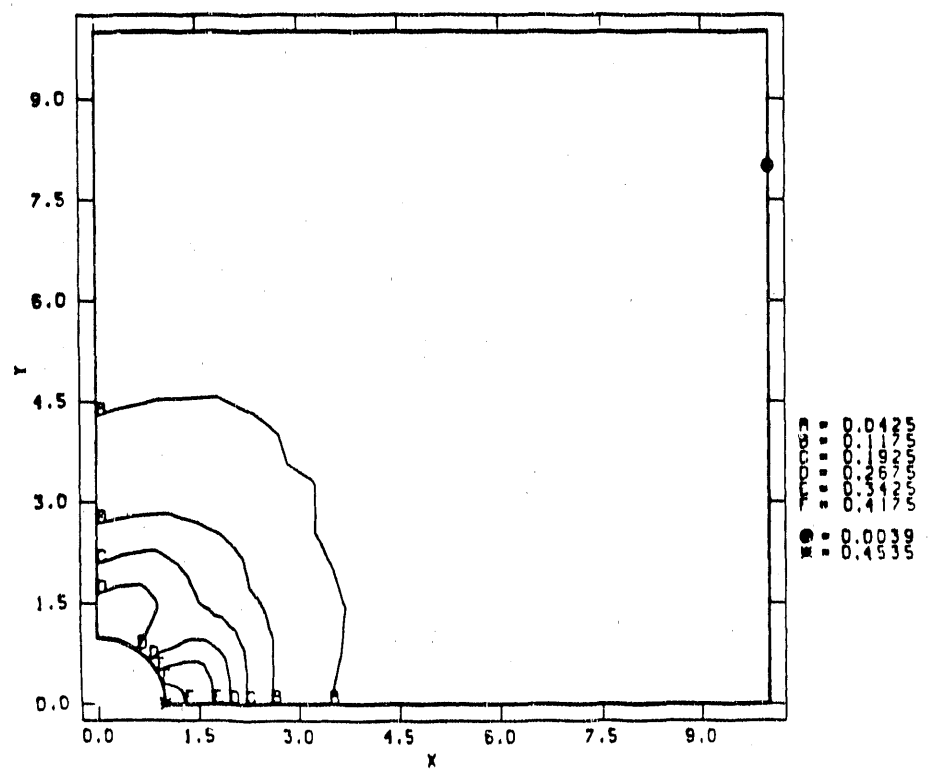

Figure 40. Stress Error Norm, Mesh 2

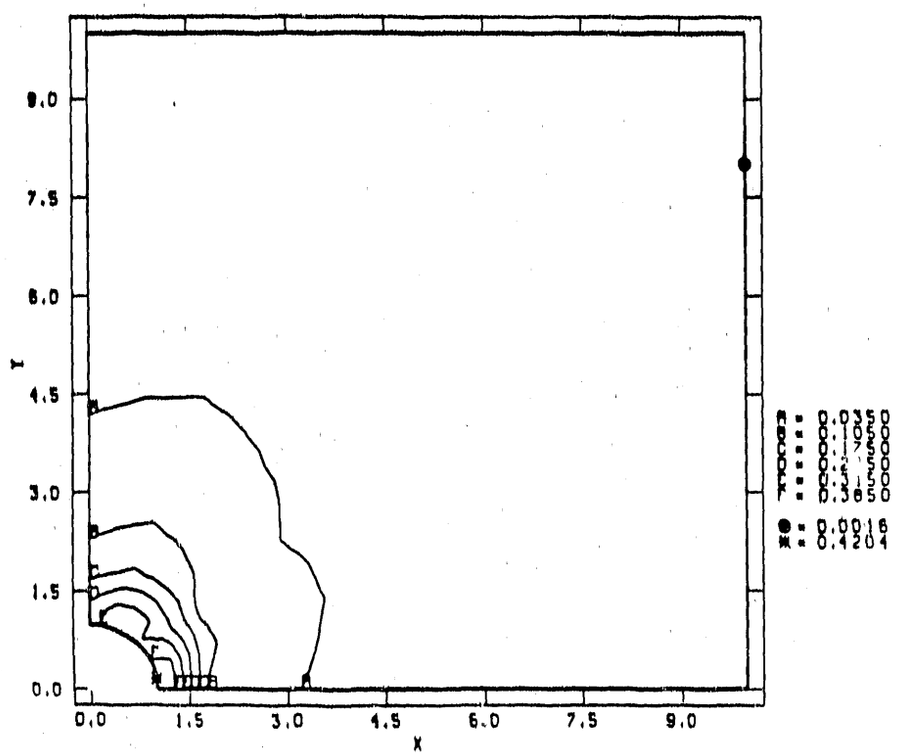

Figure 41. Stress Error Norm, Mesh 3

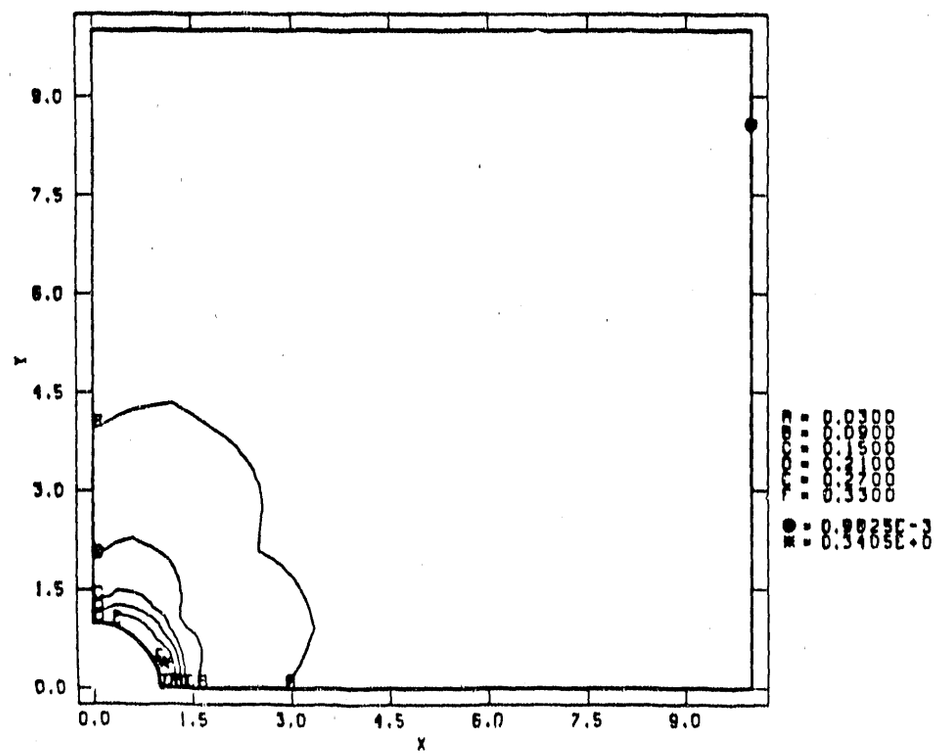

Figure 42. Stress Error Norm, Mesh 4

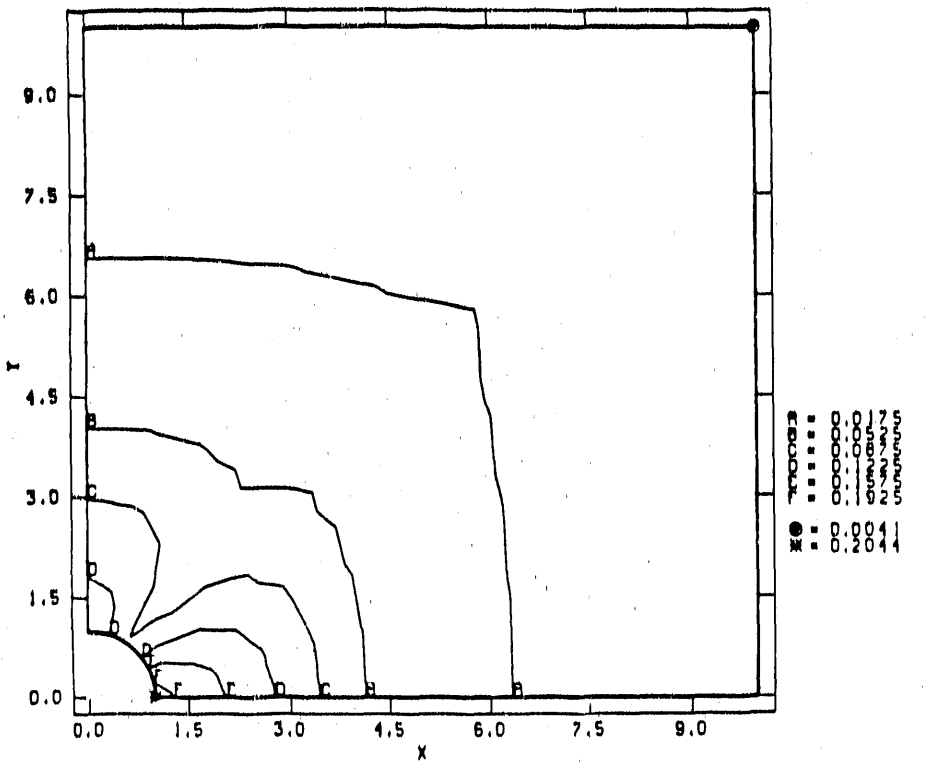

Figure 43. Del Sigma Norm, Mesh 1

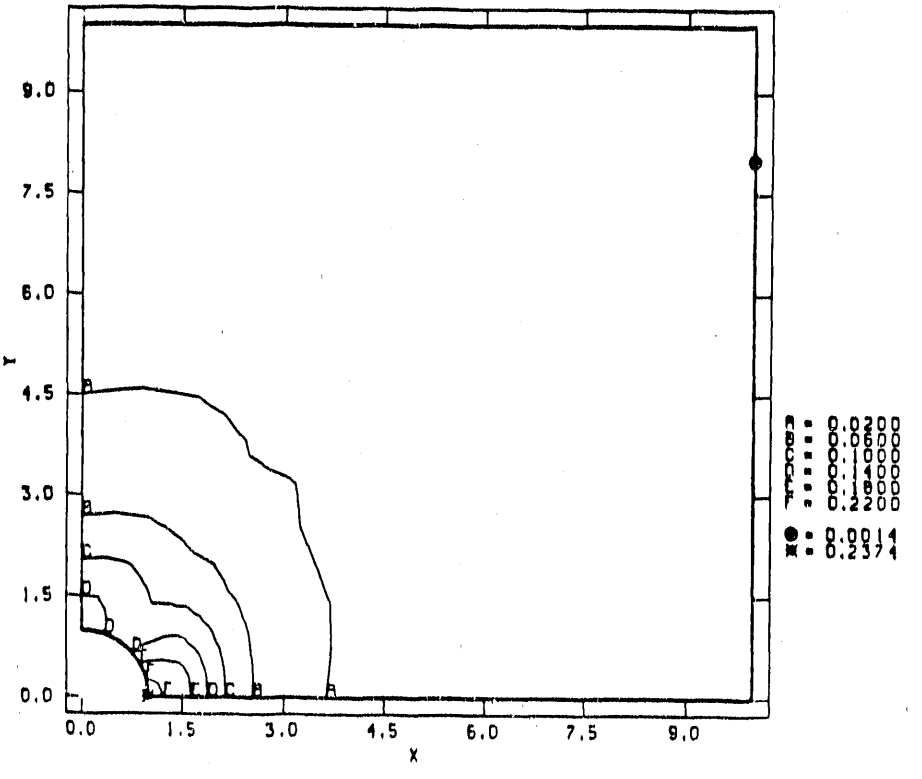

Figure 44. Del Sigma Norm, Mesh 2

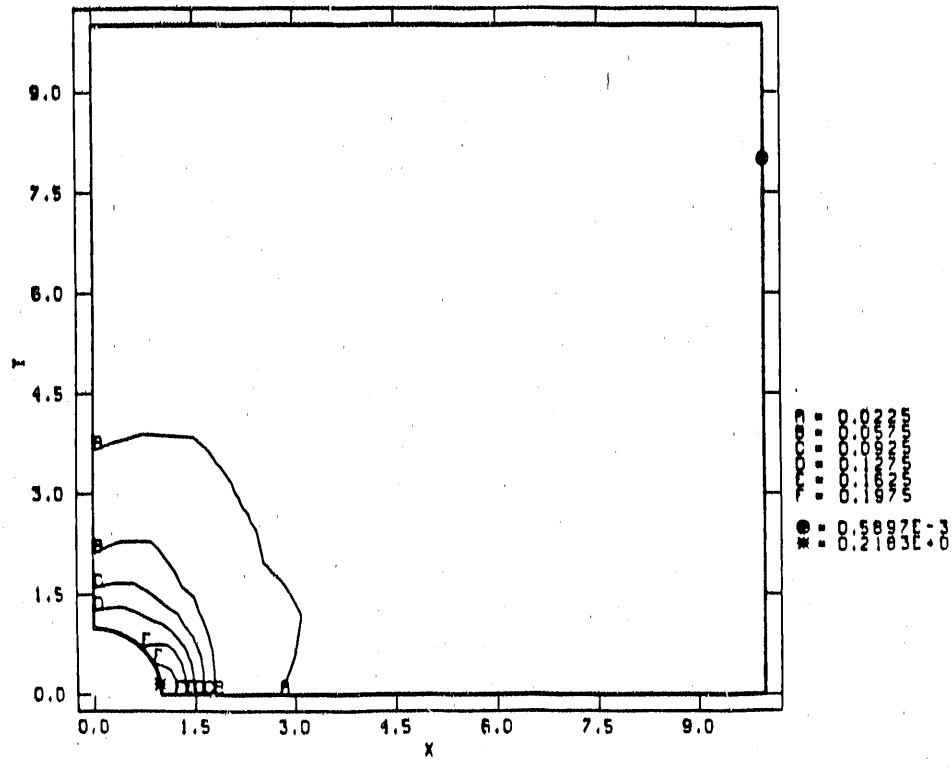

Figure 45. Del Sigma Norm, Mesh 3

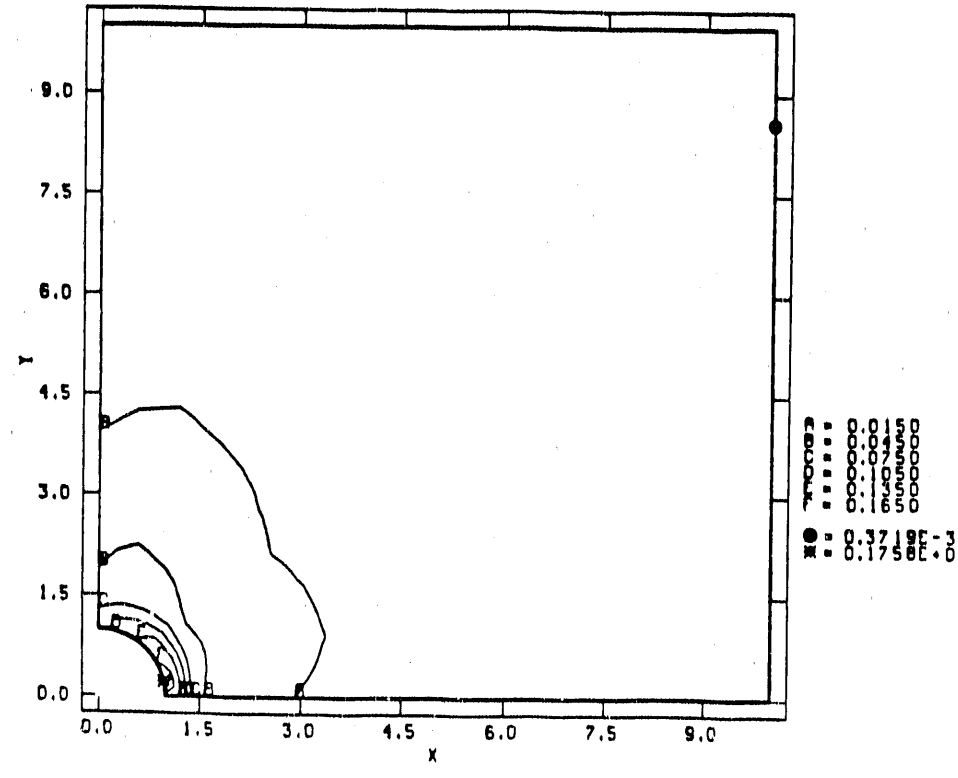

Figure 46. Del Sigma Norm, Mesh 4

4.2.2 A Uniformly Loaded Simply Supported Beam

As a second example problem, consider the case of a uniformly loaded simply supported beam, Figure 47. One-half of the beam was modeled in three finite element analyses using 18, 210, and 854 degrees of freedom, see Figures 48 through 50.

The projected stress for each mesh at the beam midspan is compared to elementary beam theory in Figure 51. Convergence to the beam theory solution is clearly shown. Also, the maximum error occurs on the boundaries as noted previously for the one-dimensional problem.

Contour plots of the element force residuals (again normalized by the net reaction forces) are shown in Figures 52 through 54. It is quite clear that the area around the support point is the location of maximum error. This is understandable since the point support (load) is a singular point. The error at the support point dominates the error in the problem. The mesh 3 contours at the center of the beam, where the highest bending stresses occur, are shown in Figure 55. If we ignore the error at the support point, the errors at the beam center are certainly sufficient to drive an adaptive scheme.

The stress error and $\Delta\sigma$ norms, Figure 56 through 61, do not appear to be particularly sensitive to the singular points, although they would be useful for the remainder of the beam.

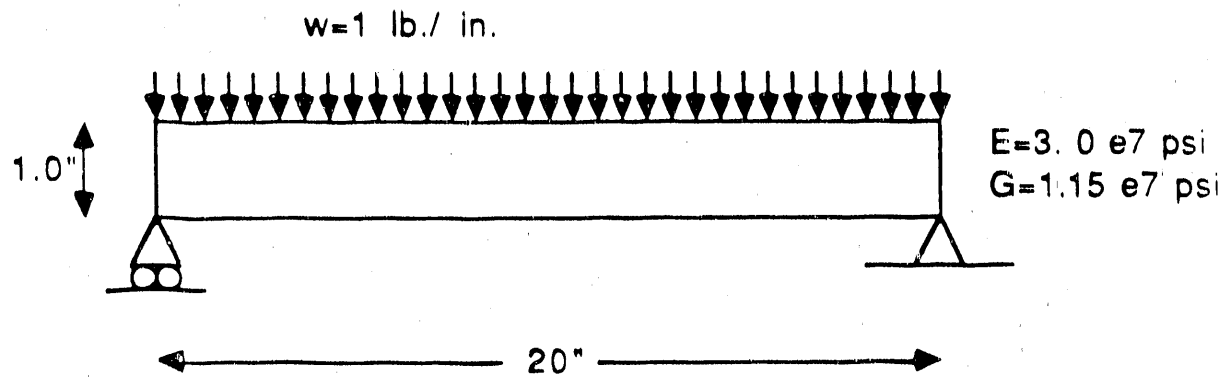

Figure 47. A Simply Supported Uniformly Loaded Beam

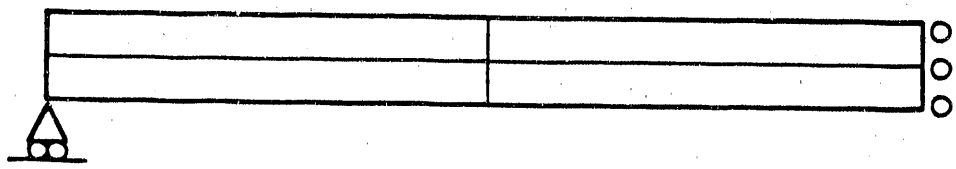

Figure 48. Mesh 1 of the Beam

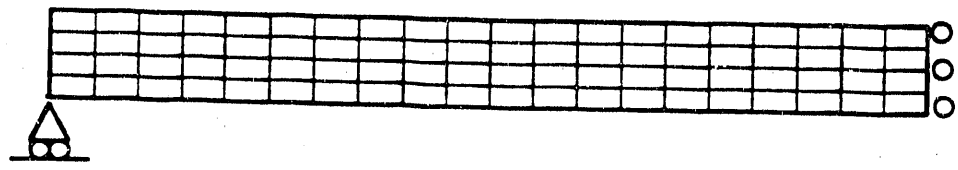

Figure 49. Mesh 2 of the Beam

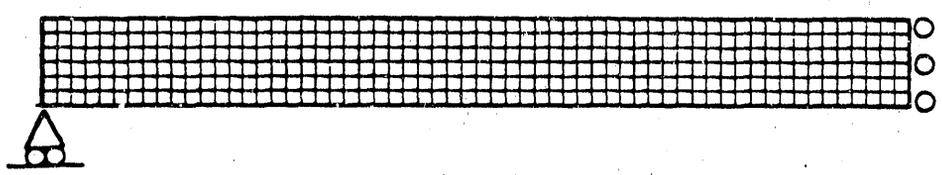

Figure 50. Mesh 3 of the Beam

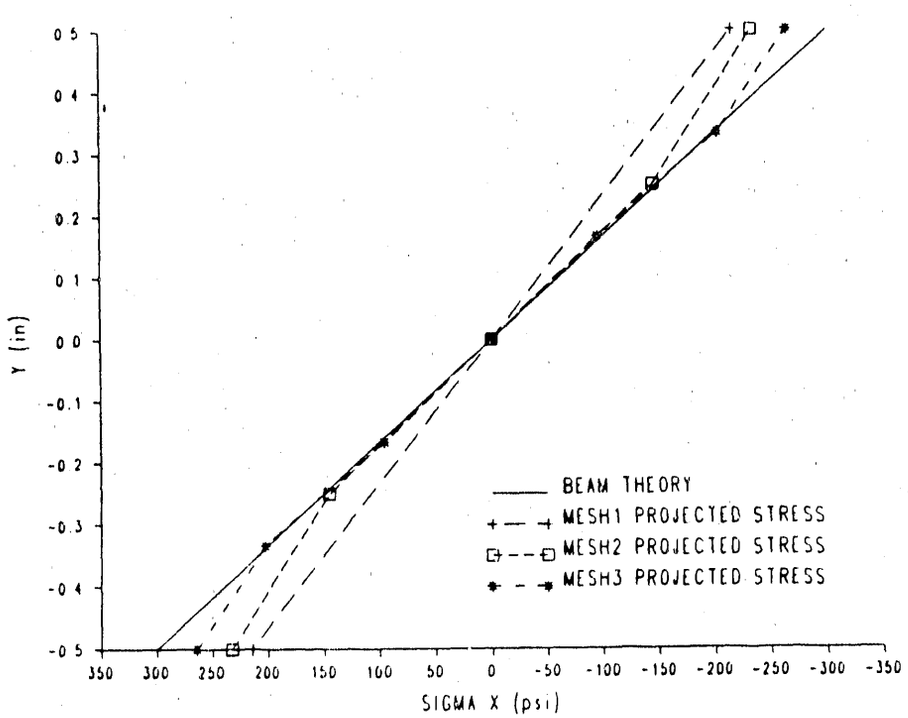

Figure 51. Comparison of Projected Bending Stresses and Beam Theory at the Midspan of the Beam

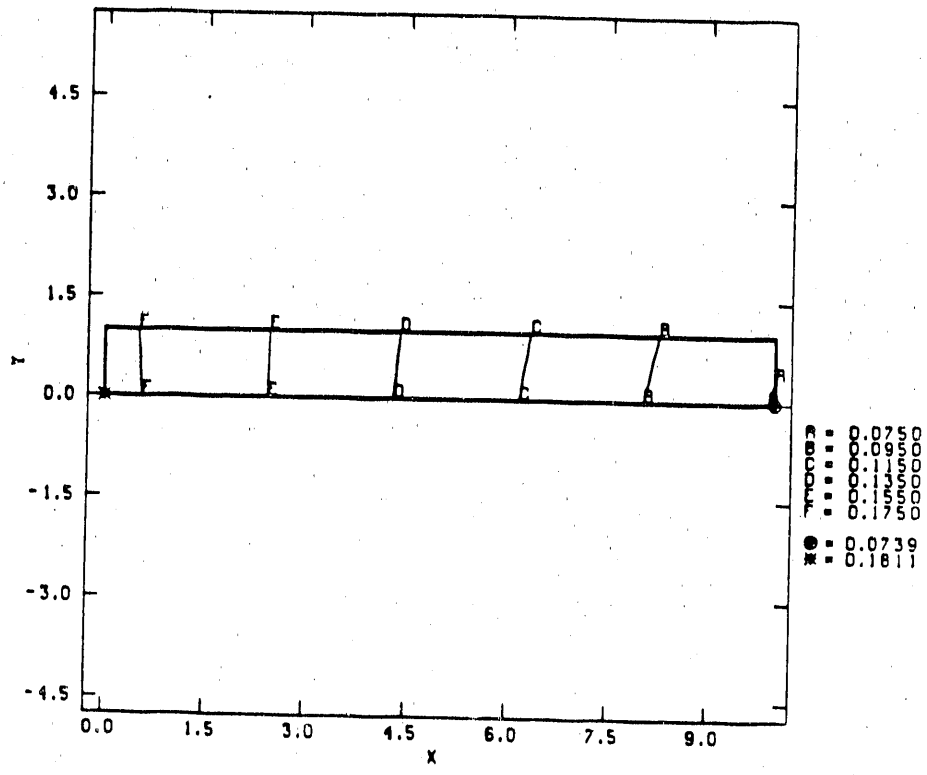

Figure 52. Element Force Residual Norm for Mesh 1

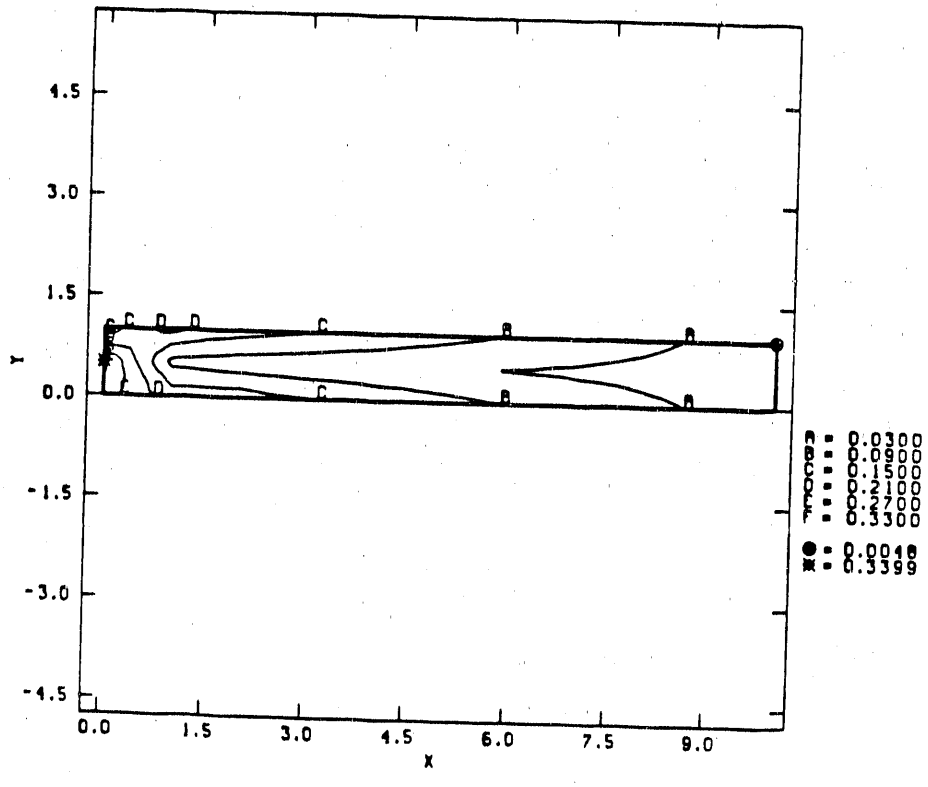

Figure 53. Element Force Residual Norm for Mesh 2

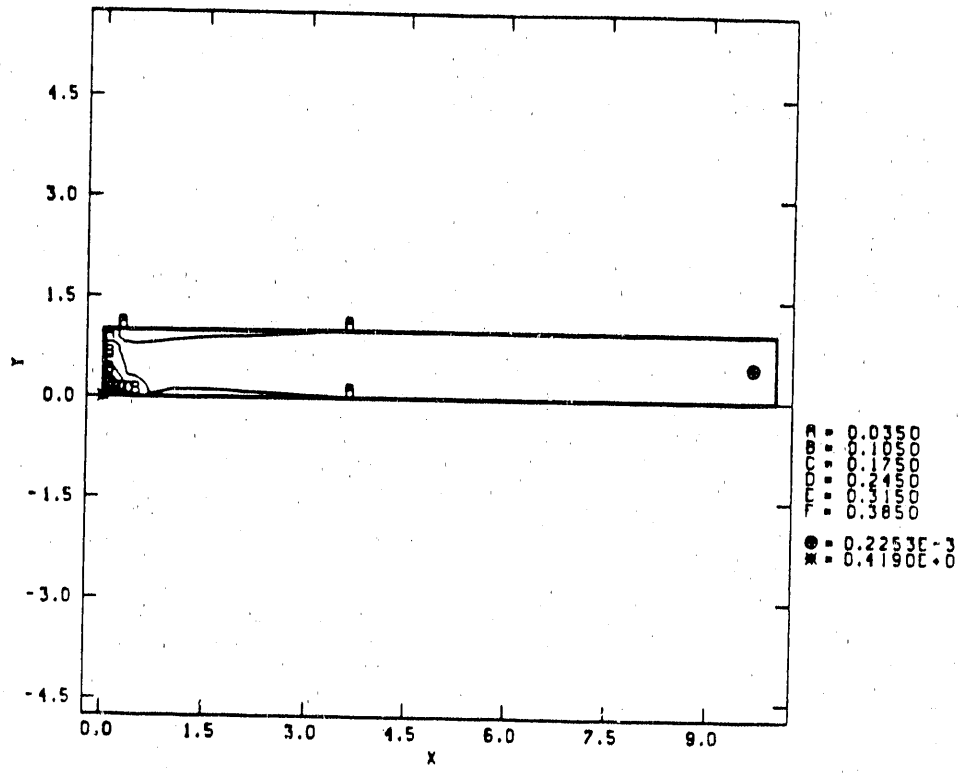

Figure 54. Element Force Residual Norm for Mesh 3

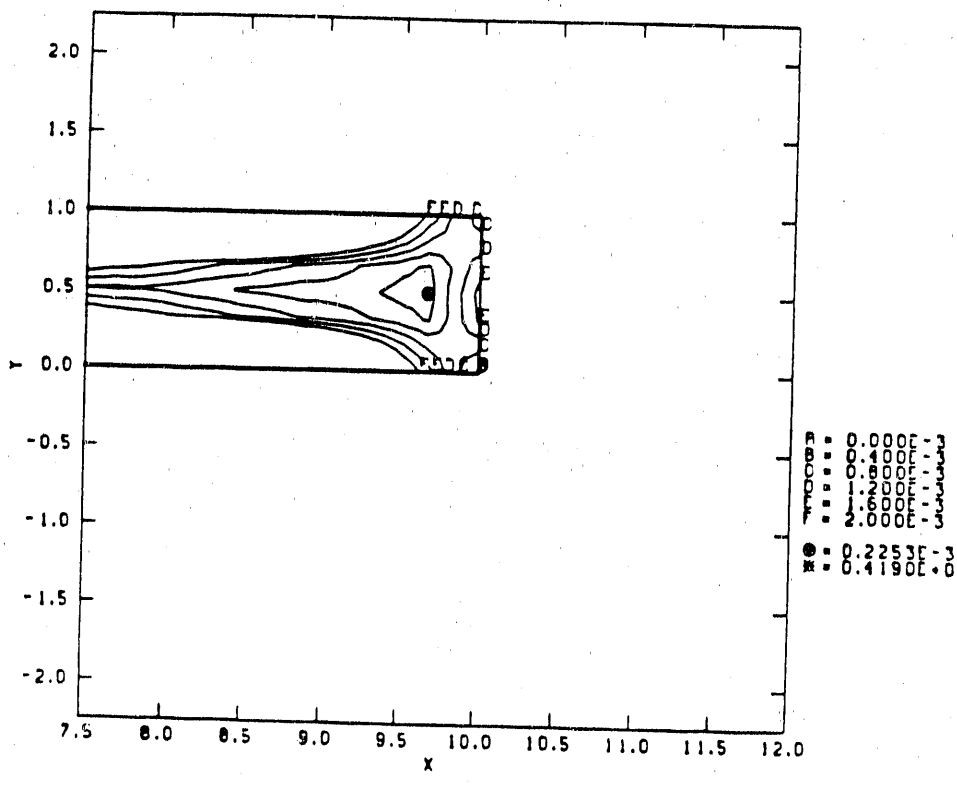

Figure 55. Element Force Residual Norm for Mesh 3 at the Midspan of the Beam

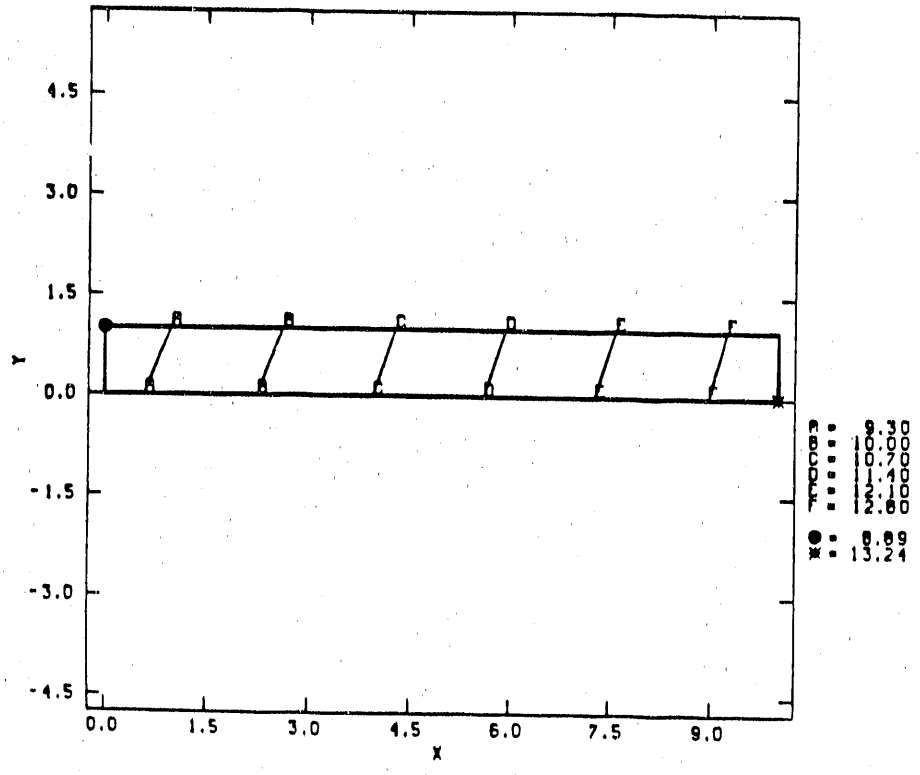

Figure 56. Stress Error Norm for Mesh 1

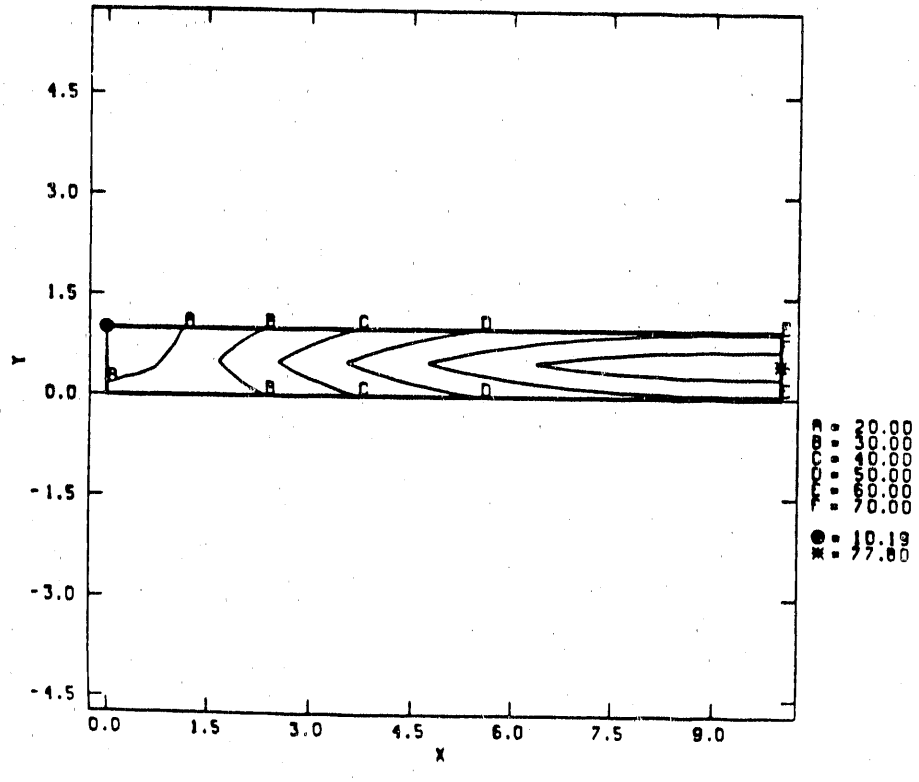

Figure 57. Stress Error Norm for Mesh 2

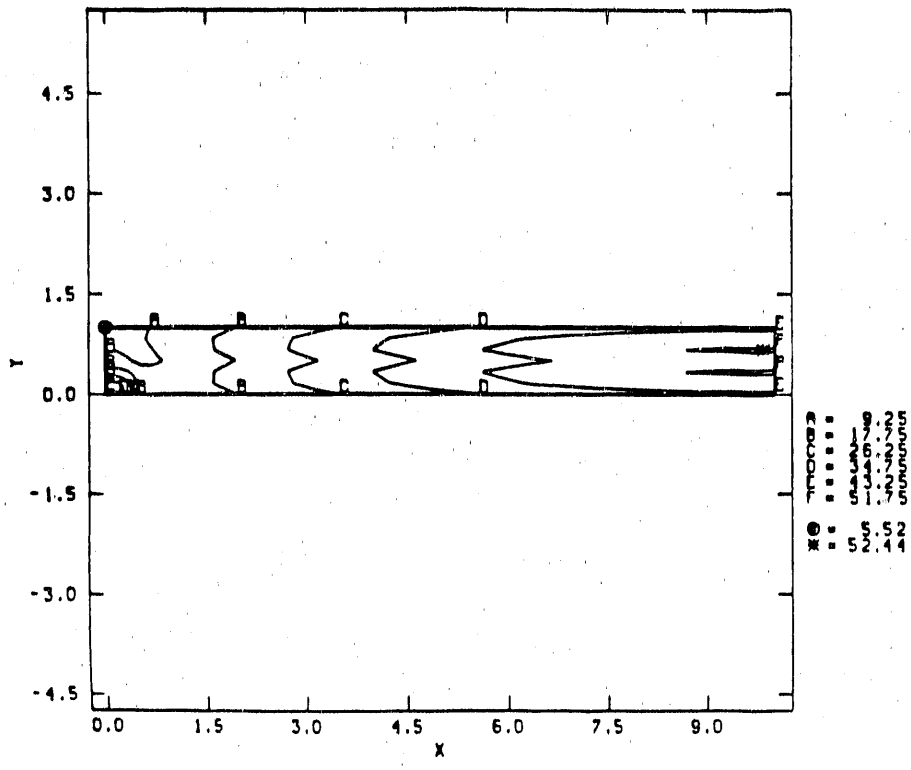

Figure 58. Stress Error Norm for Mesh 3

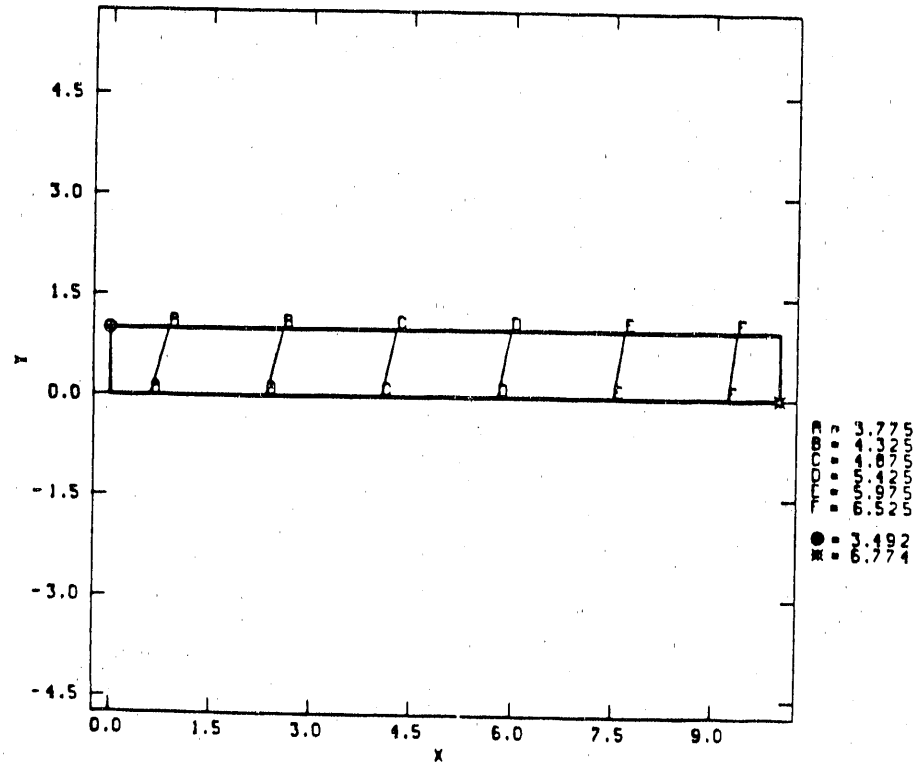

Figure 59. Del Sigma Norm for Mesh 1

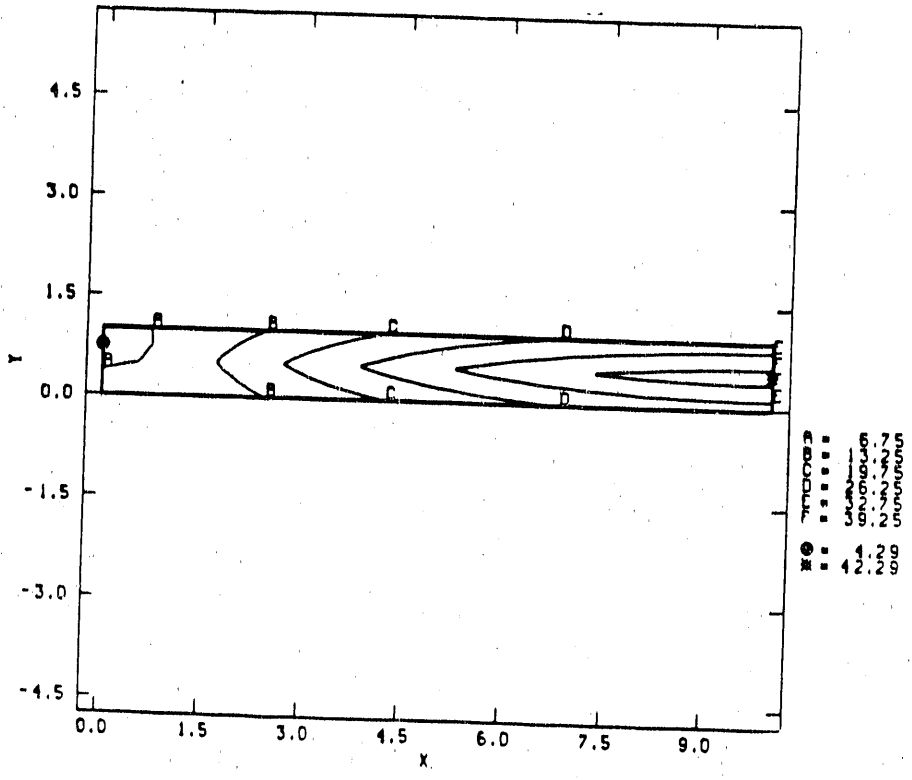

Figure 60. Del Sigma Norm for Mesh 2

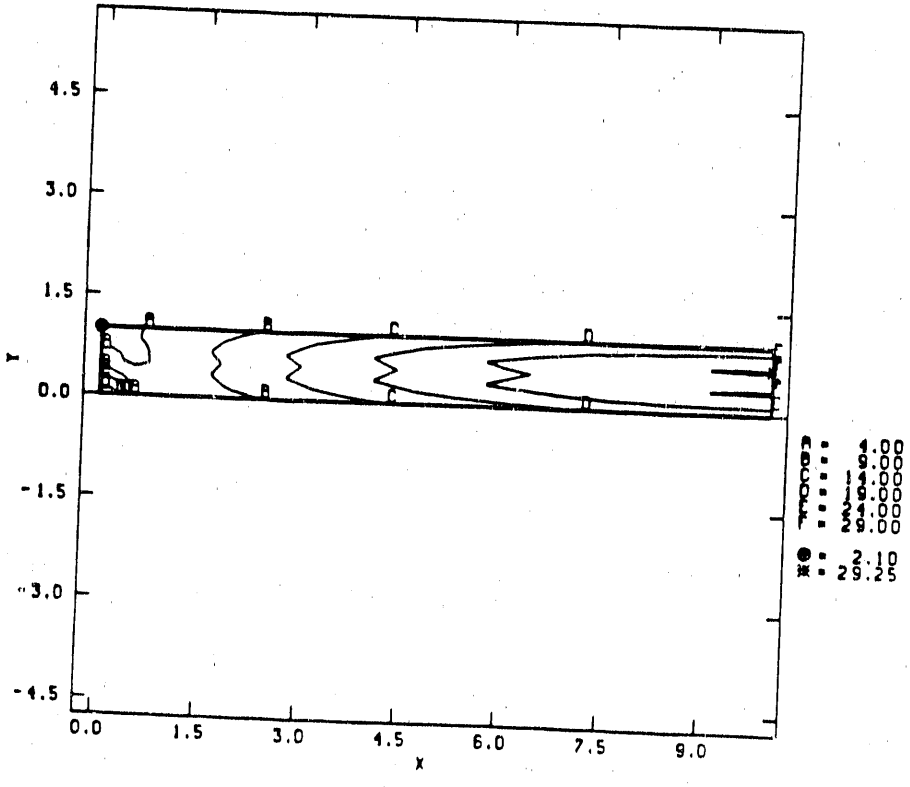

Figure 61. Del Sigma Norm for Mesh 3

4.2.3 A Short Cantilever Beam

The third problem is that of a short cantilever beam, Figure 62. The three meshes used to analyze this problem are shown in Figures 63 through 65 and have 18, 50, and 162 degrees of freedom, respectively. The element force equilibrium residuals (normalized to the net reaction force), Figures 66 through 68, clearly pick out the two corner singularities on the support edge. The stress error and $\Delta\sigma$ norms also detect the singularities, Figures 69 through 74, but do not appear to be as sensitive as the element force equilibrium residual error measure.

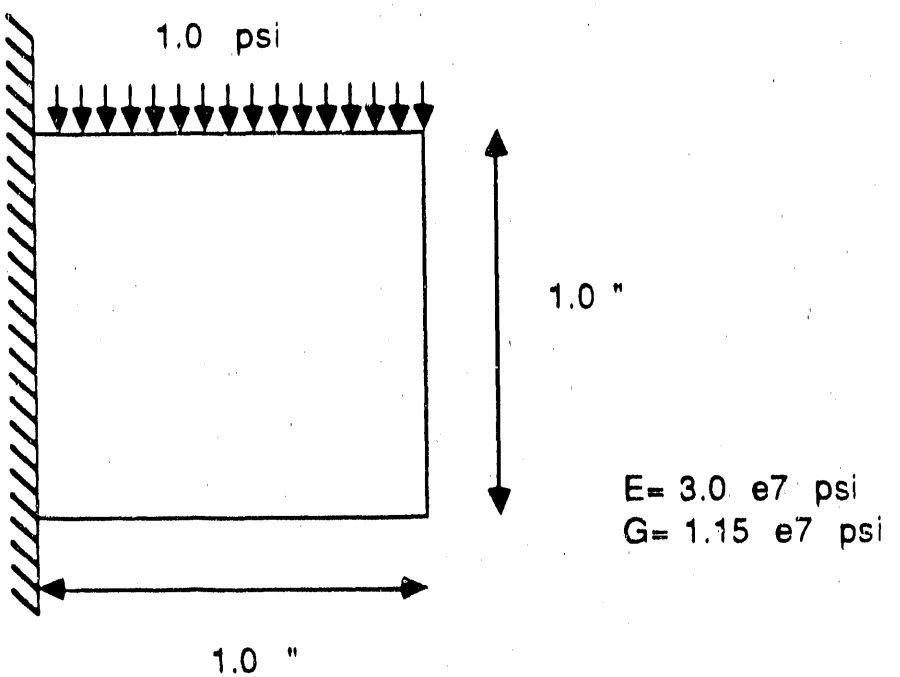

Figure 62. A Short Cantilever Beam Problem

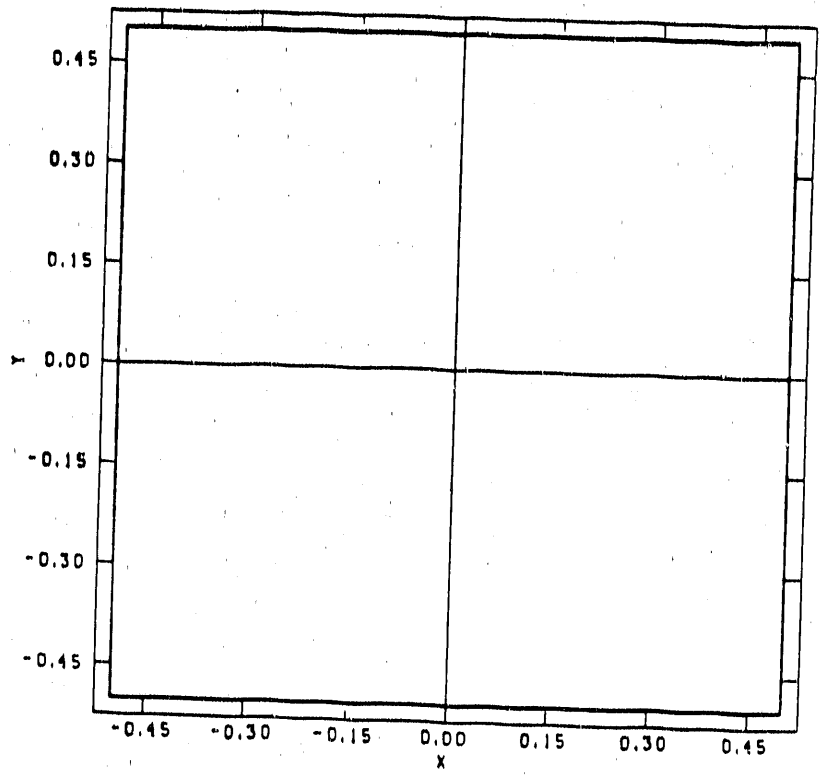

Figure 63. Mesh 1 for the Short Cantilever Problem

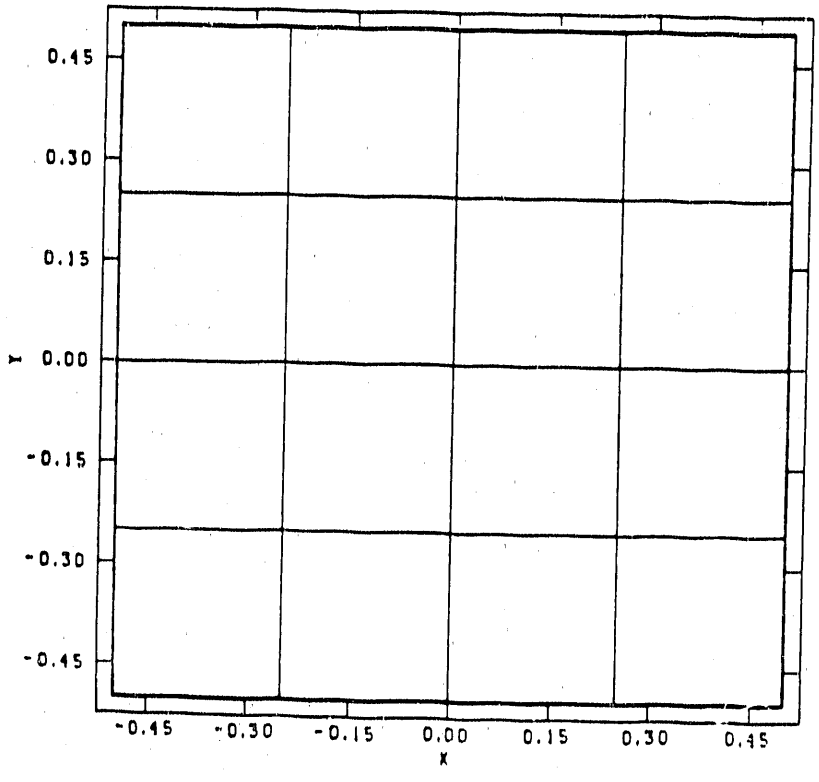

Figure 64. Mesh 2 for the Short Cantilever Problem

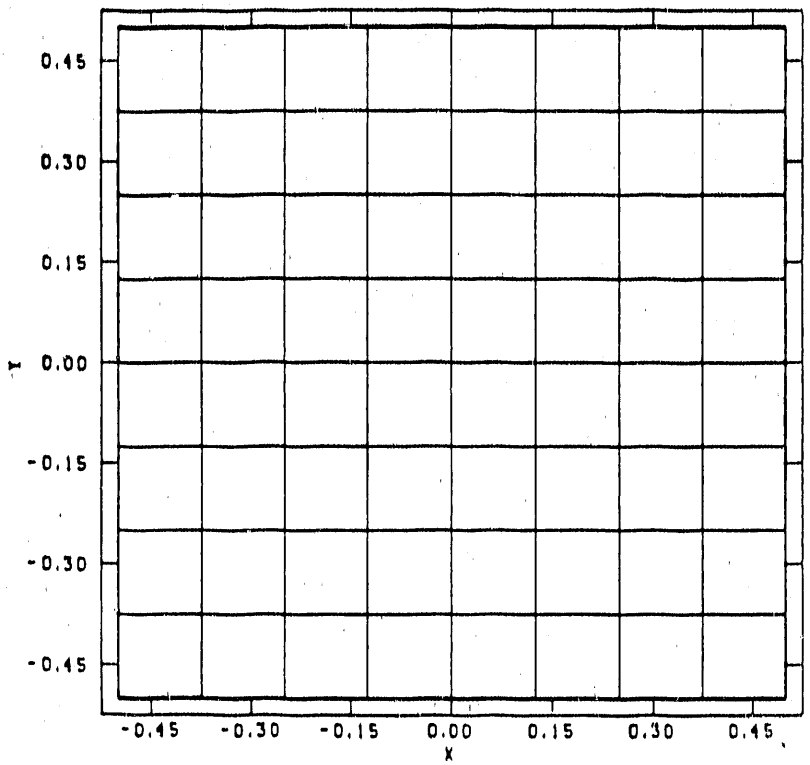

Figure 65. Mesh 3 for the Short Cantilever Problem

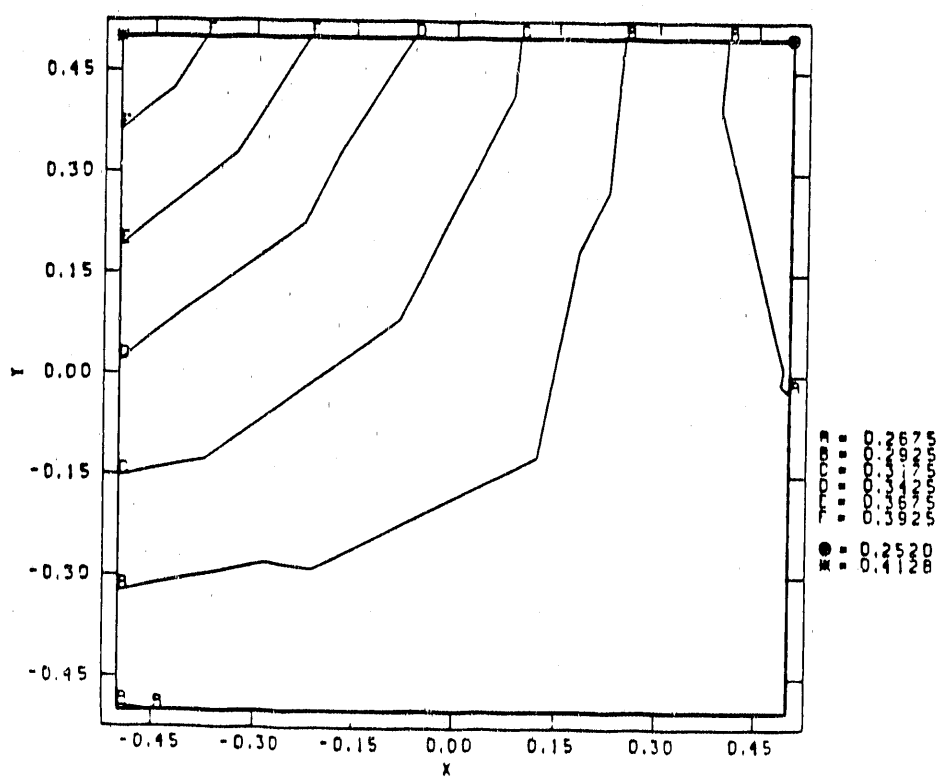

Figure 66. Element Force Error Norm for Mesh 1

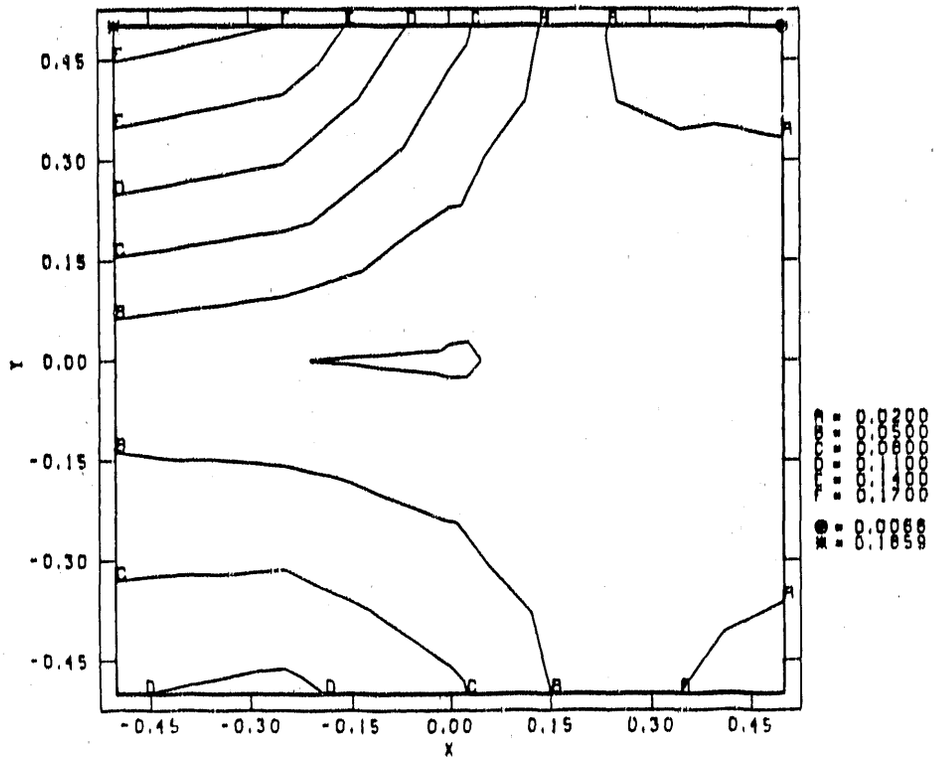

Figure 67. Element Force Error Norm for Mesh 2

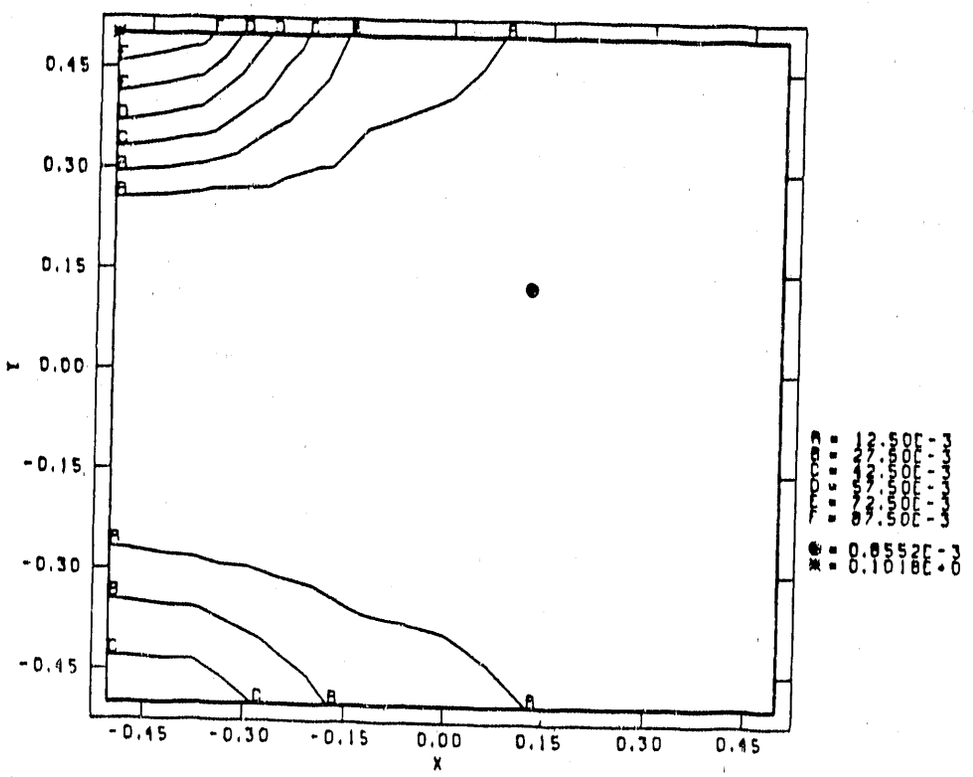

Figure 68. Element Force Error Norm for Mesh 3

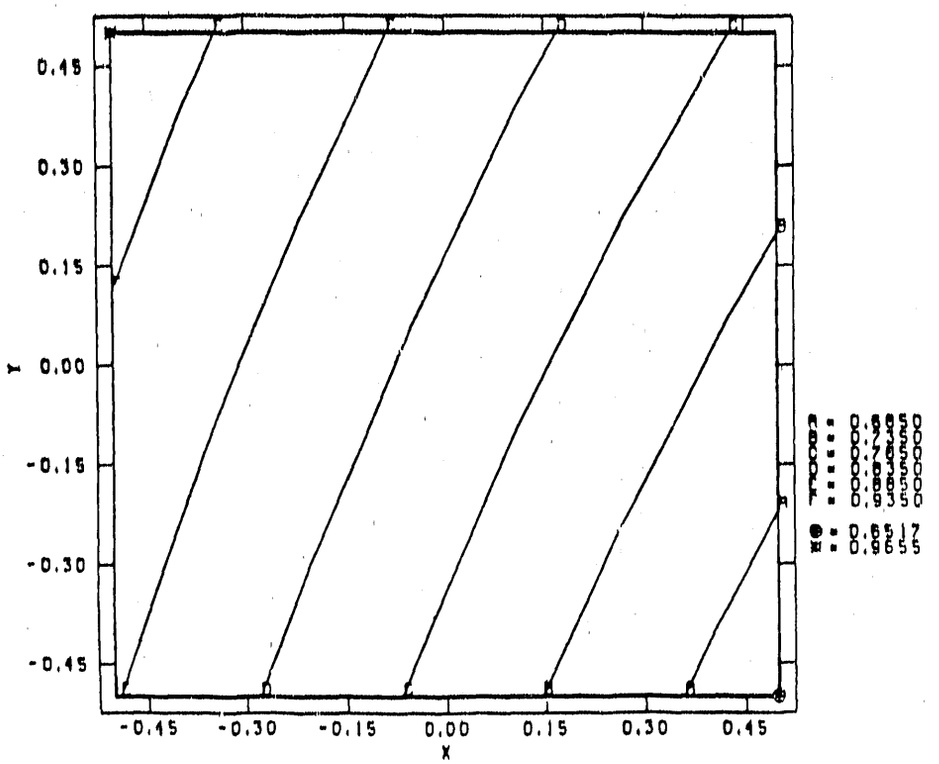

Figure 69. Stress Error Norm for Mesh 1

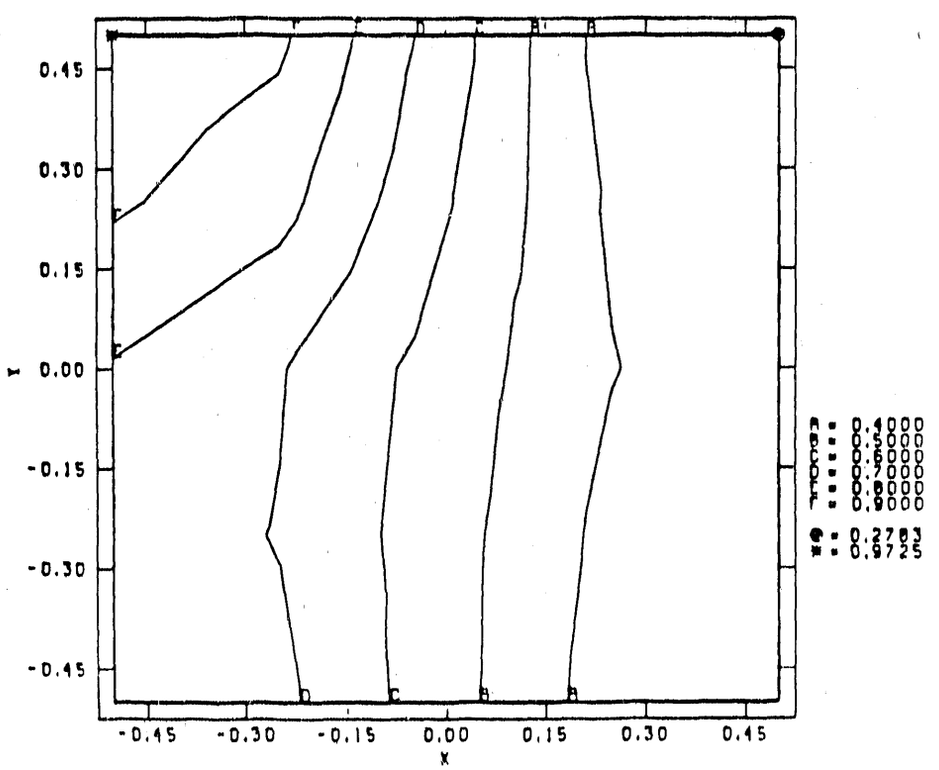

Figure 70. Stress Error Norm for Mesh 2

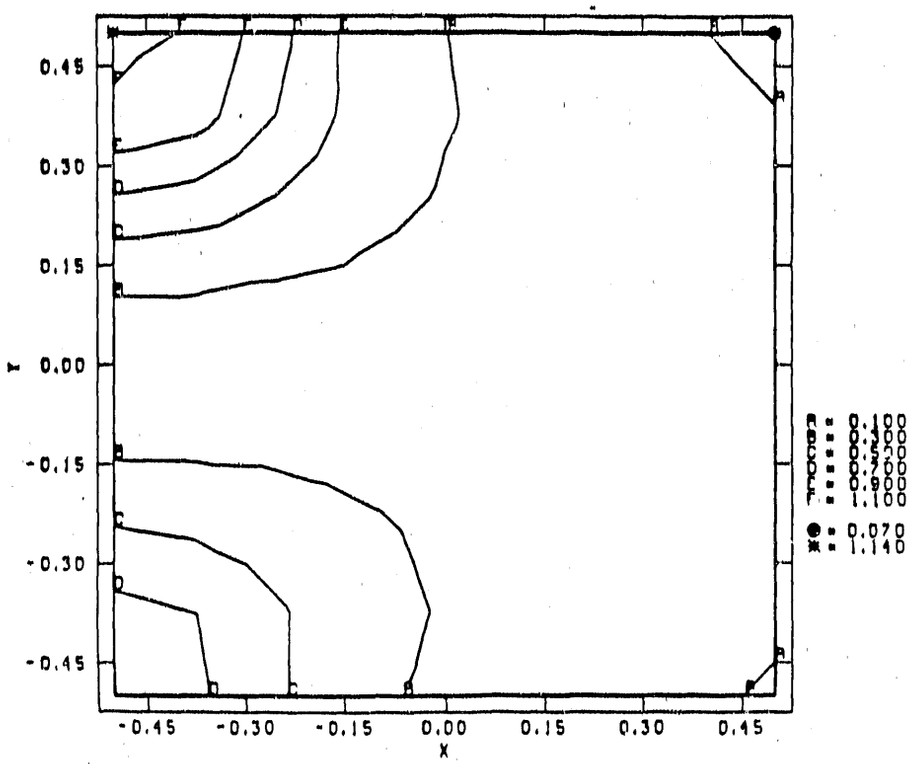

Figure 71. Stress Error Norm for Mesh 3

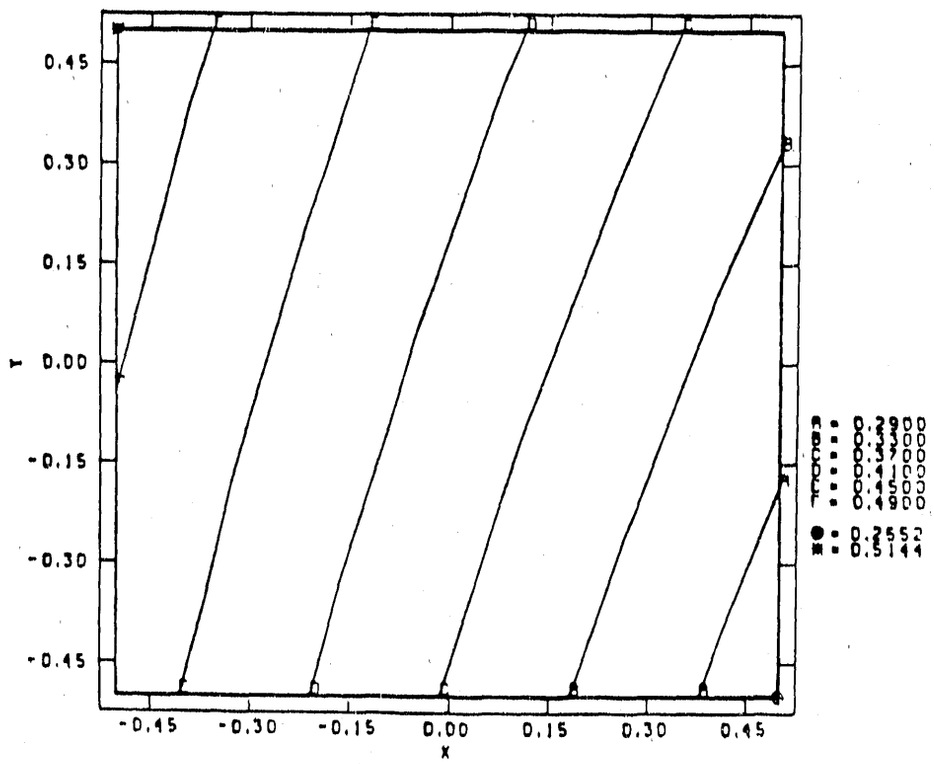

Figure 72. Del Sigma Norm for Mesh 1

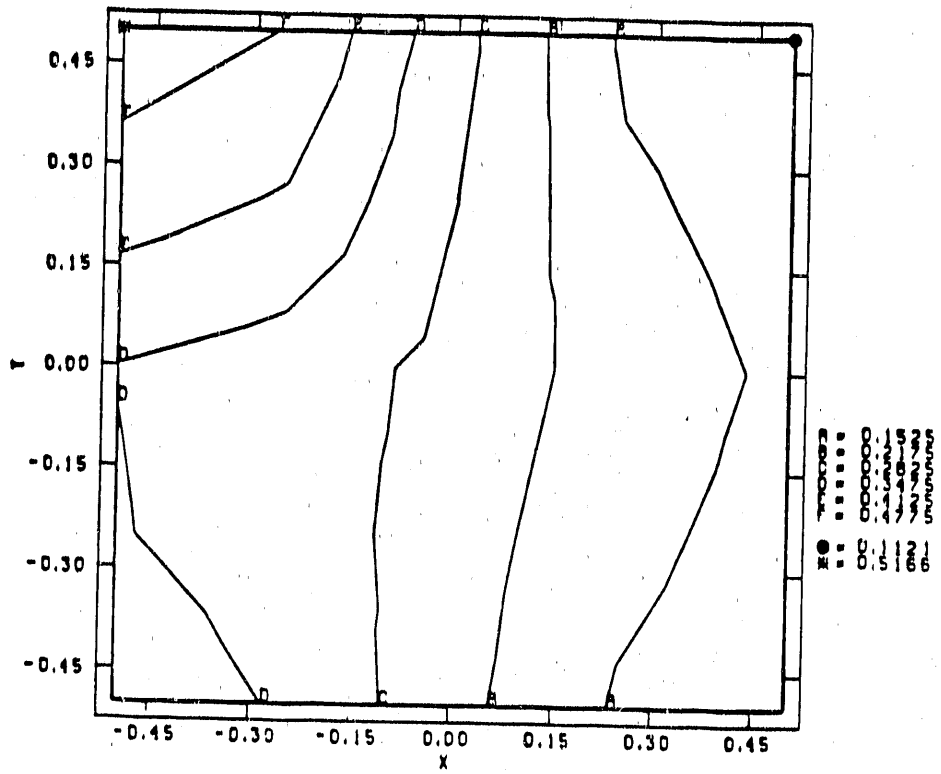

Figure 73. Del Sigma Norm for Mesh 2

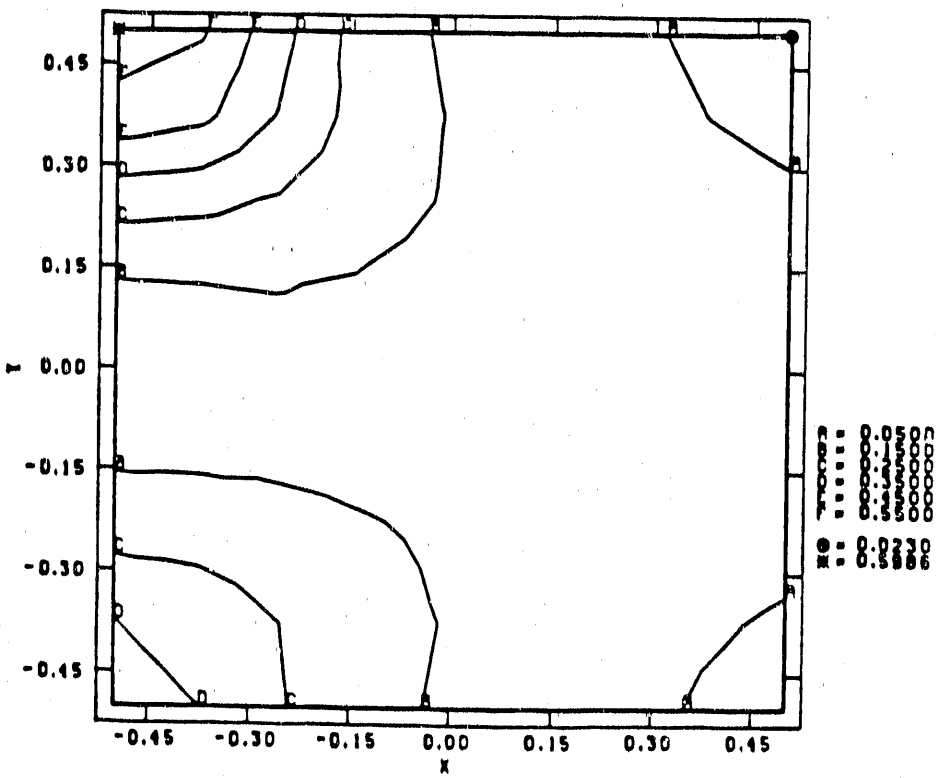

Figure 74. Del Sigma Norm for Mesh 3

5. DISCUSSION OF ERROR RESULTS

The problems considered in this report appear to indicate that the element force equilibrium residual is the most sensitive of the error measures investigated. Not only is this error measure more sensitive at singularities, but it also exhibits a boundary sensitivity that the other measures do not. This sensitivity is due to the fact that the error estimate is a measure of the departure from fundamental equations, i.e., force equilibrium, while the Zienkiewicz-Zhu family of error estimators are based on a departure from the projected stresses, which are only approximations to the true stresses. As will be demonstrated in the next section, which investigates some simple one-dimensional adaptive schemes, it could be argued that the element force equilibrium residual makes better use of the projected stresses than the Zienkiewicz-Zhu measures. As mentioned in Section 3, the Zienkiewicz-Zhu measures may indicate appreciable error even though the projected stress field approximates the exact solution well (see Figure 12).

Ainsworth, et al. (1989), performed an analysis of the Zienkiewicz-Zhu error estimator. They showed that an element force equilibrium error measure is closely enough related to the Zienkiewicz-Zhu estimator. Therefore, it may be possible to follow Ainsworth, et al.'s, work to show that an element force equilibrium error measure is also "asymptotically exact", i.e., the predicted error goes to zero when the true error goes to zero. This analysis remains to be performed, although, one could argue that as the finite element stresses converge, so do the projected stresses and element equilibrium.

In this work, element moment equilibrium was not considered. From the onset, it was intuitively believed that moment equilibrium would be a second order effect when compared to element force equilibrium. Preliminary numerical results showed this to be true. In fact, the moment residual had almost no correlation to the true error.

Although the application of any of these error measures to nonlinear problems has not been demonstrated, there is no fundamental reason why, say, the element force equilibrium error measure could not be used.

6. ADAPTIVITY

6.1 SIMPLE ONE-DIMENSIONAL H-TYPE ADAPTIVITY

The one-dimensional model problem (with n = 0 and 1) was used to explore how a simple h-type mesh refinement strategy could be used in conjunction with an element force error and $\Delta\sigma$ error measures. The refinement strategy was to simply divide an element in half if its error is above a prescribed level.

Figures 75 a-c show the computed results and mesh refinements required for the case of n = 0 to obtain an element force error of no more than 5% of the reaction force. Figure 76 shows the element force errors as the mesh is refined. Figures 77 a-c and 78 give the corresponding plots using the $\Delta\sigma$ norm with an error tolerance of 5%. A slightly more efficient solution (in terms of the number of elements used) is obtained using the element force error measure. This is due to the fact that the element force error measure makes better use of the projected stress solution than the $\Delta\sigma$ error measure. Similar statements can be made with n = 1, Figures 79 to 82.

6.2 PLANS FOR TWO-DIMENSIONAL ADAPTIVITY

Although most error measures are equally valid in one, two, or three dimensions, adaptively generating new meshes in two and three dimensions is a formidable problem. For this and other reasons, many researchers have combined h and p type adaptivity. Zienkiewicz and his co-workers have used triangular elements of linear and higher order to their advantage since it is much easier to mesh an arbitrary body with triangles than with quadrilaterals. Future efforts for this present work will focus on using Paving, a new automatic quadrilateral meshing technique (Blacker and Stephenson, 1990). This technique will allow for arbitrary selective refinements of the mesh, i.e., we will not be restricted to simple element subdivision.

6.3 CLOSURE

This report presents an investigation into the behavior of a family of finite element estimators based on projected stresses. Of those investigated, an error estimator based on the force equilibrium of an element appears to be very effective over a range of problems. This conclusion is based purely on numerical results. A mathematical analysis of this estimator is necessary to demonstrate that it is asymptotically exact. This estimator, though, is applicable to nonlinear as well as linear problems.

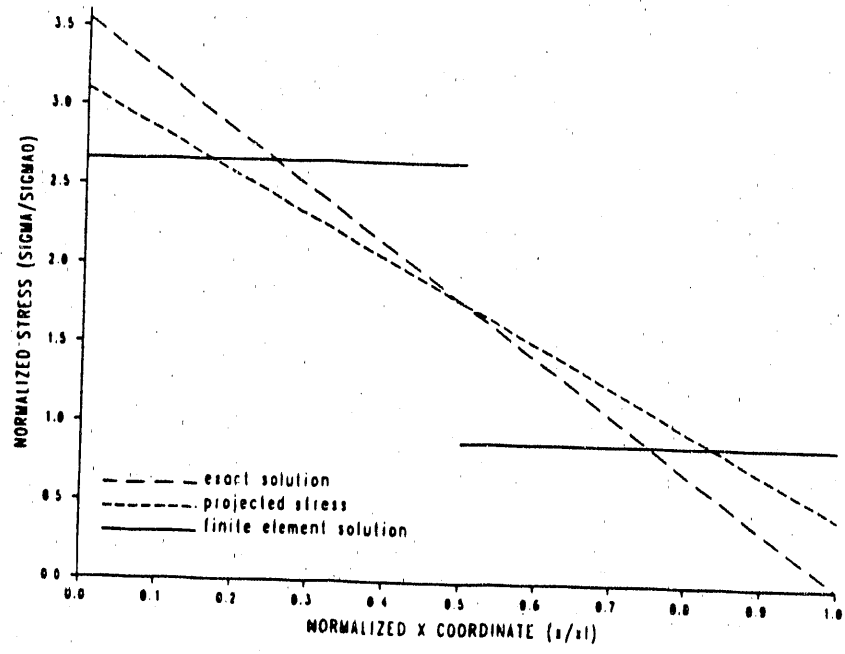

a. Iteration 1

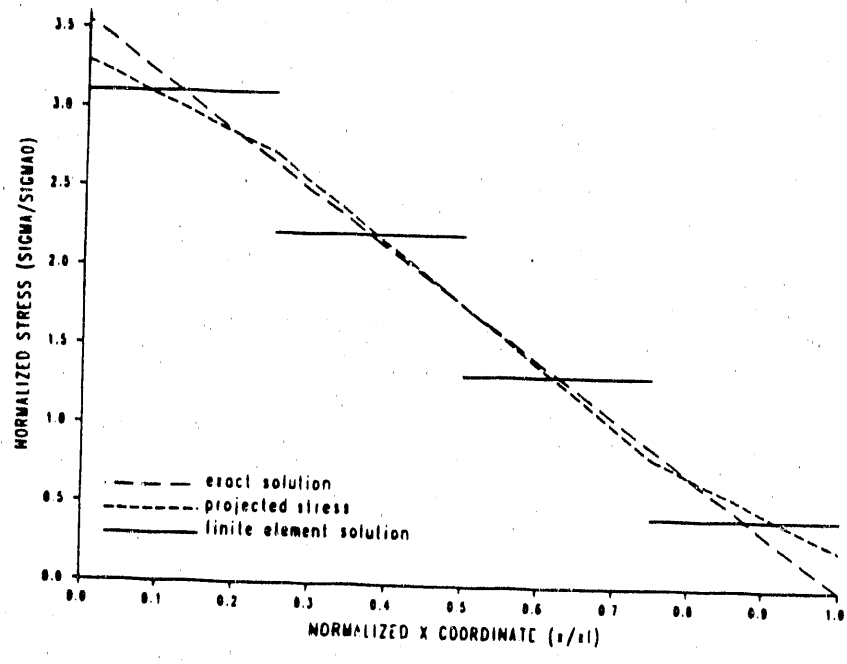

b. Iteration 2

Figure 75. H-Type Mesh Refinement for n = 0, 5% Error Tolerance Using an Element Force Residual Error Measure

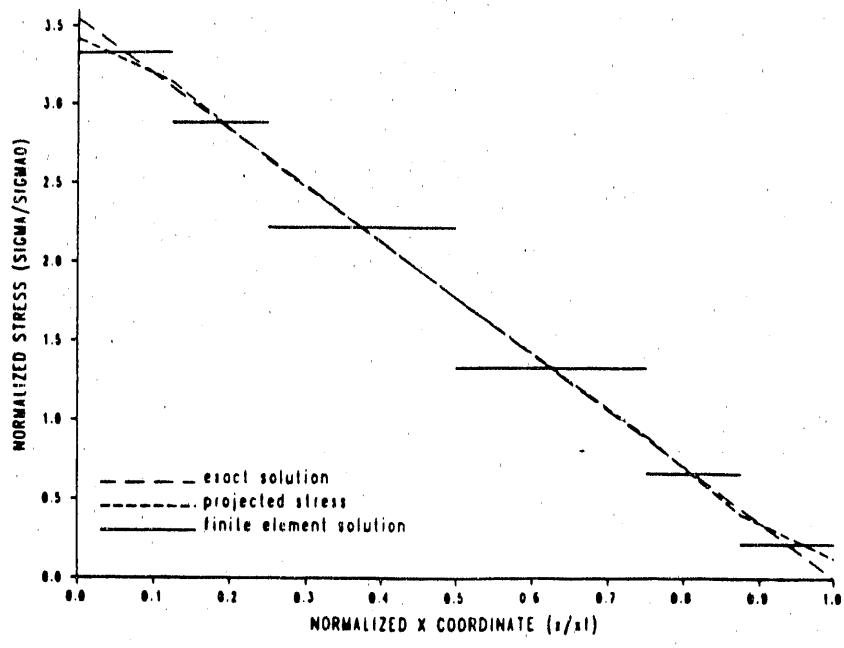

c. Iteration 3

Figure 75. H-Type Mesh Refinement for n = 0, 5% Error Tolerance Using an Element Force Residual Error Measure

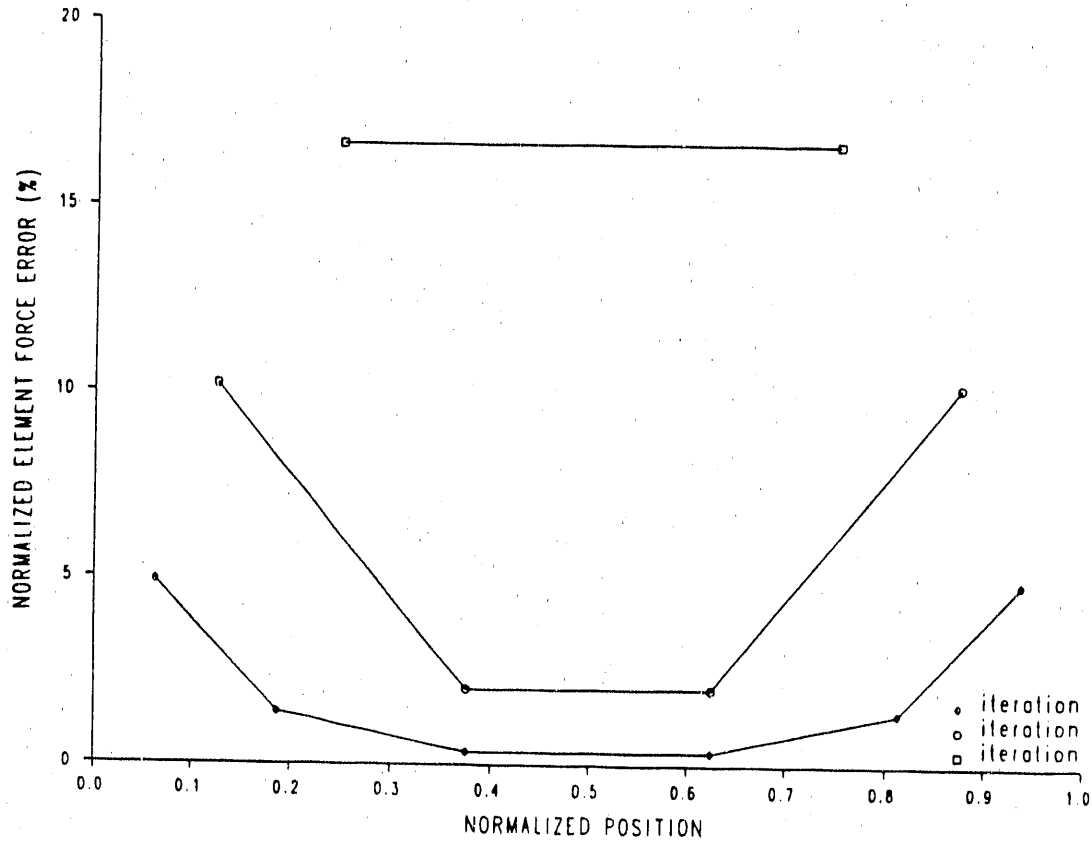

Figure 76. Element Force Residual Error for n = 0, 5% Error Tolerance

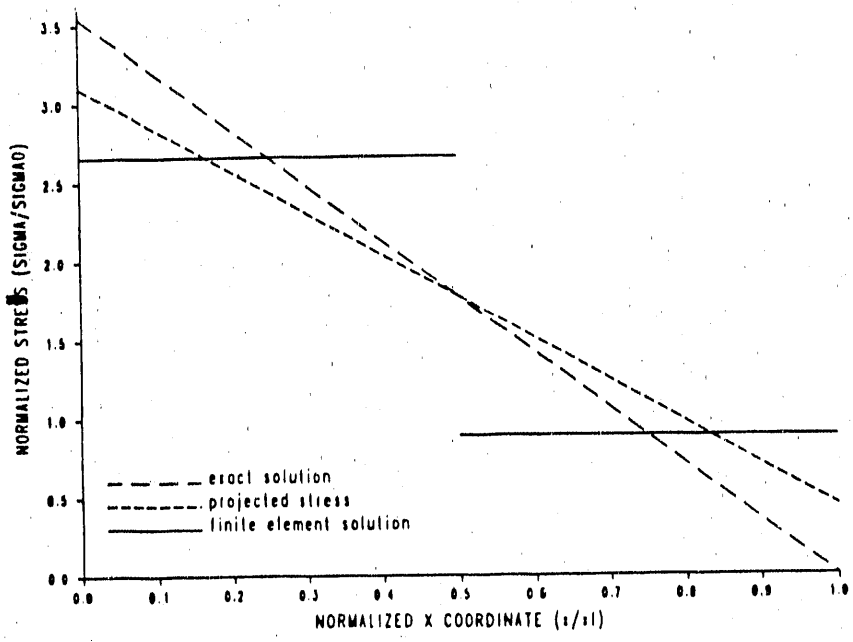

a. Iteration 1

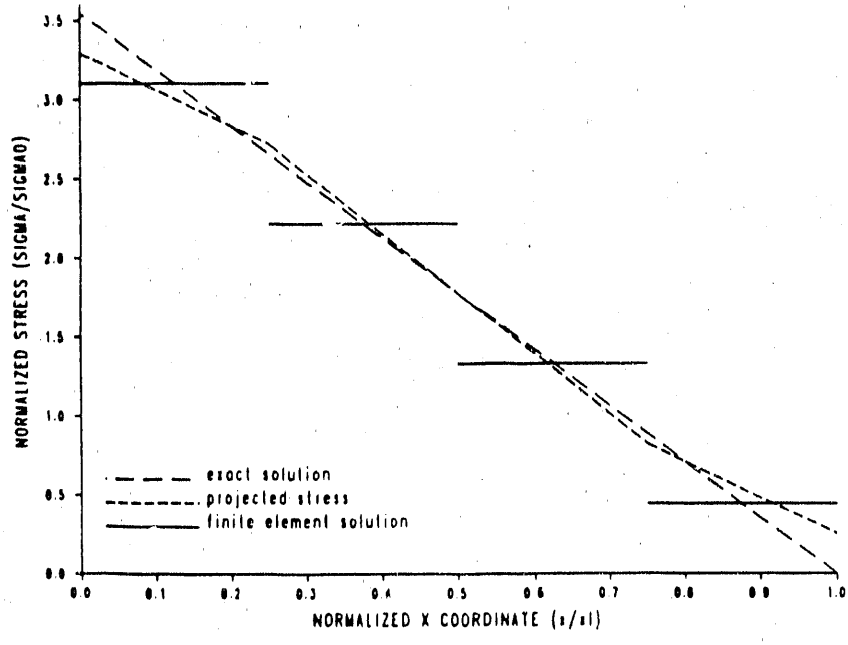

b. Iteration 2

Figure 77. H-Type Mesh Refinement for n = 0, 5% Error Tolerance Using a Del Sigma Error Measure

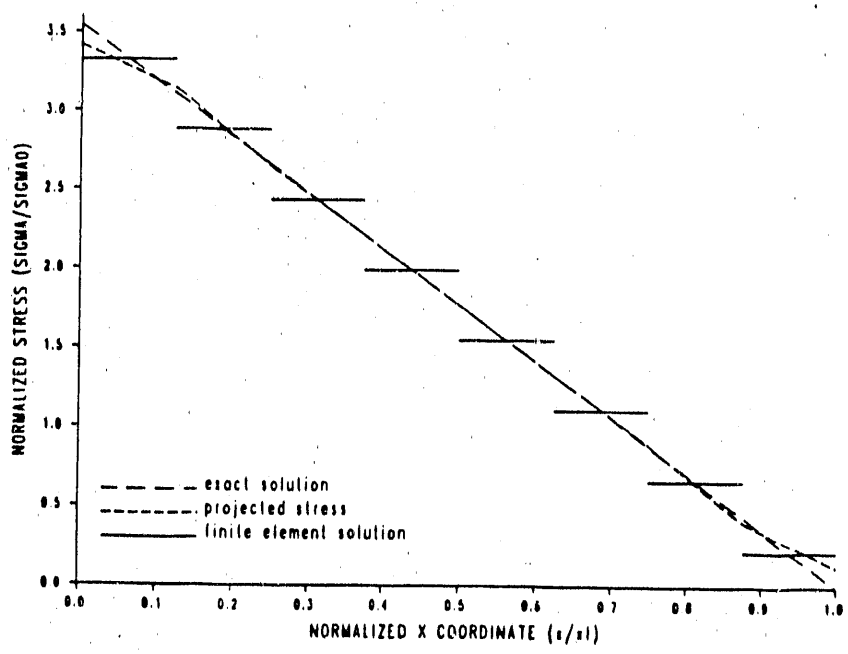

c. Iteration 3

Figure 77. H-Type Mesh Refinement for n = 0, 5% Error Tolerance Using a Del Sigma Error Measure

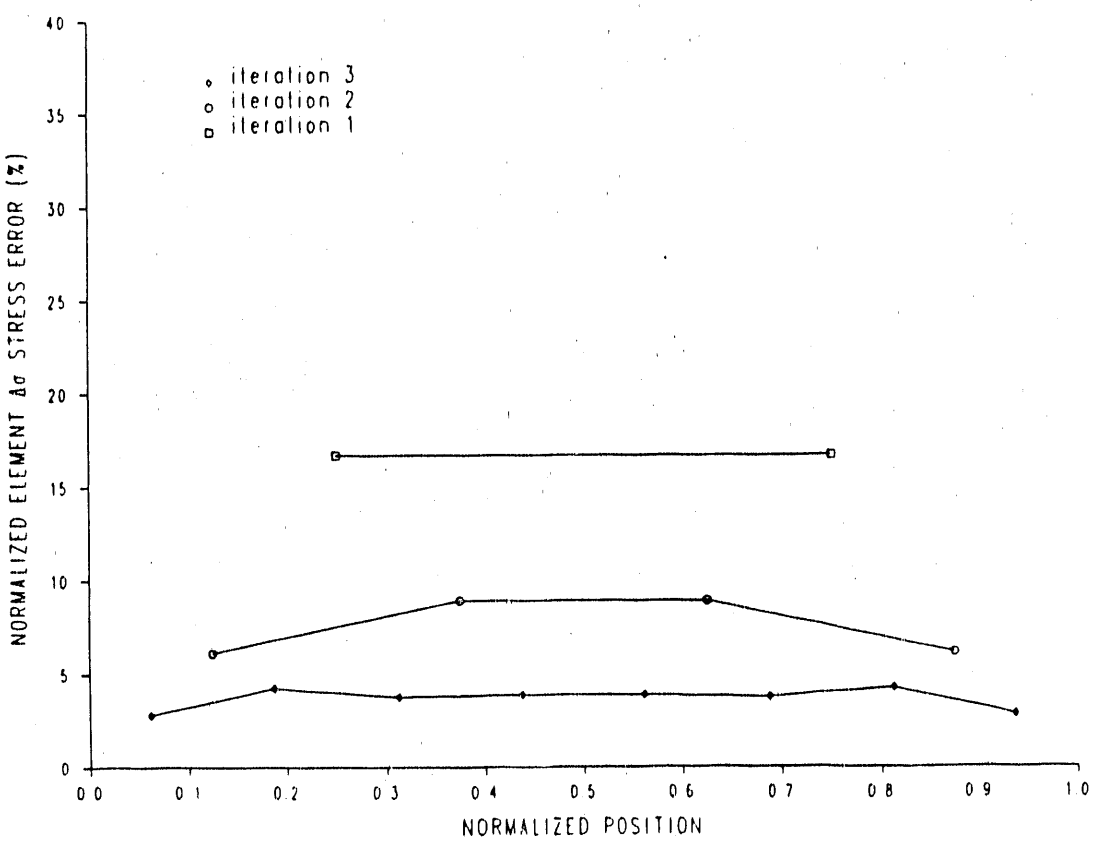

Figure 78. Del Sigma Error for n = 0, 5% Error Tolerance

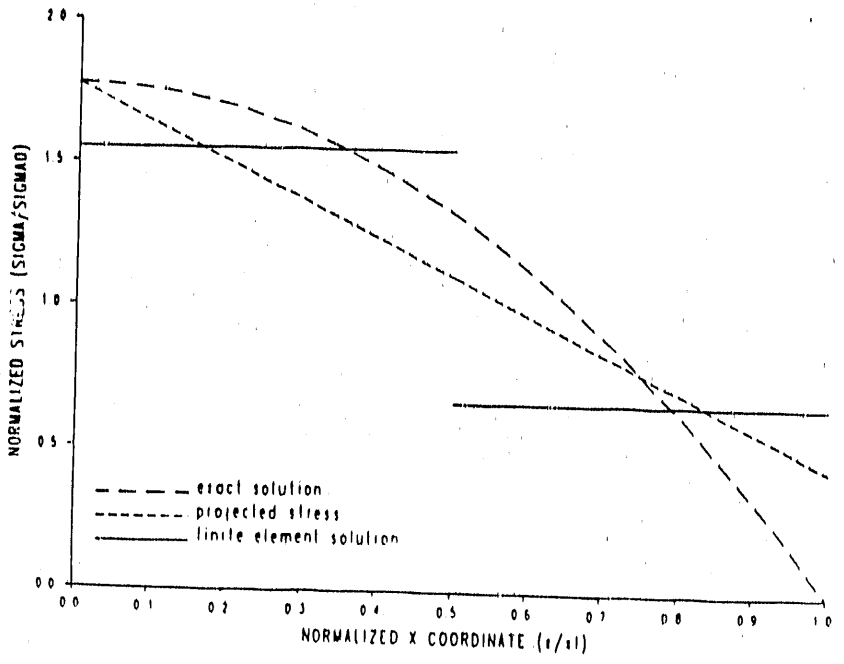

a. Iteration 1

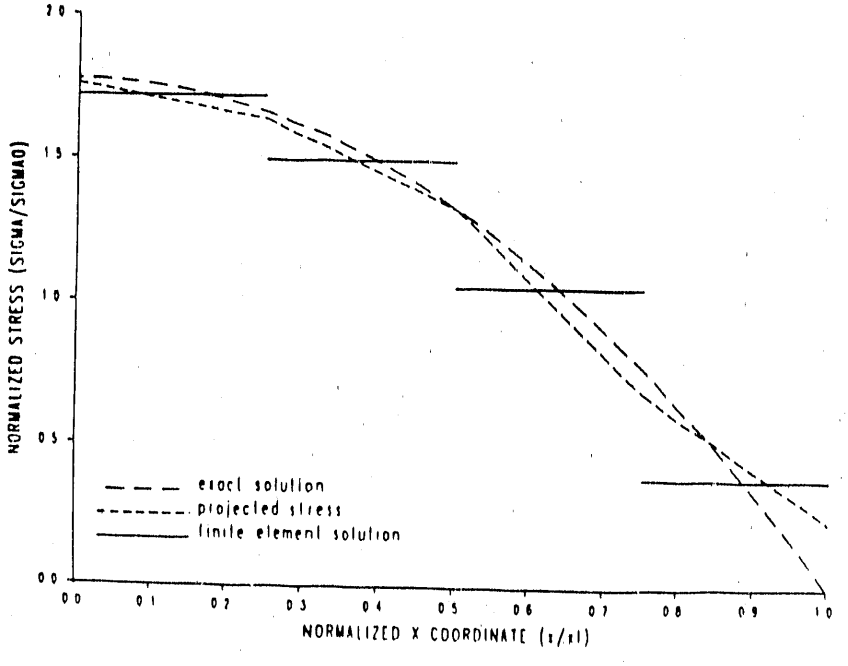

b. Iteration 2

Figure 79. H-Type Mesh Refinement for n = 0, 5% Error Tolerance Using an Element Force Residual Error Measure

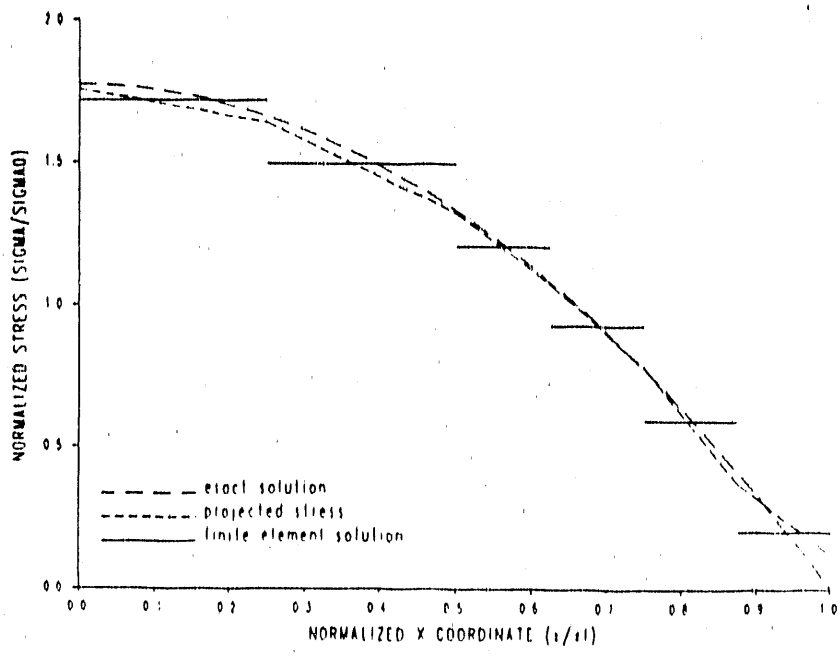

c. Iteration 3

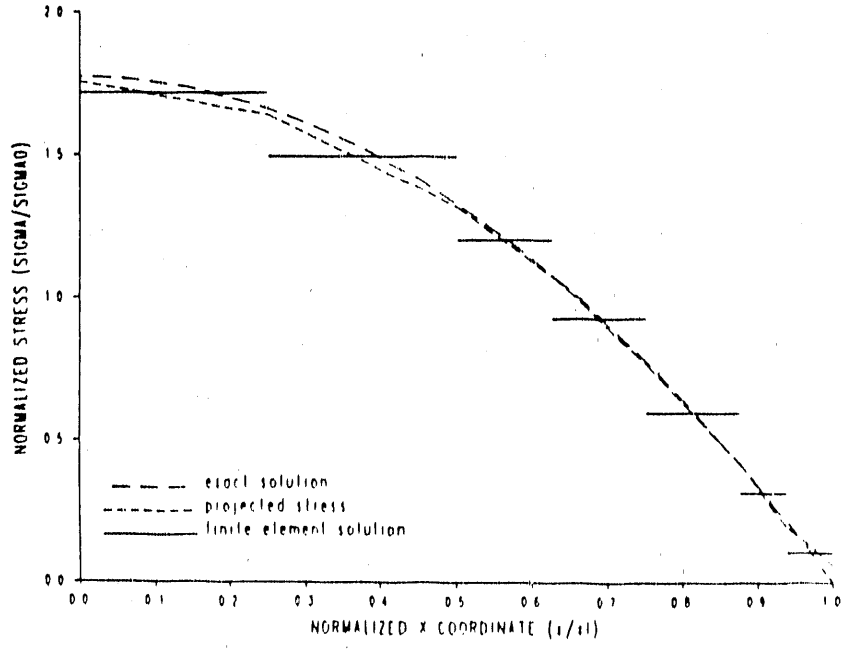

d. Iteration 4

Figure 79. H-Type Mesh Refinement for n = 0, 5% Error Tolerance Using an Element Force Residual Error Measure

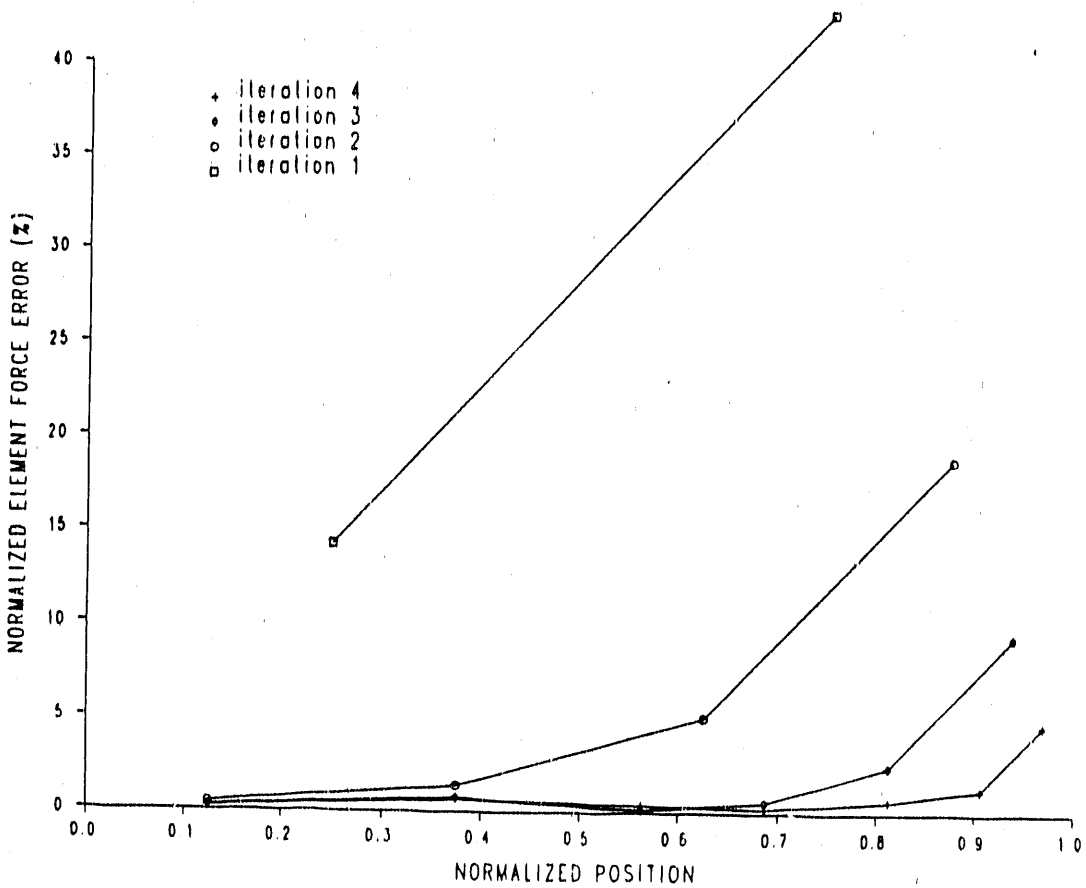

Figure 80. Element Force Residuals for n = 1, 5% Error Tolerance

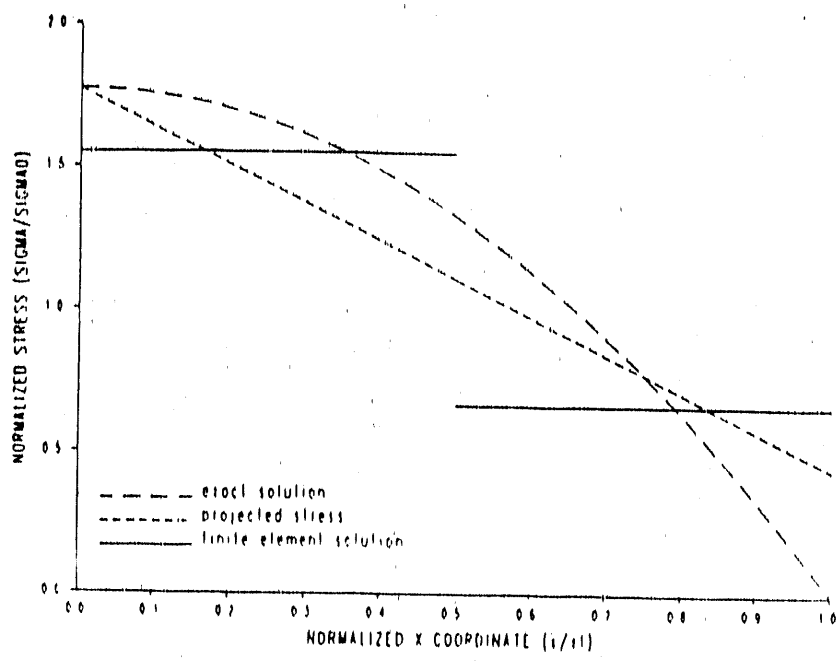

a. Iteration 1

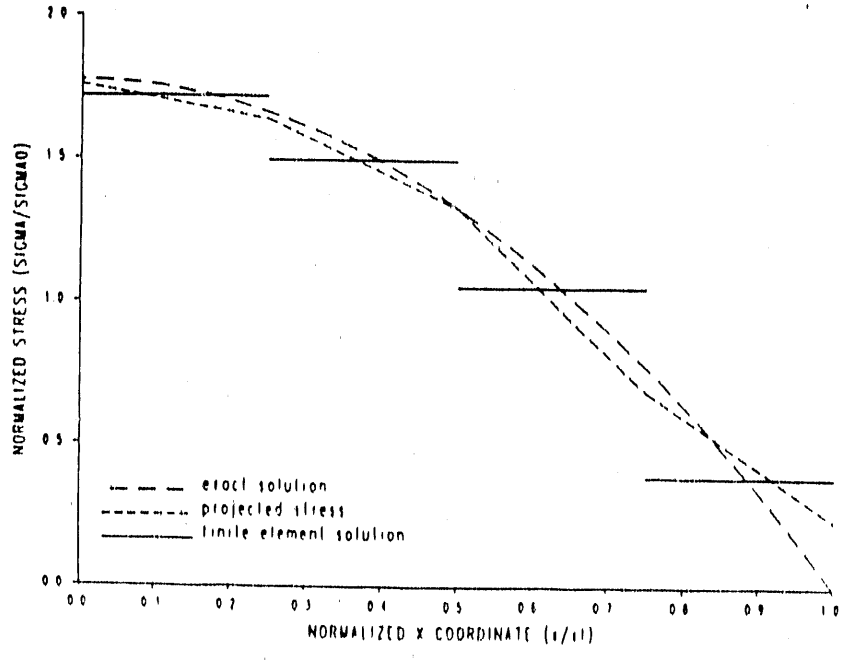

b. Iteration 2

Figure 81. H-Type Mesh Refinement for n = 1, 5% Error Tolerance Using a Del Sigma Error Measure

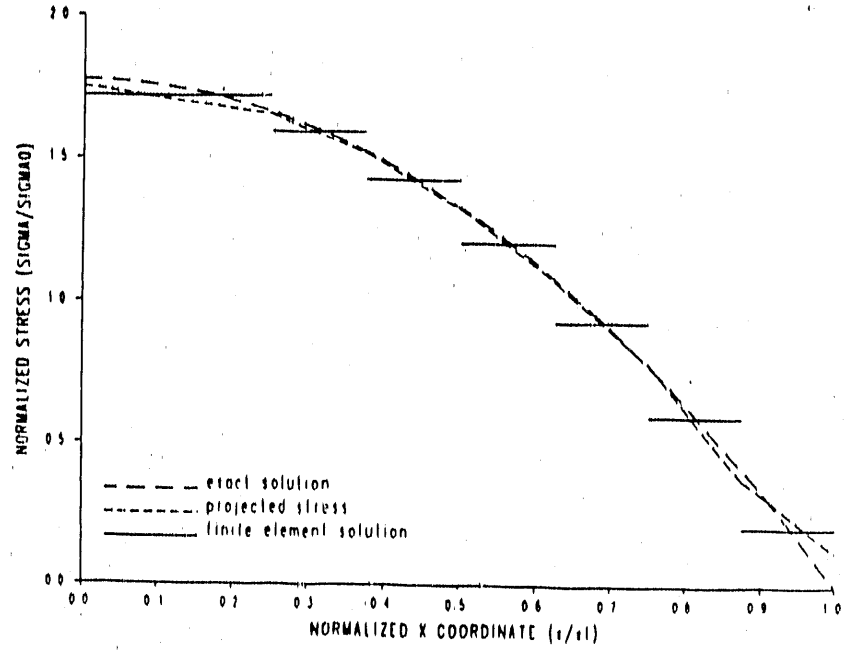

c. Iteration 3

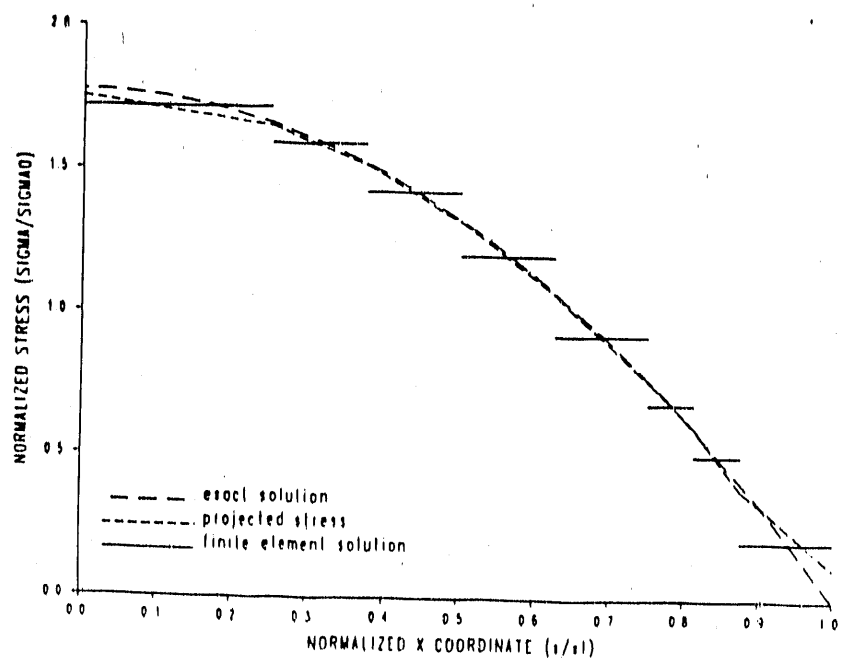

d. Iteration 4

Figure 81. H-Type Mesh Refinement for n = 1, 5% Error Tolerance Using a Del Sigma Error Measure

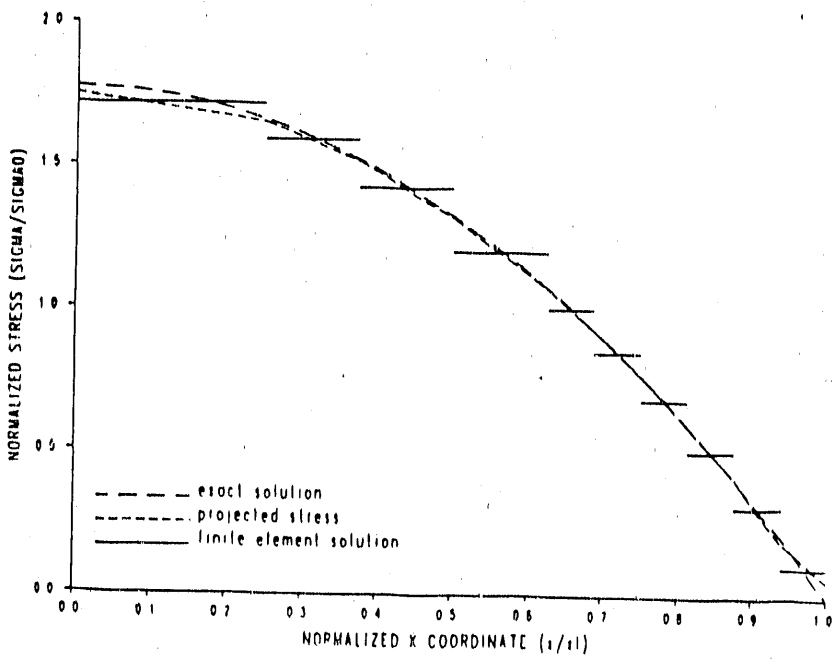

e. Iteration 5

Figure 81. H-Type Mesh Refinement for n = 1, 5% Error Tolerance Using a Del Sigma Error Measure

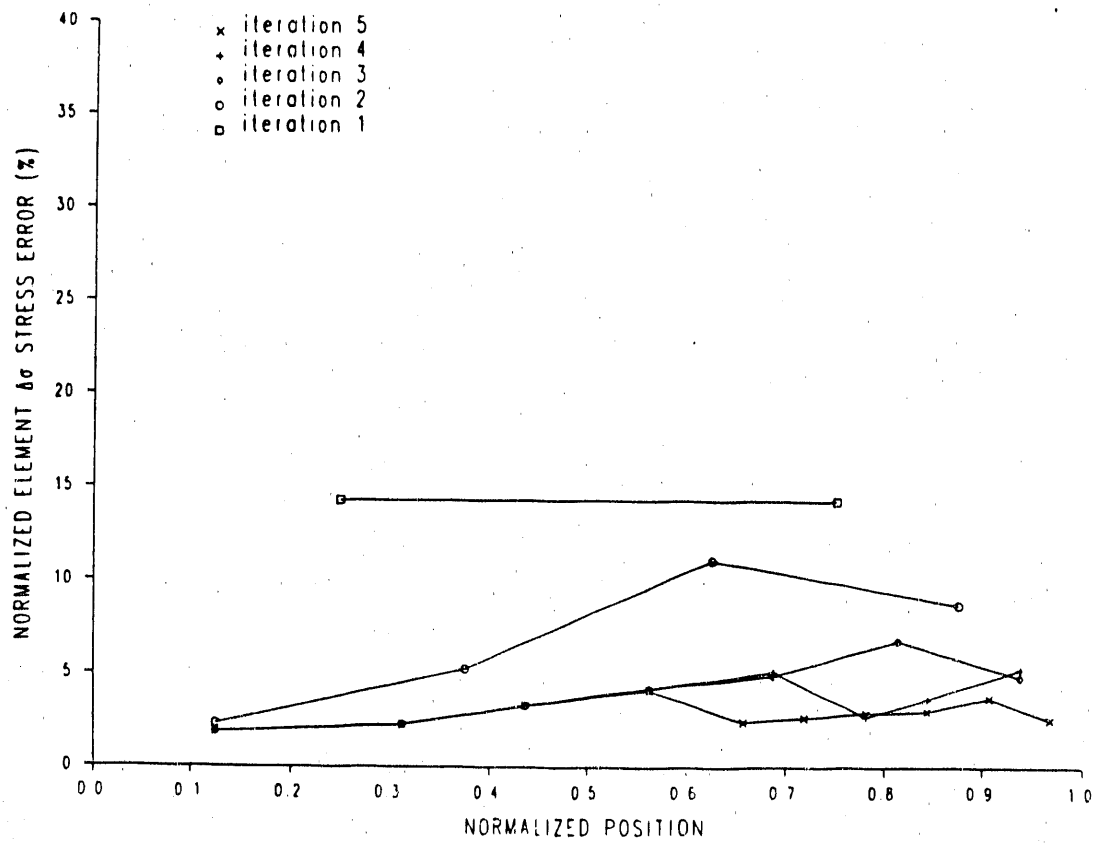

Figure 82. Del Sigma Error for n = 1, 5% Error Tolerance

7. REFERENCES

Ainsworth, M., J. Z. Zhu, A. W. Craig, O. C. Zienkiewicz, "Analysis of the Zienkiewicz-Zhu A-Posteriori Error Estimator in the Finite Element Method", Int. J. Numer. Methods Eng., 28, 2161-2174 (1989).

Babuska, I. and W. C. Rheinboldt, "Error Estimates for Adaptive Finite Elements Computations", SIAM J. Num. Analysis, 15, (4) 1978.

Babuska, I. and W. C. Rheinboldt, "Adaptive Approaches and Reliability Estimates in Finite Element Analysis", Comp. Meth. Appl. Mech. Eng., 17/18, 519-540 (1979).

Blacker, T. and M. Stephenson, "Paving: A New Approach to Automated Quadrilateral Mesh Generation," SAND90-0586, Sandia National Laboratories, Albuquerque, NM, March 1990.

Cantin, G., G. Loubignac, G. Touzot, "An Iterative Algorithm to Build Continuous Stress and Displacement Solutions", Int. J. Numer. Meth. Eng., vol. 12, 1493-1506 (1978).

Herrmann, L. R., "Interpretation of Finite Element Procedures as Stress Error Minimization Procedure", J. Eng. Mech. Div., ASCE, EM5, 1330-1336 (1972).

Hinton, E. and J. S. Cambell, "Local and Global Smoothing of Discontinuous Finite Element Functions Using a Least Squares Method", Int. J. Numer. Meth. Eng., Vol 8, 461-480 (1974).

Loubignac Gilles, Gilles Cantin, and Gilbert Touzot, "Continuous Stress Fields in Finite Element Analysis", Tech. Note, AIAA J., Vol. 15, no. 11, Nov. 1977.

Noor, Ahmed and Ivo Babuska, "Quality Assessment and Control of Finite Element Solutions", Finite Elements in Analysis and Design, 3, 1-26, 1987.

Oden, J. T. and H. J. Brauchli, "On the Calculation of Consistent Stress Distributions in Finite Element Approximations", Int. J. Numer. Meth. Eng., vol. 3, 317-325 (1971).

Zienkiewicz, O. C., Li Xi-Kui and S. Nakazawa, "Iterative Solution of Mixed Problems and the Stress Recovery Procedures", Comm. in Appl. Numer. Meth., vol. 1, 3-9 (1985).

Zienkiewicz, O. C. and J. Z. Zhu, "A Simple Error Estimator and Adaptive Procedure for Practical Engineering Analysis", Int. J. Numer. Methods Eng., 24, 337-357 (1987).

END

DATE FILMED

10 / 31 / 90